Congress report

First Sino-German Symposium on "Singlet molecular oxygen and photodynamic effects"

March 23-28, 2015; Ronggiao Riverview Hotel, Fuzhou, China

DOI 10.1515/plm-2015-0032

The First Sino-German Symposium on "Singlet molecular oxygen and photodynamic effects", supported by the Sino-German Center for Research Promotion (SGC), was successfully held in Fuzhou city from March 23–28, 2015. The SGC is co-financed by the National Natural Science Foundation of China (NSFC) and the Deutsche Forschungsgemeinschaft (DFG). The symposium was initiated and co-organized by Prof. Buhong Li from the School of Photonics and Electronic Engineering, Fujian Normal University and Prof. Beate Röder from the Institute of Physics, Humboldt-Universität zu Berlin, with strong support from top scientists in the field from China, Germany, the United States and Brazil. The aim of the symposium was to provide a bilateral scientific and technical forum to report, share and discuss the newest fundamental, clinical and technical developments in the field of singlet molecular oxygen, its detection, and its use for photodynamic treatments, both in the environment and clinics.

More than 40 experts were invited to report about their latest results in the topics of particular interest. In total 16 scholars participated from Humboldt-Universität zu Berlin, University of Regensburg, Ludwig-Maximilians-Universität München (LMU), Fraunhofer Institute of Solar Energy Systems (ISE), Charité – Universitätsmedizin Berlin, Friedrich-Alexander-Universität Erlangen-Nürnberg (FAU), Freie Universität Berlin (FU), Universität Ulm and Christian-Albrechts-Universität Greifswald. A further 25 experts participated from Shanghai Jiaotong University, Zhejiang University, Huazhong University of Science and Technology, Xi'an Jiaotong University, Xiamen University, Tongji University, Dalian University of Technology, Soochow University, China Pharmaceutical University, South China Normal University, Fuzhou University, Shenzhen University, Southern Medical University, National Center for Nanoscience and Technology of China, Technical Institute of Physics and Chemistry of Chinese Academy of Sciences, Institute of Chemistry of Chinese Academy of Sciences, Fujian Institute of Research on the Structure of Matter of Chinese Academy of Sciences, Chinese People's Liberation Army General Hospital and Fujian Normal University. There were also representatives from the City University of New York, University of Säo Paulo and The Chinese University of Hong Kong, China.

The scientific program addressed a wide range of problems in the different aspects of singlet molecular oxygen research and photodynamic effects, starting with photosensitized generation of singlet oxygen and the synthesis of novel efficient photosensitizers, problems of direct singlet oxygen luminescence detection in biological systems including possible strategies of signal enhancement, and clinical aspects up to the exciting topic of using singlet oxygen luminescence as a tool for diagnosis, and evaluation of the effectivity of photodynamic therapy in clinics. Round table discussions were also organized after each section, and a series of new bilateral collaborations were established during the symposium.

Conference Chairs



Chinese Chair: Prof. Buhong Li, Fujian Normal University, China



German Chair: Prof. Beate Röder, Humboldt University of Berlin, Germany

Submitted Short reports

Session 1:	Singlet oxygen generation and detection	299
Session 2:	Photosensitizers and targeting carrier systems (I)	315
Session 3:	Photosensitizers and targeting carrier systems (II)	322
Session 4:	Photodynamic inactivation of microorganisms	332
Session 5:	Enhancement of singlet oxygen generation	344
Session 6:	Photodynamic therapy – General aspects	352
Session 7:	Photodynamic therapy – New approaches	357
Session 8:	Optical techniques in photodynamic therapy applications	369
Session 9:	Clinical photodynamic therapy	373
Session 10:	Recent advances in clinical photodynamic therapy applications	378

Short reports

Session 1: Singlet oxygen generation and detection

[1.01] Time-resolved singlet oxygen luminescence detection under PDT-relevant light doses

Steffen Hackbarth*, Jan Caspar Schlothauer, Annegret Preuß and Beate Röder Humboldt-Universität zu Berlin, Department of Physics, Photobiophysics Group, Newtonstraße 15, 12489 Berlin, Germany *Corresponding author: Dr. Steffen Hackbarth, hacky@physik.hu-berlin.de

Abstract: Recent developments in time-resolved singlet oxygen luminescence detection allow measurements in vitro at low light doses so that the cells under investigation stay alive. This way, information can be gained about the impact of photosensitization on the cells under investigation and indirectly, their vitality can be estimated from changes in the kinetics. Such kinetics can also give information on the sub-microscopic localization of photosensitizers. This is shown in principle using liposomes as model system.

Keywords: singlet oxygen luminescence; diffusion; kinetics; subcellular localization; light dose.

1 Introduction

Measurements of the luminescence of singlet oxygen (10₂) in biological systems suffer from principal technical problems. The luminescence is very weak, the decay time of singlet oxygen is short and there are many sources of interfering signals, such as scattering or photosensitizer (PS) phosphorescence [1]. However, the kinetics of ¹O₂ may give valuable information about the illuminated sample, and detection setups have recently become much better [2]. Even though these results have been made in vitro they may be used for in vivo evaluation of a photodynamic treatment in the future.

In a homogeneous environment the temporal development of the local concentration of ${}^{1}O_{2}$, c_{3} , can be described by:

$$c_{\Delta}(t) = c_{\text{PS}} \cdot \phi_{\Delta} \cdot \frac{\tau_{T}^{-1}}{\tau_{T}^{-1} - \tau_{\Delta}^{-1}} [e^{-(t/\tau_{\Delta})} - e^{-(t/\tau_{T})}], \tag{1}$$

where c_{PS} represents the concentration of excited PS directly after excitation, Φ_{Δ} the $^1\!O_2$ quantum yield, τ_{Δ} and τ_{T} are the $^{1}O_{2}$ decay and the PS triplet decay time, respectively. τ_{T} is dependent on the local oxygen concentration and its diffusivity. The ¹O₂ decay in biological systems is influenced by the omnipresence of water, which is an effective physical quencher. The ${}^{1}O_{3}$ decay time in pure water is $3.7\pm0.2\,\mu s$ [3]. Intracellular quenchers, like proteins further shorten this decay time. The shortest reported decay time of ¹O₂ in cells so far was 0.3 µs [4], which means that in this experiment the quenching by proteins was 10 times more efficient than it was by water. If these proteins react with ¹O₂, both the protein and the oxygen are consumed, which affects both the PS triplet and the ¹O₃ decay [5].

2 Statement 1

"One has to be aware that any in-vitro measurement using other than just small light doses bear the risk of not being PDT relevant anymore. The cells under investigation will be in many cases just dead biomaterial."

Chemical quenching and the related changes in decay times of PS in vitro were observed first in 2008 [6] and have been investigated in more detail since explaining the contradictary kinetics in cells which was reported earlier [3, 4, 7]. Any measurement of ¹O₂ in cells influences the local environment of the PS by consumption of oxygen and the quencher. Illumination with an effective light dose (ELD) of around 400 nJ/cell already causes in many cases a doubling of the observed ¹O, decay time, where ELD describes the amount of light that actually passes the cross section of a cell and is defined as the average light intensity in the sample multiplied by the geometric cross section of the cell.

This was chosen as the upper limit for measurements in living cells. The reason for this is that about half of all chemical quenchers, among them cellular proteins, within the diffusion range of a PS are destroyed at that point and so the cell is doomed to die. After illumination with only 20 nJ/cell, the vitality of the examined androgen-sensitive human prostate adenocarcinoma (LNCaP) cells in suspension, which were incubated with 3 µM or more Pheophorbide-a (Pheo) in the cell medium for 24 h and determined with the microculture tetrazolium (MTT) test, dropped to <40% after further 24 h (Figure 1).

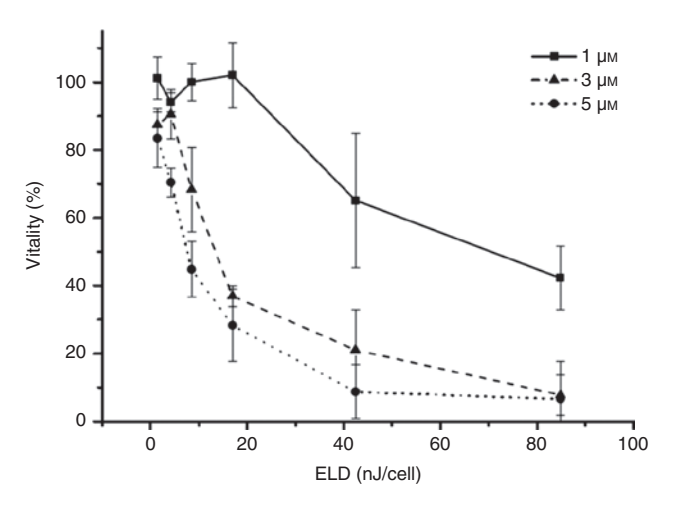


Figure 1: Cell vitality of LNCaP cells 24 h after illumination with low light doses (ELD, effective light dose) for different incubation concentrations of Pheo in the cell medium (incubated for 24 h). Cells were kept in cell medium at 37°C with 5% CO₂ constantly and only removed from the incubator for a short illumination period. The illumination was performed with white-light emitting diodes, but the illumination dose was corrected according to the absorption spectrum of Pheo as if it had been performed with 666 nm to enable comparison with the luminescence measurements.

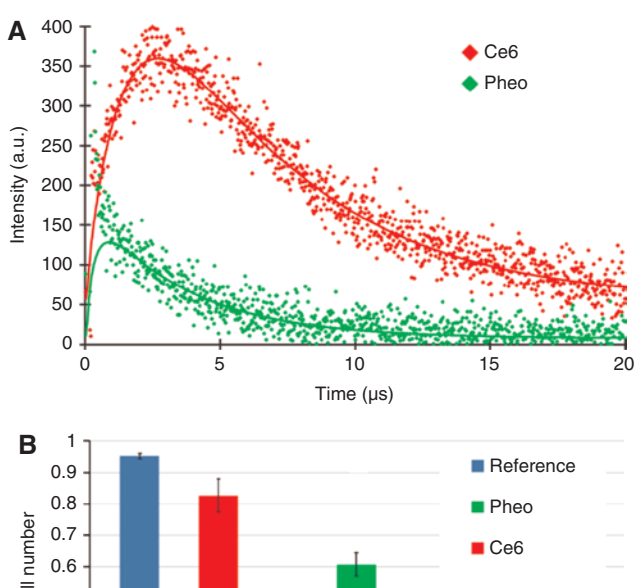
3 Statement 2

"The treatment efficiency does not only depend on the amount of generated 1O_2 , but also, where the 1O_2 is generated."

There is common agreement in the literature that the diffusion coefficient of oxygen in water is about 2×10^{-5} cm²/s and also that it will be even smaller in cells. Therefore the diffusion length of $^1\mathrm{O}_2$ in the cells is considerably lower than the diffraction limit for optical imaging, so even co-staining techniques cannot predict the treatment efficiency. However, luminescence kinetics can.

After just 30 min incubation of Jurkat cells with chlorin e_6 (Ce6) and Pheo, the 1O_2 luminescence signal of Ce6 was much bigger than that of Pheo (Figure 2A). In biological material in most cases the 1O_2 decay time is shorter than the PS triplet decay. According to Eqn. (1) this means, that the 1O_2 decay mainly influences the shape of the rising flank of the 1O_2 luminescence signal.

It is obvious that the ${}^{1}O_{2}$ decay time of Pheo is much shorter than that of Ce6 indicating that the interaction of ${}^{1}O_{2}$ with cellular quenchers is much greater if generated by Pheo. Hence the impact of Pheo on the cell after only 30 min of incubation is much more significant than that of Ce6. The cell vitality counting which took place about 90 min post-illumination supports this interpretation (Figure 2B). While the percentage of vital cells is reduced to 40% for Pheo, it is more than 80% for Ce6. This result



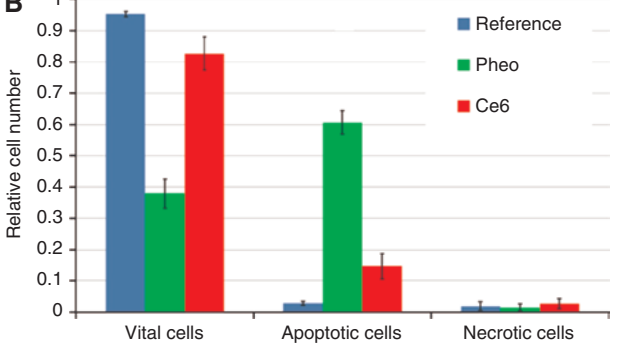


Figure 2: While the intensity of the $^1\mathrm{O}_2$ luminescence signal of Ce6 is bigger than that of Pheo after incubation of Jurkat cells for 30 min (A), the treatment impact is lower for Ce6 (B). The reason is probably the lower interaction of the $^1\mathrm{O}_2$ with cellular quenchers due to different localization of $^1\mathrm{O}_2$ generation, resulting in a longer $^1\mathrm{O}_2$ decay time for Ce6 compared to Pheo.

underlines the importance of measuring the kinetics of $^1{\rm O}_2$ luminescence rather than just the intensity.

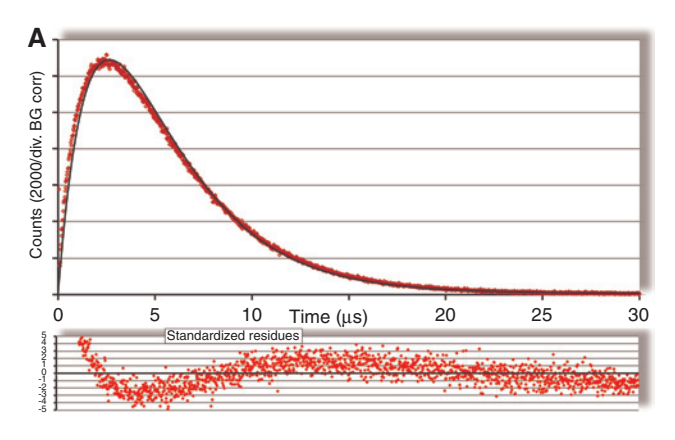
4 Statement 3

"Encoded in the kinetics there is information about the submicroscopic localization of the PS."

 $^{1}O_{2}$ has different radiative rate constants in different cell compartments (meaning the same amount of $^{1}O_{2}$ may emit a different number of photons depending on the local environment) and different decay times. The diffusion of $^{1}O_{2}$ from one cell compartment to another then causes deviations in the luminescence kinetics from the perfect exponential behavior as described in Eqn. (1).

The first example for deriving the sub-microscopic localization from the kinetics was given recently [8]. The kinetics of meso-Tetra(4-N-methylpyridyl) porphyrin (TMPyP) and Pheo in the liposomes of 1,2-dipalmitoyl-rac-glycero-3-phosphocholine hydrate (DPPC) were investigated. Since the geometry of the formed liposomes can be determined with a high degree of accuracy, a detailed theoretical simulation of the diffusion and luminescence

of ¹O₂ in these suspensions was possible. Whereas for TMPvP, which is located in the agueous phase, the simple two exponential descriptions resulted in a χ^2 value very close to 1, the measured signals of Pheo in liposomes could not be fitted this way (see Figure 3). Only a spherical symmetric diffusion fit, assuming the Pheo is located in or in direct vicinity of the DPPC membrane resulted in a good fit.



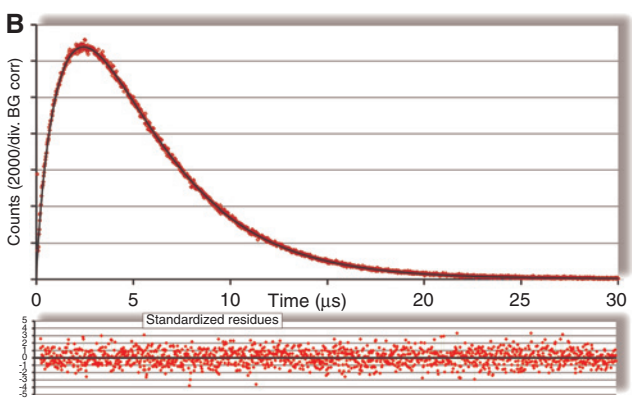


Figure 3: Any trial to fit the 10, luminescence signal of Pheo in liposomes using Eqn. (1) will fail, particularly if the PS triplet decay time is determined independently (f.i. with flash photolysis) and the result is included in the fitting process as fixed parameter (A). A fit can be reached using the spherical symmetric diffusion model for fitting a perfect coincidence of measured data (B, reprinted from [8]).

5 Conclusions

Strong limitations apply to 10, luminescence measurements of biological systems if relevant results are pursued. Nevertheless, if this challenge is managed, analysis of the ¹O₂ kinetics can help in gaining information on the situation in the cell, the treatment impact and cell vitality or even the sub-microscopic localization of the PS.

Acknowledgment: The authors want to thank Carmen Ludwig for carrying out measurements on cell vitality.

References

- [1] Kanofsky JR. Measurement of singlet-oxygen in vivo: progress and pitfalls. Photochem Photobiol 2011;87(1):14-7.
- [2] Hackbarth S, Schlothauer JC, Preuss A, Röder B. Highly sensitive time resolved singlet oxygen luminescence detection using LEDs as the excitation source. Laser Phys Lett 2013;10(12):125702.
- [3] Hackbarth S, Schlothauer J, Preuss A, Röder B. New insights to primary photodynamic effects - Singlet oxygen kinetics in living cells. J Photochem Photobiol B 2010;98(3):173-9.
- [4] Hackbarth S, Schlothauer JC, Preuß A, Ludwig C, Röder B. Time resolved sub-cellular singlet oxygen detection - ensemble measurements versus single cell experiments. Laser Phys Lett 2012:9(6):474-80.
- [5] Hackbarth S, Schlothauer J, Preuß A, Röder B. Singlet oxygen kinetics inside living cells: observation of endogenous quencher consumption and consequences for the spatial resolution in time-resolved measurements. Proc SPIE 2009;7380:738045. doi: 10.1117/12.822830.
- [6] Schlothauer JC, Hackbarth S, Röder B. A new benchmark for time-resolved detection of singlet oxygen luminescence revealing the evolution of lifetime in living cells with low dose illumination. Laser Phys Lett 2009;6(3):216-21.
- [7] Schlothauer JC, Hackbarth S, Jäger L, Drobniewski K, Patel H, Gorun SM, Röder B. Time-resolved singlet oxygen luminescence detection under photodynamic therapy relevant conditions: comparison of ex vivo application of two photosensitizer formulations. J Biomed Opt 2012;17(11):115005.
- [8] Hackbarth S, Röder B. Singlet oxygen luminescence kinetics in a heterogeneous environment - identification of the photosensitizer localization in small unilamellar vesicles. Photochem Photobiol Sci 2015;14(2):329-34.

[1.02] Singlet oxygen and its role in drug delivery

Miao Guo, Yanli Li, Zhihui Wan, Huajian Mao and Huabing Chen* Jiangsu Key Laboratory of Translational Research and Therapy for Neuro-Psycho-Diseases, College of Pharmaceutical Sciences, Soochow University, Suzhou 215123, Jiangsu, China *Corresponding author: Prof. Huabing Chen, chenhb@suda.edu.cn

Abstract: Singlet oxygen from photosensitizers plays an important role in photodynamic therapy. Generally, singlet oxygen is considered as a highly reactive oxygen species

which can directly damage cancer cells under light irradiation. Here we demonstrate a new role of singlet oxygen in intracellular delivery of anticancer compounds using nanocarriers. Singlet oxygen can mediate the disruption of lysosomes, induce the translocation of the nanocarriers from lysosomes into cytoplasma, and finally achieve synergistic anticancer efficiency.

Keywords: vesicles; micelles; singlet oxygen; lysosomal disruption; intracellular delivery.

1 Background

Photodynamic therapy (PDT) is a good approach for selectively destroying cancer cells by singlet oxygen that is generated by photosensitizers upon light irradiation at an appropriate wavelength [1]. However, it is still a major challenge to develop the nanocarriers for efficient intracellular delivery of photosensitizers, even though some nanocarriers such as liposomes and polymersomes are also being used to improve their delivery into cytoplasma.

2 Vesicle system

We have recently explored a vesicle system for the photoinduced intracellular delivery of photosensitizers, which possesses the ability to selectively disrupt lysosomal membranes through a photochemical internalization effect. The vesicles are fabricated through a pair of oppositely charged polyethylene glycol (PEG)-based block aniomer and homocatiomer [2]. A photosensitizer, Al(III) phthalocyanine chloride disulfonic acid (AlPcS2a) was further encapsulated into the vesicles through a simple vortex mixing of solution at a drug loading percentage of 11%.

Interestingly, the vesicles exhibited a photo-induced release of AlPcS2a under irradiation. The combination of high-resolution fluorescent confocal microscopy and lysosome membrane-specific staining showed that the photoinduced release was also observed even in the lysosomes after endocytic internalization. Simultaneously, the released AlPcS2a disrupted the lysosomal membranes through photochemical internalization effect, leading to the translocation of AlPcS2a and vesicles themselves to the cytoplasm. Thus, the vesicles exhibited stronger photocytotoxicity compared with free AlPcS2a. It is worth of note that the vesicles exhibit a promising potential for PDT application.

3 Micelle system

The focus has recently turned to the exploration of a nanocarrier for multimodal cancer therapy. We have recently demonstrated a micelle system for PDT-based multimodal therapy. The copolymers, consisting of monomethoxy poly(ethylene glycol) and alkylamine-grafted poly(L-aspartic acid), were assembled with carbocyanine dyes into the micelles, which exhibited small size,

high loading capacity, good stability, sustained release behavior, and enhanced cellular uptake [3]. The micelles achieved the desired biodistribution and long-term retention of carbocyanine dyes in the tumor. The micelles caused severe photothermal damage to the cancer cells by the destabilization of subcellular organelles after photoirradiation, causing superior photothermal tumor regression. Interestingly, singlet oxygen was also generated from carbocyanine dyes at a low dose under irradiation, and was found to disrupt the lysosomes upon light irradiation through photochemical internalization effect. The acridine orange staining was used to validate the disruption of lysosomes at a very low dose of carbocyanine dye under irradiation. Therefore, the micelles encapsulating the carbocyanine dye are potentially able to facilitate the intracellular translocation of other anticancer compounds into cytoplasm through lysosomal disruption.

We subsequently encapsulated carbocyanine dye and photosensitizer within the micelles, which exhibited significant photothermal effect and singlet oxygen from carbocvanine dye with irradiation at 785 nm [4]. The photothermal effect triggered hyperthermia, while singlet oxygen also triggered the disruption of lysosomes at a low dose of 0.2 µg/ml carbocyanine dye, which further induced the translocation of photosensitizer into cytoplasma. The enhanced distribution of photosensitizer in cytoplasma effectively led to the enhancement of PDT at 660 nm irradiation owing to the enhanced access of singlet oxygen to subcellular organelles. Finally it triggered off synergistic anticancer efficacy between PDT and photothermal therapy. In addition, we developed the micelles to encapsulate cyanine dye and a chemotherapeutic drug, which also exhibited singlet oxygen-mediated disruption of lysosomal membranes under irradiation [5]. The micelles proved to be highly capable of triggering the synergistic cytotoxicity of chemotherapeutic drug with photothermal therapy for achieving tumor eradication without any tumor re-growth. The enhanced distribution of a chemotherapeutic drug in cytoplasma plays a key role for synergistic anticancer efficacy. Consequently, it indicates that the micelles encapsulating carbocyanine dye provide an effective pathway to transport anticancer compounds into the cytoplasma by efecting photo-induced lysosomal disruption, which can improve the susceptibility of residual cancer cells to anticancer compounds, and generate synergistic anticancer efficiency.

References

[1] Chatterjee DK, Fong LS, Zhang Y. Nanoparticles in photodynamic therapy: an emerging paradigm. Adv Drug Deliv Rev 2008;60(15):1627-37.

- [2] Chen H, Xiao L, Anraku Y, Mi P, Liu X, Cabral H, Inoue A, Nomoto T, Kishimura A, Nishiyama N, Kataoka K. Polyion complex vesicles for photoinduced intracellular delivery of amphiphilic photosensitizer. J Am Chem Soc 2014;136(1):157-63.
- [3] Yang H, Mao H, Wan Z, Zhu A, Guo M, Li Y, Li X, Wan J, Yang X, Shuai X, Chen H. Micelles assembled with carbocyanine dyes for theranostic near-infrared fluorescent cancer imaging and photothermal therapy. Biomaterials 2013:34(36):9124-33.
- [4] Guo M, Mao H, Li Y, Zhu A, He H, Yang H, Wang Y, Tian X, Ge C, Peng Q, Wang X, Yang X, Chen X, Liu G, Chen H. Dual imagingguided photothermal/photodynamic therapy using micelles. Biomaterials 2014;35(16):4656-66.
- [5] Wan Z, Mao H, Guo M, Li Y, Zhu A, Yang H, He H, Shen J, Zhou L, Jiang Z, Ge C, Chen X, Yang X, Liu G, Chen H. Highly efficient hierarchical micelles integrating photothermal therapy and singlet oxygen-synergized chemotherapy for cancer eradication. Theranostics 2014:4(4):399-411.

[1.03] Current prospects of detectors for high performance time-resolved singlet oxygen luminescence detection

Jan Caspar Schlothauer, Steffen Hackbarth and Beate Röder*

Humboldt-Universität zu Berlin, Department of Physics, Photobiophysics Group, Newtonstraße 15, 12489 Berlin, Germany *Corresponding author: Prof. Dr. Beate Röder, roeder@physik.hu-berlin.de

Abstract: The very weak phosphorescence of singlet oxygen is the best option for the direct detection of singlet oxygen. Time-resolved luminescence detection in the nearinfrared gives detailed insight into the generation and decay of photosensitized generated singlet oxygen. Highly sophisticated instrumentation is necessary to obtain luminescence kinetics with high signal-to-noise ratio. Here we present the current state of time-resolved singlet oxygen luminescence detection. For the improvement of the detection systems possible alternative near-infrared detectors are discussed with respect to their usefulness for timeresolved singlet oxygen luminescence detection.

Keywords: infrared spectroscopy; photon counting; photomultiplier; single photon avalanche diode; superconducting nanowire.

1 Introduction

Direct detection of singlet oxygen is possible via its weak phosphorescence emission in the near-infrared (NIR), at about 1270 nm. In contrast to steady-state detection timeresolved detection allows the determination of kinetics which give information about the generation and decay of singlet oxygen. For quantitative investigation of singlet oxygen, especially in biological environments, the timeresolved detection of the singlet oxygen luminescence can be considered a "gold standard".

For the determination of kinetics the light dose of the experiment must be minimized, since the kinetics in biologic environments change due to light. However, due to the low quantum efficiency of the phosphorescence emission, the luminescence signals are very weak. This already makes the detection a challenging task. In addition, for NIR wavelengths around 1270 nm only a few detectors are available.

In contrast to silicon-based technologies for the visible spectrum, the development of NIR detectors proceeds slower. Photomultipliers suitable for wavelengths around 1270 nm are almost exclusively offered by Hamamatsu. Nevertheless, the demand for NIR detectors has increased, also due to applications in cryptography and the telecommunication industry. In addition to classic photomultipliers (PMT), different technological approaches are pursued such as single photon avalanche diodes (SPAD) or single photon superconducting nanowire detectors (SPSND).

For this, it is the aim of this work to look at the current state of technological development of commercially available devices for NIR detection with respect to their possible application for time-resolved detection of the singlet oxygen luminescence.

2 Analog detectors vs. photon counting devices

Analog detection of the luminescence kinetics is a very straightforward method (see Figure 1). The sample is excited by a pulsed laser and the detector output is an electronic signal proportional to the luminescence. This signal must be amplified and digitized for further processing. In contrast to analog detection a counting detector converts incoming photons into electronic pulses. A histogram of

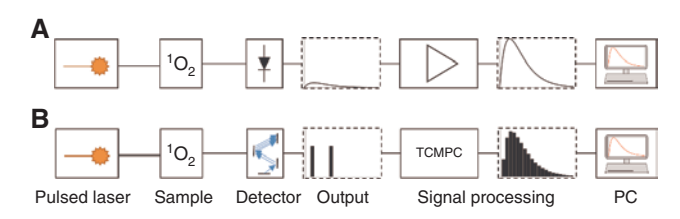


Figure 1: Luminescence detection schemes of (A) analog detection and (B) photon counting.

the temporal distribution of these pulses with respect to the excitation laser pulse has to be constructed. This is usually done by time-correlated single photon counting devices. In the case of singlet oxygen luminescence detection the use of multiscalers or time correlated multi photon counting is advised.

The best detector for analog detection is a Ge diode (EO817-p), which is available from Northcoast. For photon counting the H10330-45 PMT by Hamamatsu is considered the optimal device [1]. A comparison of the luminescence signal of pheophorbide-a in ethanol, obtained from the analog detection setup with that obtained using photon counting is shown in Figure 2. When the signal obtained from the analog measurement of the sample with OD 0.00067 and the counting measurement of the sample with OD 0.00017 are compared, taking into account the irradiation energy of the measurement and the channel width, the signal obtained by

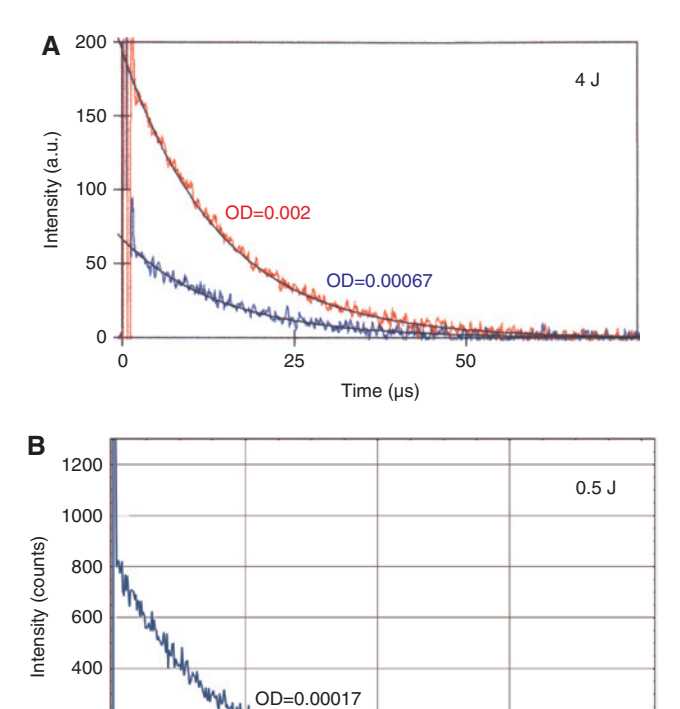


Figure 2: Comparison of the singlet oxygen luminescence signal acquired by (A) analog detection with the Northcoast EO817-p and (B) photon counting with the Hamamatsu H10330-45 PMT from solutions of pheophorbide-a in ethanol with different optical densities. The samples were illuminated with 4 J for analog detection and 0.5 J for photon counting. The signal acquired with the photon counting setup is approximately a factor of 30× higher.

40

Time (µs)

60

20

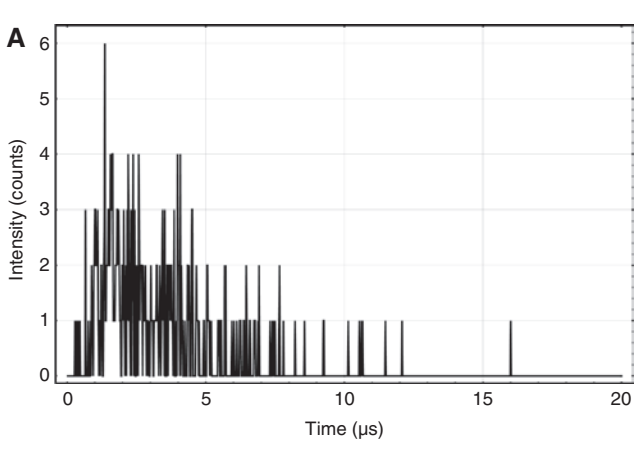
200

the photon counting setup is more than an order of magnitude higher (Figure 2) [2].

3 Sensitivity of biological cells to light

Following the illustrative look of Hackbarth et al. [3], showing how many photons can be detected from a single cell, before the cell has been critically damaged by the measurement light and using more realistic values for the kinetics and maximum light dose, a signal of 330 photons can be obtained from a single cell. A simulated signal of this magnitude, without any noise, is depicted in Figure 3A. The signal does not allow accurate quantification of rise- or decay times.

Kinetics of singlet oxygen luminescence can only be obtained from measurements of suspensions of many cells. Typical experiments use around 1 million cells. The setup used in our group typically allows around 7–9 measurements before the decay times have doubled. Assuming a good optical efficiency of 20% and a detector quantum efficiency of 2% the simulated signal for such a measurements looks like in Figure 3B.



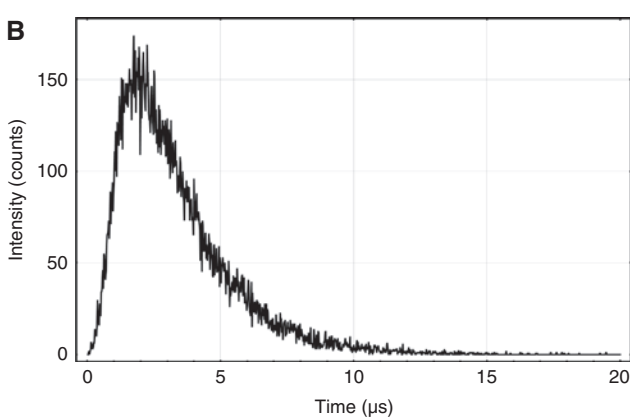


Figure 3: (A) Simulated signal obtained from a single cell by collecting all emitted photons and (B) simulated signal for one realistic measurement of a suspension of 1 million cells; seven such measurements can be conducted before the light dose limit is reached.

4 Detector technologies

Apart from PMTs other detector technologies exist for single photon detection in the NIR [4]. SPADs and SNSPDs may be of interest for a possible application in singlet oxygen luminescence detection setups.

SPADs are avalanche diodes biased above the breakdown voltage. An occurring avalanche has to be quenched by reducing the bias voltage below breakdown. Due to trapped charges these devices exhibit a high afterpulsing probability. This is reduced by keeping the bias below the breakdown voltage for a hold-off time in the order of microseconds. Two operating modes must be distinguished, gated mode and free running operation. In gated operation the bias in only applied for a short time, the gate time. Photons can only be detected during the gate time. In free-running mode the device can asynchronously detect photons, however, when a photon event occurs, the bias is reduced for a hold-off time resulting in a dead time after the detection of a photon. Gated operation reduced the dark counts, but gate times of <2 us make the gated mode unsuitable for singlet oxygen luminescence detection with kinetics in the range of microseconds.

SNSPDs consist of a superconducting nanowire that is about 100 nm wide. To maximize the detector, the wire is layed out meandering across the detector area. The wire is biased slightly below the critical current density for superconduction. When a photon is absorbed, a local hotspot disturbs the superconduction within the nanowire and the critical current is exceeded. This causes the breakdown of the superconduction, which can be detected by a voltage drop across the wire. The device recovers quickly from this condition, once the temperature is reestablished. These devices are sensitive once the temperature is reached and the bias is applied, no gating is necessary and after pulsing does not occur.

5 Discussion of NIR photon counting devices for singlet oxygen luminescence detection

The detector area, the quantum efficiency, and the dark count rate are parameters suitable for a first evaluation of a detector. An overview of these parameters for the devices considered here is given in Table 1. Regarding PMTs only the H10330-45 was considered in Table 1 since datasheet values, own investigations as well as reports in literature indicate that this PMT is optimal for time-resolved singlet oxygen luminescence detection. However, other PMTs with similar characteristics are available, such as the H12694-45 (Hamamatsu). To the knowledge of the authors, no other manufacturer apart from Hamamatsu offers PMTs for single photon counting at wavelengths around 1270 nm. NIR sensitive SPADs are offered by ID Quantique (id210, id220, and id230) and Micro Photon Devices (InGaAs SPAD - gated and InGaAs SPAD - free-running). For the overview devices for gated and free-running operation were considered. SNSPDs are offered by SCONTEL, PhotonSpot and Single Quantum. However, datasheets for SNSPDs are not readily available, therefore data was compiled here from scientific publications using SNSPDs.

The timing characteristics of all these detectors exceed the requirements, since time-resolution on the scale of several nanoseconds is sufficient to resolve singlet oxygen kinetics in most environments. Thus, this parameter is not further considered. Long term stability of these parameters may be of more concern for quantitative measurements, but is not scope of this work.

Usually for PMTs it is not reasonable to make adjustments that significantly affect quantum efficiency or dark counts since the count rate dependence on the operating voltage exhibits a plateau region and the optimal operating point is easily found. For SNSPDs, an optimal adjustment of the bias current is necessary to optimize the trade-off between quantum efficiency and dark counts. Similar to PMTs, for SNSPDs continuous operation is possible and

Table 1: Overview of selected properties of the different detector types.

	PMT (H10330-45)	SPAD ^a	SNSPD ^b
Sensitive area	Ø 1.6 mm	Ø 20-50 μm	10×10−30×30 μm²
Quantum efficiency at 1270 nm (%)	typ. 2	3-40	10-25
Dark count rate (cps) Other considerations	typ. 2500 – Thermoelectric cooling – Fixed lens in detector unit	50–2000 - Thermoelectric cooling - Gated operation or free-running mode - Trade-off between after-pulsing and dead time	1000–2000 – Closed cycle cooling –Natively fiber coupled

^aCompiled from datasheets of commercial devices by ID Quantique and Micro Photon Devices; ^bCompiled from scientific publications (SCONTEL, PhotonSpot and Single Quantum offer commercial devices).

after-pulsing is not a concern. SPADs allow the adjustment of several parameters by software: The quantum efficiency, dark count rate, hold-off time and after-pulsing probability are interdependent on each other and an optimal operating point considering all parameters must be determined by the user.

It is of interest that even though SPAD datasheets and publications on SNSDPs claim singlet oxygen luminescence detection as an application, scientific publications where SPADs or SNSPDs were used for singlet oxygen luminescence detection still seem quite rare. Just a few examples were found by the authors; all of the investigated systems had a very high luminescence intensity on the scale of singlet oxygen. The time-resolved luminescence of singlet oxygen, generated by photosensitizer-loaded nanofibers was investigated using a SPAD [5]; however, the investigated system is complex and conclusions about details of the detection system are omitted. Singlet oxygen luminescence detection using a SNSPD was reported for a photosensitizer in solution [6]. The kinetics obtained in both experiments demonstrate that, in principle, SPADs and SNSPDs can be used for singlet oxygen luminescence measurements.

However, up to now the very small size and, associated with this, the limited possible optical layouts for setups incorporating SPADs or SNSPDs restrict their use. For spectroscopic applications in biological environments multimode fibers are usually used [7]. For singlet oxygen luminescence detection the weak signal requires the fiber to collect as much light as possible and therefore is rather large. Currently it seems, that the development of fiber coupling to larger multi-mode fibers must become available for these detectors to become a realistic alternative to the PMT. SPAD datasheets already mention possible coupling to a 100-µm multimode fiber. SNSPDs have only recently been coupled to multimode fibers; in the visible wavelength range a fiber diameter was reported of up to 50 µm [8]. However, the problem of polarization sensitivity of SNSPDs must be overcome to achieve high coupling efficiencies with multimode fibers [9].

6 Conclusions

Time-resolved singlet oxygen luminescence detection relies on photon counting. To select an optimal detector for such measurements several different properties of the detection system must be assessed. Not all detector properties such as the detector area, quantum efficiency, and dark count rate can be maximized all at once. Technical details such as cooling effort, fiber coupling, and electronic timing requirements have to be considered.

At present, the authors consider the H10330-45 PMT from Hamamatsu still to be the most suitable device for time-resolved singlet oxygen luminescence detection. Other detector types show very promising quantum efficiencies, but still have sensitive detector areas that are orders-of-magnitude smaller.

References

- [1] Jiménez-Banzo A, Ragàs X, Kapusta P, Nonell S. Time-resolved methods in biophysics. 7. Photon counting vs. analog time-resolved singlet oxygen phosphorescence detection. Photochem Photobiol Sci 2008;7(9):1003-10.
- [2] Schlothauer J, Hackbarth S, Röder B. A new benchmark for timeresolved detection of singlet oxygen luminescence - revealing the evolution of lifetime in living cells with low dose illumination. Laser Phys Lett 2009;6(3):216-21.
- [3] Hackbarth S, Schlothauer J, Preuß A, Ludwig C, Röder B. Time resolved sub-cellular singlet oxygen detection - ensemble measurements versus single cell experiments. Laser Phys Lett 2012;9(6):474-80.
- [4] Buller GS, Collins RJ. Single-photon detectors for infrared wavelengths in the range 1-1.7 μm. In: Kapusta P, Wahl M, Erdmann R, editors. Advanced photon counting: applications, methods, instrumentation. Berlin and Heidelberg: Springer; 2014, p. 43-66.
- [5] Mosinger J, Lang K, Kubát P, Sýkora J, Hof M, Plístil L, Mosinger B Jr. Photofunctional polyurethane nanofabrics doped by zinc tetraphenylporphyrin and zinc phthalocyanine photosensitizers. J Fluoresc 2009;19(4):705-13.
- [6] Gemmell NR, McCarthy A, Liu B, Tanner MG, Dorenbos SD, Zwiller V, Patterson MS, Buller GS, Wilson BC, Hadfield RH. Singlet oxygen luminescence detection with a fiber-coupled superconducting nanowire single-photon detector. Opt Express 2013;21(4):5005-13.
- [7] Utzinger U, Richards-Kortum RR. Fiber optic probes for biomedical optical spectroscopy. J Biomed Opt 2003;8(1):121-47.
- [8] Liu D, Miki S, Yamashita T, You L, Wang Z, Terai H. Multimode fiber-coupled superconducting nanowire single-photon detector with 70% system efficiency at visible wavelength. Opt Express 2014;22(18):21167-74.
- [9] Dauler EA, Grein ME, Kerman AJ, Marsili F, Miki S, Nam SW, Shaw MD, Terai H, Verma BB, Yamashita T. Review of superconducting nanowire single-photon detector system design options and demonstrated performance. Opt Eng 2014;53(8):081907.

[1.04] Two-dimensional time-resolved detection of singlet oxygen luminescence

Beate Röder*, Jan Caspar Schlothauer and Michael Pfitzner

Humboldt-Universität zu Berlin, Department of Physics, Photobiophysics Group, Newtonstraße 15, 12489 Berlin, Germany *Corresponding author: Prof. Dr. Beate Röder, roeder@physik.hu-berlin.de

Abstract: The use of imaging techniques has given a boost to the gain in knowledge about biological systems. This talk discusses the current state of time-resolved singlet oxygen luminescence detection as an especially important technique, since it allows the discrimination of singlet oxygen and other luminescence sources and the investigation of singlet oxygen interaction with its surroundings. The technical approaches of spatially resolved detection (scanning in contrast to wide-field imaging) are evaluated. Investigations on the macroscopic scale of tissue are covered, including their advantages and limitations.

Keywords: singlet oxygen luminescence; time-resolved luminescence spectroscopy; imaging; in vivo singlet oxygen detection.

1 Introduction

The use of imaging techniques has given a boost to the gain in knowledge about biological systems. Photodynamic therapy (PDT) imaging is in general used in applications ranging from research to clinical use [1] focusing on imaging of the photosensitizer (PS) fluorescence, which correlates with the localization of the PS. However, imaging of the main mediator of PDT, singlet oxygen, is of great interest as this could help to understand the local efficiency of photodynamic action. In future it might help to optimize therapeutic relevant parameters, such as the light dose [1, 2]. The possibility of direct imaging of singlet oxygen under PDT relevant conditions would be a leap in clinical methodology. It is a well-known fact that direct detection of singlet oxygen is at its most promising when detecting its weak luminescence at 1270 nm [3]. However, signal intensities are quite low due to the very low quantum yield of luminescent deactivation of singlet oxygen [4]. Only a few research groups worldwide go beyond measurements in solution or suspension and investigate singlet oxygen luminescence in a spatially resolved mode.

2 Macroscopic time-resolved singlet oxygen luminescence detection

Macroscopic time-resolved luminescence detection would enable simultaneous monitoring of singlet oxygen generation and its decay in malignant tissue giving deeper insights in the current therapy progress and facilitating individual optimization of the treatment parameters. Up to now, macroscopic time-resolved singlet oxygen luminescence monitoring has been employed for the investigation of several systems from ex-vivo tissue models up to in-vivo models such as tumor bearing mice or rats. Work performed by Schlothauer et al. [5, 6] on topically photosensitized ex-vivo pig ear skin shows singlet oxygen kinetics with a sufficiently high signal-to-noise ratio to derive signal rise and decay times. Clear changes in the rise and decay time were observed during illumination of the sample, whilst using PDT-like excitation conditions. The signal rise and decay times of a bi-exponential fit of the data obtained from pig ear skin are of the order of less than about 1 µs for the rise time and about 10-20 µs for the decay time [7]. These times are similar to reports by Baier et al. [8] and Nonell et al. [9] for singlet oxygen kinetics obtained by direct excitation of pig ear samples and Jarvi et al. [10] for experiments on rat skin.

Based on measurements made on the ex-vivo pig ear, the question remains as to whether in-vivo application is possible on human skin. Using the fiber setup, a measurement was conducted on *in-vivo* human skin with topically applied pheophorbide-a. The investigations on model systems ex vivo as well as in vivo clearly demonstrate that macroscopic scanning of time-resolved singlet oxygen luminescence is feasible. This method has the great advantage of gathering the kinetics and information about the interaction of singlet oxygen with the micro-environment. This allows a deeper insight into the photophysical processes within the tissue. Future evaluation of this method must show the comparability of skin samples and tissue of other organs. Currently, requirement of having to raster scan samples is still a serious drawback of the method because of the long time needed. Using high resolution scanning with a typical integration time of some seconds per pixel and a pixel size in the order of 100 µm, a scan of a macroscopic area would easily take hours. As a result, changes in the sample - light-induced as well as others - presents a problem for the investigation of biological samples.

To reduce the light dose and measurement time, improvement of the detection systems is highly desirable. The photomultiplier tube (type H10330-45; Hamamatsu), which is considered most suitable for time-resolved singlet oxygen luminescence detection [3], has a datasheet value for the quantum efficiency of typically 2%. Detectors with higher quantum efficiencies are available. For example, superconducting nanowire single photon detectors have shown promising quantum efficiencies of more than 20%, [11], and single photon avalanche diodes have quantum efficiencies of up to around 40% at 1270 nm. Despite the higher quantum efficiencies, other technical properties make these devices less useful for singlet oxygen luminescence detection. Nevertheless, for use in scanning and fiber applications these devices may become suitable alternatives.

3 Conclusions

From the little literature available in the field of spatially resolved direct singlet oxygen detection, it becomes clear that measuring and in particular imaging are still extremely challenging tasks. In contrast to steady-state singlet oxygen luminescence detection, time-resolved measurements allow the exclusion of luminescence that does not originate from singlet oxygen by spectral discrimination as well as due to the different kinetics. Furthermore, the kinetics gives information about the singlet oxygen interaction with the micro-surroundings of the where it has been generated. Until now, scanning is necessary to acquire spatially and time-resolved singlet oxygen luminescence signals concurrently.

The time-resolved macroscopic scanning of *ex-vivo* pig ear shows that singlet oxygen luminescence detection under PDT-relevant experimental conditions is possible with today's detector systems. The same method can be applied to *in vivo* systems, for which similar luminescence signals are obtained. Nevertheless, scanning of samples is slow and since singlet oxygen kinetics are influenced by the measurement excitation light and duration, this particular feature must be optimized.

References

- [1] Celli JP, Spring BQ, Rizvi I, Evans CL, Samkoe KS, Verma S, Pogue BW, Hasan T. Imaging and photodynamic therapy: mechanisms, monitoring, and optimization. Chem Rev 2010;110(5):2795–838.
- [2] Kanofsky JR. Measurement of singlet-oxygen *in vivo*: progress and pitfalls. Photochem Photobiol 2011;87(1):14-7.
- [3] Jiménez-Banzo A, Ragàs X, Kapusta P, Nonell S. Time-resolved methods in biophysics. 7. Photon counting vs. analog timeresolved singlet oxygen phosphorescence detection. Photochem Photobiol Sci 2008;7(9):1003–10.
- [4] Schweitzer C, Schmidt R. Physical mechanisms of generation and deactivation of singlet oxygen. Chem Rev 2003;103(5):1685-757.
- [5] Schlothauer J, Röder B, Hackbarth S, Lademann J. In vivo detection of time-resolved singlet oxygen luminescence under PDT relevant conditions. Proc SPIE 2010;7551:755106. doi: 10.1117/12.839851.
- [6] Schlothauer JC, Hackbarth S, Jäger L, Drobniewski K, Patel H, Gorun SM, Röder B. Time-resolved singlet oxygen luminescence detection under photodynamic therapy relevant conditions: comparison of *ex vivo* application of two photosensitizer formulations. J Biomed Opt 2012;17(11):115005.
- [7] Schlothauer JC, Falckenhayn J, Perna T, Hackbarth S, Röder B. Luminescence investigation of photosensitizer distribution in skin: correlation of singlet oxygen kinetics with the microarchitecture of the epidermis. J Biomed Opt 2013;18(11):115001.
- [8] Baier J, Maisch T, Maier M, Landthaler M, Bäumler W. Direct detection of singlet oxygen generated by UVA irradiation in human cells and skin. J Invest Dermatol 2007;127(6):1498-506.
- [9] Nonell S, García-Díaz M, Viladot JL, Delgado R. Singlet molecular oxygen quenching by the antioxidant dimethylmethoxy chromanol in solution and in *ex vivo* porcine skin. Int J Cosmet Sci 2013;35(3):272–80.
- [10] Jarvi MT, Niedre MJ, Patterson MS, Wilson BC. Singlet oxygen luminescence dosimetry (SOLD) for photodynamic therapy: current status, challenges and future prospects. Photochem Photobiol 2006;82(5):1198–210.
- [11] Gemmell NR, McCarthy A, Liu B, Tanner MG, Dorenbos SD, Zwiller V, Patterson MS, Buller GS, Wilson BC, Hadfield RH. Singlet oxygen luminescence detection with a fiber-coupled superconducting nanowire single-photon detector. Opt Express 2013;21(4):5005-13.

[1.05] Recent advances in optical imaging techniques for singlet oxygen luminescence

Buhong Li^{1,*}, Lisheng Lin¹, Ying Gu² and Brian C. Wilson³

¹Key Laboratory of OptoElectronic Science and Technology for Medicine of Ministry of Education, Fujian Provincial Key Laboratory for Photonics Technology, Fujian Normal University, Fuzhou 350007, China

²Department of Laser Medicine, Chinese People's Liberation Army General Hospital, Beijing 100853, China

³Department of Medical Biophysics, University of Toronto/Ontario Cancer Institute, Toronto, Ontario M5G 2M9, Canada

*Corresponding author: Prof. Buhong Li, bhli@fjnu.edu.cn

Abstract: Singlet oxygen (${}^{1}O_{2}$) is widely believed to be the major cytotoxic reactive oxygen species generated during photodynamic therapy (PDT). In this talk, recent advances

in optical imaging techniques for 1O_2 luminescence at \sim 1270 nm will be summarized, and a newly developed novel configuration of a near-infrared sensitive camera

and adaptive optics for fast imaging of ¹O₂ luminescence in vivo will be introduced. With regard to PDT application, the future challenges for direct imaging of 10, luminescence will be discussed briefly.

Keywords: singlet oxygen luminescence; imaging; timeresolved; spatially resolved.

1 Introduction

The excited singlet state of oxygen (102), is recognized as being the major cytotoxic reactive oxygen species (ROS) generated during photodynamic therapy (PDT) for a number of photosensitizers used clinically (porphyrin- and chlorin-based) and for some new components under investigation [1, 2]. 10, is generated in a type-II reaction in which the excited singlet state of the photosensitizer produced upon photon absorption by the ground-state photosensitizer molecule undergoes intersystem crossing to a relative long-living triplet state. This state can then exchange energy with the triplet ground state of molecular oxygen. ¹O₂ can have radiation decay, emitting near-infrared (NIR) luminescence at around 1270 nm. This phenomenon has driven intense research to develop novel sensitive techniques for time- and spatial- resolved measurement of ¹O₂ luminescence at 1270 nm. In this talk, recent advances in optical imaging techniques for 10, luminescence will be summarized, and a newly developed novel configuration of a NIR sensitive camera and adaptive optics will be introduced for fast imaging of ¹O₂ luminescence. With regard to PDT application, the future challenges will be briefly discussed concerning direct imaging of ¹O₂ luminescence.

2 Imaging systems for ¹O₂ luminescence

As summarized in Table 1, there were two patterns developed for direct imaging of ¹O₂ luminescence.

One pattern is based on the utilization of NIR photomultiplier tube (PMT) in combination with scanningbased methods, and the advantage of these measurements is that the ¹O₂ luminescence could be simultaneously validated by time-resolved measurement, which is beneficial in processing the raw data to obtain ¹O₂ luminescence images. However, motion artifacts during the long scan time are still a serious concern, while the treatment itself may cause changes to the 10, kinetics that are then missed or incorrectly recorded [3-6]. The second approach is based on the use of a NIR camera with a set of band-pass filters to discriminate the 10, luminescence from background fluorescence and phosphorescence [7–9]. However, the long acquisition time of 40–50 s per image and the low signal-to-noise ratio in physiological environments are likely to preclude this method being practical for PDT dosimetry.

Most recently, we have developed a novel configuration of a thermoelectrically-cooled NIR-sensitive InGaAs camera for imaging photodynamically generated 10, luminescence, using custom-designed NIR optics to collect the luminescence [10]. The validation of ¹O₂ luminescence in the acquired images was performed using the model photosensitizer rose bengal (RB) in aqueous solution. In this study, the well-controlled dorsal skinfold window chamber model in mice was used in vivo to image the ¹O₂ luminescence in blood vessels immediately after the mice had been intravenously injected with RB. Images of ¹O₂ luminescence in blood vessels in vivo were obtained for the first time.

3 Future challenges

¹O₂ is generally considered to have an extremely short lifetime (probablility <<1 μs) in cells and tissues due to its high reactivity with biomolecules, so that the luminescence signal is very weak (~1:108 probability). Additionally, 1270 nm is not in a favorable range for efficient photodetection using standard

Table 1: Imaging systems for ¹O₂ luminescence.

NIR detector	Object	Scanning	Resolution (μm)	Integrated time (s)	References
InGaAs Linear array detector (Princeton Instrument)	Cells with D ₂ O	Yes	2.5	30	[3]
PMT (R5509, Hamamatsu)	Tumor model	Yes	1000	400	[4]
PMT (H10330-45, Hamamatsu)	Skin model	Yes	200	4000	[5]
PMT (R5509, Hamamatsu)	C ₆₀ powder	Yes	17.96	589.824	[6]
Camera (XEVA, Xenics)	Mouse skin	No	39.4	1	[7]
Camera (MOSIR 950, Intevac)	Tumor Model	No	46.0	40-50	[8]
Camera (NIRvana:640, Princeton Instruments)	Cells with D ₂ O	No	1.4	5	[9]
Camera (XEVA, Xenics)	Dorsal skin window chamber	No	30	1	[10]

devices. In order to establish a robust 10, luminescencebased PDT dosimetry, the NIR-PMT or a camera with extraordinarily high sensitivity is highly desired. Furthermore, the validation of ¹O₂ luminescence from the obtained NIR luminescence image is still a challenge, which hopefully can be directly validated by time-resolved measurement. For this, the combination of time- and spatial-resolved measurements with NIR-PMT and camera respectively, is currently the major aim of our study.

Acknowledgments: This work was supported by the National Natural Science Foundation of China (Grant numbers: '61275216' and '61520106015'), the Fujian Provincial Natural Science Foundation (Grant number: '2014J07008') and the Joint Funds of Fujian Provincial Health and Education Research (Grant number: 'WJK-FJ-30').

References

- [1] Li B, Lin H, Chen D, Wilson BC, Gu Y. Singlet oxygen detection during photosensitization. J Innov Opt Heal Sci 2013;6(1):1330002.
- [2] Wilson BC, Patterson MS, Li B, Jarvi MT, Correlation of in vivo tumor response and singlet oxygen luminescence detection in mTHPC-mediated photodynamic therapy. J Innov Opt Health Sci 2015;8(1):1540006.

- [3] Andersen LM, Gao Z, Ogilby PR, Poulsen L, Zebger I. A singlet oxygen image with 2.5 µm resolution. J Phys Chem A 2002:106(37):8488-90.
- [4] Niedre MJ, Patterson MS, Giles A, Wilson BC. Imaging of photodynamically generated singlet oxygen luminescence in vivo. Photochem Photobiol 2005;81(4):941-3.
- [5] Schlothauer JC, Falckenhayn J, Perna T, Hackbarth S, Röder B. Luminescence investigation of photosensitizer distribution in skin: correlation of singlet oxygen kinetics with the microarchitecture of the epidermis. J Biomed Opt 2013;18(11):115001.
- [6] Tian W, Deng L, Jin S, Yang H, Cui R, Zhang Q, Shi W, Zhang C, Yuan X, Sha G. Singlet oxygen phosphorescence lifetime imaging based on a fluorescence lifetime imaging microscope. J Phys Chem A 2015;119(14):3393-9.
- [7] Hu B, Zeng N, Liu Z, Ji Y, Xie W, Peng Q, Zhou Y, He Y, Ma H. Two-dimensional singlet oxygen imaging with its near-infrared luminescence during photosensitization. J Biomed Opt 2011;16(1):016003.
- [8] Lee S, Isabelle ME, Gabally-Kinney KL, Pogue BW, Davis SJ. Dual-channel imaging system for singlet oxygen and photosensitizer for PDT. Biomed Opt Express 2011;2(5):1233-42.
- [9] Scholz M, Dědic R, Valenta J, Breitenbach T, Hála J. Real-time luminescence microspectroscopy monitoring of singlet oxygen in individual cells. Photochem Photobiol Sci 2014;13(8):1203-12.
- [10] Lin L, Lin H, Chen D, Xie S, Gu Y, Wilson BC, Li B. Imaging of singlet oxygen luminescence in blood vessels. SPIE Newsroom 2014. doi: 10.1117/2.1201405.005511. http://spie.org/documents/Newsroom/Imported/005511/005511_10.pdf [Accessed on July 10, 2015].

[1.06] Properties and usage of water after quenching of singlet oxygen

Michael Köhl*

Fraunhofer Institut für Solare Energiesysteme, Heidenhofstr. 2, 79110 Freiburg, Germany *Corresponding author: Dr.-Ing. Michael Köhl, michael.koehl@ise.fraunhofer.de

Abstract: Water is a well-known quencher for singlet molecular oxygen. The dissipation of the energy from singlet molecular oxygen was found to cause physical changes of the water that could be detected by infraredspectroscopic investigation of the water absorption bands and the behavior during the liquid/solid phase transitions. Water treated with singlet oxygen accelerated the activity of the enzyme beta-glucosidase and accelerated the growth of corn plants.

Keywords: singlet oxygen; water; quenching; infrared spectroscopy; enzyme activity.

1 Introduction

The energy for the excitation of singlet oxygen could be provided by the energy transfer between a photosensitizer (PS) and an oxygen molecule. The lifetime of the singlet oxygen state, the so-called ${}^{\scriptscriptstyle 1}\!\Delta_{\scriptscriptstyle g},$ depends on the surrounding medium. The oxygen molecule in this excited singlet state relaxes by emitting a photon at a wavelength of 1268 nm (7886 cm⁻¹). The typical lifetime of this process is of the order of milliseconds. Radiationless deactivation (energy transfer) is induced if a so-called quencher is present. Water is a well-known quencher for singlet oxygen and reduces the lifetime of singlet oxygen to a few microseconds [1, 2]. That is especially the case when using singlet oxygen for inhalation therapies. However, healing effects have been reported.

2 Singlet oxygen and water

What could be of interest in combining singlet oxygen and water? The water will simply deactivate the singlet oxygen, as may be seen from the diminished near-infrared (NIR) luminescence of singlet-molecular oxygen. But what happens with the water? Will the energy be dissipated by the water, resulting in a slight temperature

increase? The energy content of 0.98 eV in ¹O₂ is above the vibration-stretching modes of water. These modes can be seen in the water absorption spectrum in the NIR and mid-infrared. Infrared (IR) spectroscopic investigations of liquid water and air saturated with water vapor and water clusters, treated with singlet oxygen, showed changes in the absorption bands when the water quenched the singlet oxygen. This would not be such a surprise, if these changes were not also detected minutes, hours and even days after the water had quenched the singlet oxygen, far beyond the time-scale for a thermal relaxation.

3 Investigation of the interaction between singlet oxygen and water

Singlet oxygen was generated in the gas phase. The water-insoluble PS (metal-phthalocyanine) was deposited on various substrate materials by evaporation in a high vacuum. The PS was illuminated and excited by means of a suitable broadband light source. A gas containing oxygen was blown across the surface of the PS and fed into de-ionized water for deactivation.

4 NIR spectra of singlet oxygen treated air

The spectroscopic analysis was performed either in the gas phase by feeding the outlet air, which was humidified by the water used for quenching the singlet oxygen, into integrating spheres attached to a Fourier-transform spectrometer: A PTFE-coated sphere fitted with an InGaAs detector for the shorter wavelength range (1.0-2.4 µm or 10,000-4300 cm⁻¹) and a diffuse-gold coated sphere with a Mercury-Cadmium-Telluride (MCT) detector attached to the sphere wall for the IR spectral range (1.7–17 µm or 6000-600 cm⁻¹).

The NIR absorption bands caused by the water molecules of humidified air treated with singlet molecular oxygen show small, but reproducible changes compared to non-treated humidified air. The rotational fine structure of the water bands had disappeared in the ratio of the spectra measured after quenching singlet oxygen to the reference, whereas a somewhat weaker shift in the vibrational modes was observed (Figure 1) which could still be seen for a long time after the treatment. One explanation could be that the changes only occur in water clusters formed by hydrogen bonds, where the water molecules are not able to rotate.

Analysis of the time dependence of the spectral changes at 5600 cm⁻¹ yielded some interesting features (Figure 2). A saturation level was reached after treating the water for approximately 2 h, presumably depending on the singlet oxygen production rate and the amount of treated water. An exponential decrease of the changes

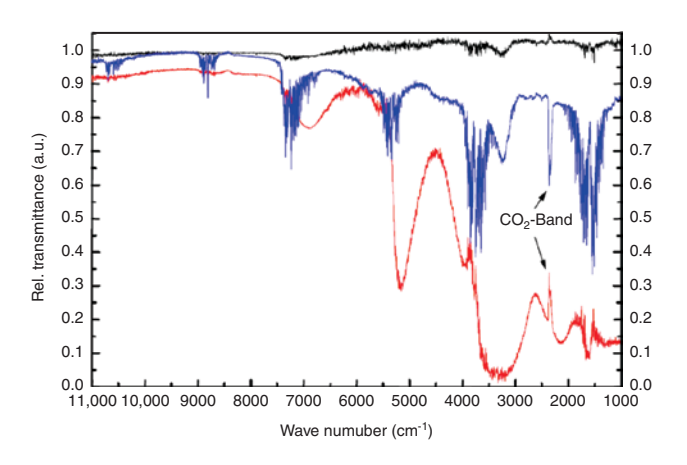


Figure 1: Transmittance spectra of humidified air before (black) and after quenching singlet oxygen (red) in relation to the reference spectrum (blue).

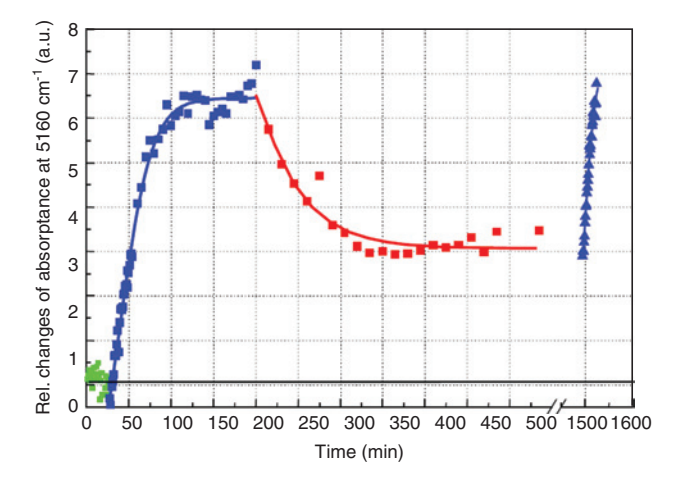


Figure 2: Relative changes of the water absorptance at 5160 cm⁻¹ while purging with air without singlet oxygen (green), while quenching singlet oxygen (blue squares), after stopping the quenching (red), and after restarting quenching (blue triangles, note the change in time scale).

after the end of the treatment was observed. This process reached a constant level after approximately 2.5 h. The absorption changes could be reproduced by restarting the singlet oxygen impact.

5 Effect of water treated with singlet oxygen on metabolic processes

Enzymes are usually active in water. Their chemical activity to change molecules involves hydrogen bonds. Therefore the influence of water treated with singlet oxygen was investigated on the enzyme activity of betaglucosidase. The exogenous beta-glucosidase enzyme is used for the decomposition of cellulose into glucose. The

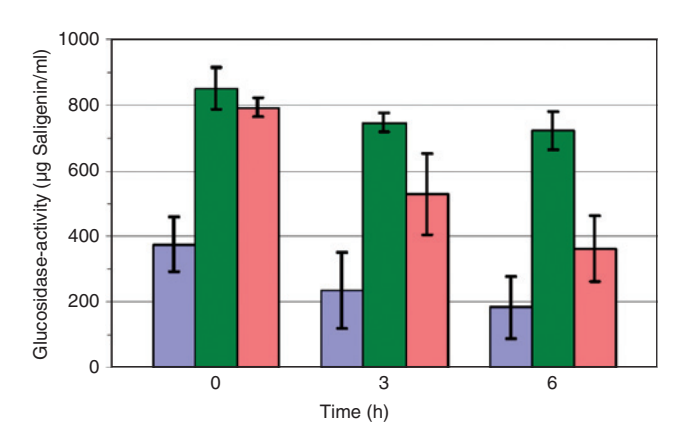


Figure 3: Activity of 10 mg/l beta-glucosidase in water after addition of 5 g/l salicin. The data are averages taken from eight experiments. Untreated de-ionized water (blue bars), de-ionized water freshly treated with singlet oxygen (green bars) and de-ionized water, which was treated with singlet oxygen 3 days before the enzyme test started (red bars).

enzyme concentration was 10 mg/l in all experiments. Salicine (5 g/l) was added as the carbohydrate substrate instead of cellulose in order to keep the enzymes active. The saligenine concentration was used as a measure of the enzyme activity. Samples were taken and analyzed immediately after adding salicine as well as 3 h and 6 h later. All experiments were repeated a total of eight times.

Beta-glucosidase showed a drastically increased enzymatic activity in treated water (Figure 3). Soil suspensions reached different equilibrium levels for the pH value and the redox potential, when the water had been treated with singlet oxygen. Irrigation with activated water increased above ground dry-matter production of corn plants by 20%. The mechanisms of the improvements of these biochemical and metabolic processes are unknown and still require further investigation.

6 Conclusions

After the quenching of singlet molecular oxygen, unexpected changes were found in some of the physical properties of water. IR spectroscopy demonstrated these changes and showed that they were not caused by temperature effects or the formation of hydrogen peroxides.

Differences in the thermal behavior during and after liquid/solid phase transitions also indicated structural differences. The lifetime of the observed changes was found to be of the order of hours and days. Thermal treatment (microwave) reversed the observed changes. The nature of these changes in the water is still unclear. Changes in the structure or size of water clusters might be assumed, but this hypothesis needs to be validated.

We are convinced that we have found a new method for water treatment which could facilitate fruitful applications in various fields such as biotechnology, agriculture and food processing. We also recognize that a much better understanding of the properties of water is still needed.

Acknowledgments: The author thanks F. Brucker, K. Forcht and T. Kaltenbach (Fraunhofer ISE, Germany) for setting up the experiments, V. Lieske for his initiatives, Prof. Neue and Dr. Kathrin Heinrich (Umweltforschungszentrum Leipzig-Halle GmbH) for performing the experiments with enzymes and plants and Prof. Beate Röder for her encouraging support.

References

- [1] Foote CS. Mechanisms of photosensitized oxidation. There are several different types of photosensitized oxidation which may be important in biological systems. Science 1968;162(3857):963–70.
- [2] Wilkinson F, Helman WP, Ross AB. Quantum yields for the photosensitized formation of the lowest electronically excited singlet-state of molecular oxygen in solution. J Phys Chem Ref Data 1993;22:113–262.

[1.07] Influence of pulse repetition rate on singlet oxygen production during photosensitization using a pulsed laser

Defu Chen¹, Ying Wang², Buhong Li³ and Ying Gu^{2,*}

School of Information and Electronics, Beijing Institute of Technology, Beijing 100081, China

²Department of Laser Medicine, Chinese People's Liberation Army General Hospital, Beijing 100853, China

³Key Laboratory of OptoElectronic Science and Technology for Medicine of Ministry of Education, Fujian Provincial Key Laboratory for Photonics Technology, Fujian Normal University, Fujian 350007, China

*Corresponding author: Prof. Ying Gu, guyinglaser@sina.com

Abstract: Pulsed lasers have been widely applied in photodynamic therapy (PDT). However, the effects of pulsed laser parameters on PDT efficacy have not been fully understood. Singlet oxygen (¹O₂) is known to be a major

cytotoxic agent in PDT. In this study, the influence of pulse repetition rate on $^1\mathrm{O}_2$ production was evaluated by detecting $^1\mathrm{O}_2$ luminescence at 1270 nm. We studied the generation of $^1\mathrm{O}_2$ using a pulsed laser by changing its repetition

rate (1–90 kHz). The results showed that there was no significant difference in ¹O₂ production among different repetition rates with the same irradiation power of 20 mW.

Keywords: photodynamic therapy; singlet oxygen; luminescence; pulsed laser; pulse repetition rate.

1 Introduction

Photodynamic therapy (PDT) is an effective therapeutic modality that uses light source with a specific wavelength to activate a photosensitizer (PS) for the treatment of both oncological and non-oncological diseases. Upon absorption of the light, the PS initiates photochemical reactions that lead to generation of reactive oxygen species (ROS), particularly singlet oxygen (10), which may cause targeted cells damage or death. Therefore, the production of ¹O₂ during PDT is a direct indicator for PDT dosimetry.

In clinical practice, different types of pulsed light sources have been widely used as the excitation light sources in PDT. Several investigations have reported that the efficacy of PDT using a pulsed laser may vary with the pulsed laser parameters, for instance, repetition rate, fluence rate, and so on [1, 2]. However, the effects of pulsed laser parameters on PDT efficacy have not been fully understood. In this study, we demonstrate the influence of laser pulse repetition rate on the ¹O₂ production during photosensitization by directly detecting its luminescence at 1270 nm.

2 Materials and methods

We studied the production of ¹O₂ that was generated from photosensitization of rose bengal (RB) using a pulsed laser by changing its repetition rate from 1 to 90 kHz. RB-mediated ¹O₂ luminescence were detected at different repetition rates with the same irradiation power of 20 mW using time- and spectra-resolved ¹O₂ luminescence detection system.

RB was purchased from Sigma-Aldrich (St. Louis, MO, USA) and was used as a model PS in the solutionbased measurements for generation of ¹O₂ in the following studies. A 100 µM stock solution of RB was made up in initially air-statured phosphate buffered saline (PBS) at pH 7.5, and 1 µM RB were prepared from this stock immediately before use. Preparation was done in near-dark conditions to prevent photosensitized degradation of RB.

The time- and spectra-resolved ¹O₂ luminescence was measured by a custom-developed near-infrared (NIR) luminescence detection system, which has been described in detail previously [3]. Briefly, a 523 nm pulsed laser (QG-523-500; Crystalaser Inc., Reno, NV, USA) was used to excite the PS. The laser light passed through a splitter, an optical attenuator and was directed into the measured

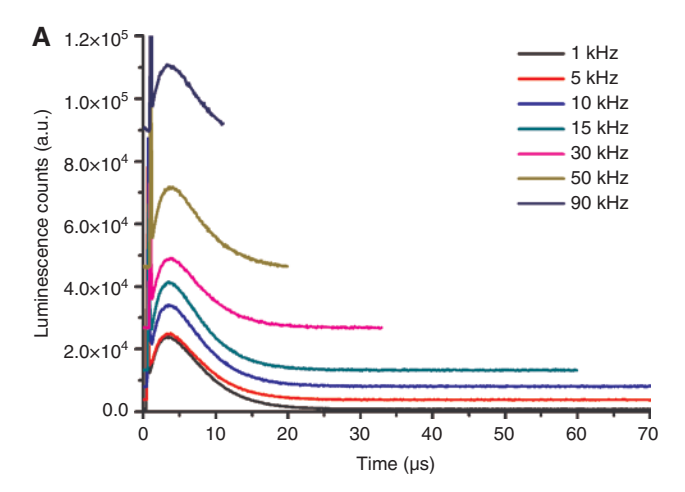
2.5 ml RB solution placed in a standard 10 mm pathlength quartz cuvette. The average output power can be adjusted by using the optical attenuator. The exciting luminescence was collected at right angle to the excitation beam through a 1000 nm long-pass filter, the collection optics and a series of three NIR narrow-band filters centered at 1270, 1230, and 1310 nm that were placed in front of the NIR-PMT (H10330-45; Hamamatsu Corp.) at an operating voltage of -900 V. The NIR-PMT output signals were finally recorded by the fast photon counter (MSA-300; Becker & Hickl GmbH, Berlin, Germany). In order to differentiate ¹O₂ emission at 1270 nm from the PS fluorescence (and/ or phosphorescence) and other background signals, the exciting luminescence for each sample was detected by using each of the 1230, 1270 and 1310 nm filters in turn. The 1230 and 1310 nm filters, which contain only the PS fluorescence (and/or phosphorescence) and other background signals, were used to determine the luminescence background in the 1270 nm region. Therefore, the ¹O₂ luminescence counts at 1270 nm for RB in PBS were corrected for background by subtracting the average luminescence counts of the 1230 and 1310 nm.

In order to evaluate the influence of pulse repetition rate on the production of ¹O₂, 1 μM RB in initially air-statured PBS was freshly prepared for each ¹O₂ luminescence measurement with the selected pulse repetition rate of 1, 5, 10, 15, 30, 50 and 90 kHz, respectively. Under each pulse repetition rate, the laser power and irradiation time were set to 20 mW and 30 s, respectively. The obtained timeresolved 10, luminescence curve and the corresponding integrated ¹O₂ luminescence counts with background subtraction in PBS solution were comparatively studied.

3 Results

Figure 1A shows the representative time-resolved NIR luminescence curves at the filter of 1270 nm for different repetition rates, respectively. In order to keep the same laser irradiation time of 30 s, the time-resolved luminescence counts were summed over a different number of laser pulses for different repetition rates (30,000-2,700,000 laser pulses for 1-90 kHz). As a result, the background counts increased with the repetition rate. The integrated ¹O₂ luminescence counts were calculated by counting the total luminescence counts following the laser pulse and subtracting background contributions. Figure 1B shows the comparison of the integrated 10, luminescence counts at different repetition rates. No significant difference in ¹O₂ production was observed among the different repetition rates with the same irradiation power of 20 mW (p>0.05).

Furthermore, the influence of laser power on the ¹O₂ production was also assessed at the repetition rate of



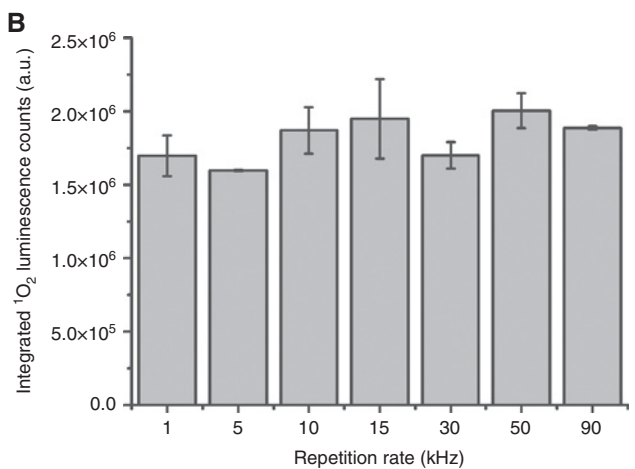


Figure 1: (A) The time-resolved NIR luminescence curves at the filter of 1270 nm, and (B) the integrated $^{1}O_{2}$ luminescence counts as a function of the pulse repetition rate.

15 kHz with a fixed laser irradiation time of 30 s. The laser power was set to 20, 50, 100, 150 and 200 mW, respectively. As shown in Figure 2, the integrated $^{1}O_{2}$ luminescence counts almost linearly increased with increasing laser power, but reached a plateau at above the laser power of 150 mW. We estimated the peak fluence rate with laser power of 150 mW, repetition rate of 15 kHz and pulse width of 29.1 ns to be about 4.4×10^{4} W/cm² in the present study.

In clinical practice, the PDT efficacy may be influenced by the penetration of light in tissue, distribution of PS, and so on. In this study, the experiments were performed in the solution of RB. Therefore, we do not have to take into account factors such as light penetration depth; this allowing us to focus on discussion the influence of the pulse repetition rate on the production of $^{1}O_{2}$, which is the major cytotoxic agent in PDT. In a previous theoretical analysis [2], the authors concluded that the effectiveness of pulsed excitation in PDT drop significantly when the peak fluence rate was above a threshold, which was probably

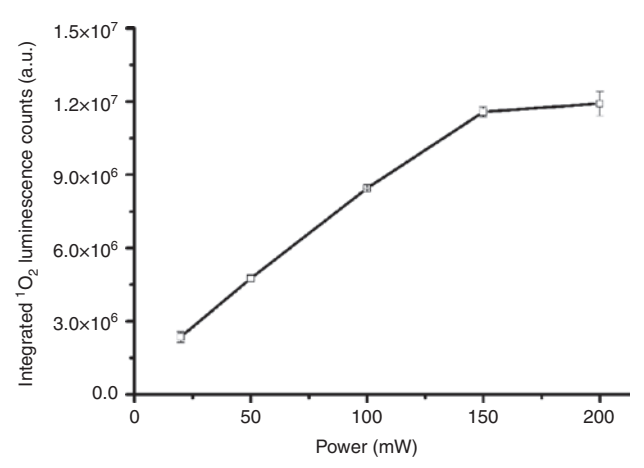


Figure 2: The integrated ${}^{1}O_{2}$ luminescence counts at the repetition rate of 15 kHz as a function of the laser power.

due to the saturation of the PS absorption. Furthermore, the threshold may vary with the laser pulse parameters, for instance, repetition rate, pulse width, and so on [2]. In this study, the peak fluence rate is inversely proportional to the pulse repetition rate, while the laser power and irradiation time were kept constant. The $^1\mathrm{O}_2$ production was almost identical among different pulse repetition rates, and the peak fluence rate for each repetition rate was below the threshold.

4 Conclusion

In conclusion, we investigated the influence of pulse repetition rate on the $^{1}O_{2}$ generation from the photosensitization of RB by using a $^{1}O_{2}$ luminescence detection system. The obtained results indicate that there was no significant difference in $^{1}O_{2}$ production among different repetition rates with the same irradiation power of 20 mW.

Acknowledgments: This study was supported by the National Natural Science Foundation of China (Grant numbers: '61108078', '61450005', '81171633' and '61036014'), and the Industry Research Special Funds for Public Welfare Projects (Grant number: '2015SQ00057').

References

- [1] Seguchi K, Kawauchi S, Morimoto Y, Arai T, Asanuma H, Hayakawa M, Kikuchi M. Critical parameters in the cytotoxicity of photodynamic therapy using a pulsed laser. Lasers Med Sci 2002;17(4):265–71.
- [2] Sterenborg HJ, van Gemert MJ. Photodynamic therapy with pulsed light sources: a theoretical analysis. Phys Med Biol 1996;41(5):835–49.
- [3] Lin H, Chen D, Wang M, Lin J, Li B, Xie S. Influence of pulse-height discrimination threshold for photon counting on the accuracy of singlet oxygen luminescence measurement. J Opt 2011;13(12):125301.

Session 2: Photosensitizers and targeting carrier systems (I)

[2.01] Carrier systems for the photodynamic therapy of tumors

Norbert Jux*, Miriam Biedermann, Kathrin Eder, Matthias Helmreich, Helen Hoelzel and Astrid Hopf Friedrich-Alexander-Universität Erlangen-Nürnberg, Lehrstuhl für Organische Chemie II, Henkestraße 42, 91054 Erlangen, Germany

*Corresponding author: Prof. Dr. Norbert Jux, norbert.jux@fau.de

Abstract: In this contribution we will discuss the selectivity challenge in the photodynamic therapy of tumors, various approaches to increase selectivity and present some of our results with regard to this issue.

Keywords: PDT; active targeting; passive targeting; enhanced permeation and retention effect (EPR).

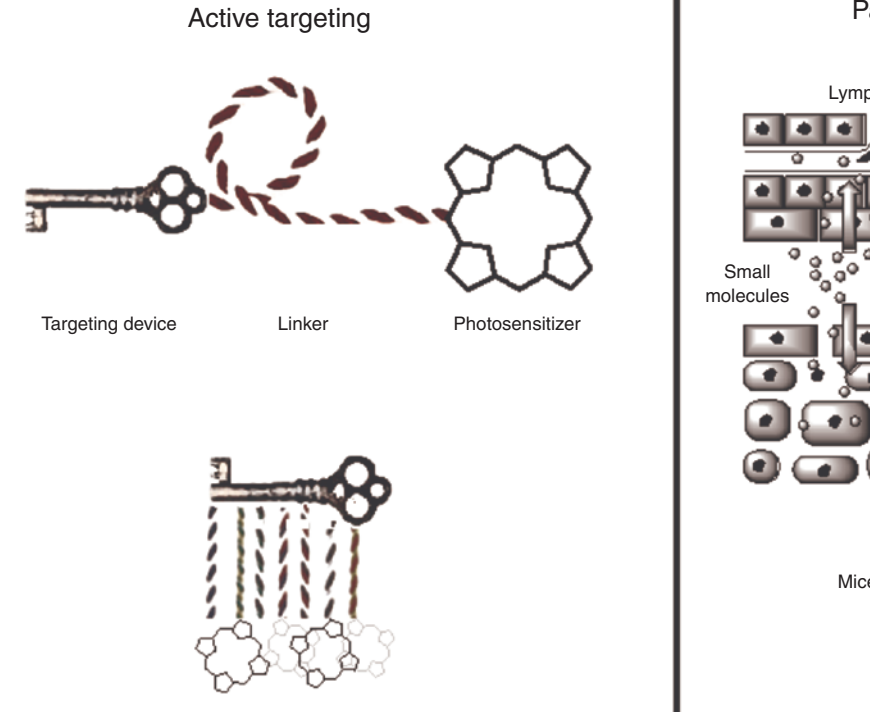
1 Introduction

The selective enrichment of photosensitizers in tumor tissue with respect to healthy tissue is still a major issue in photodynamic therapy (PDT), as it is with many other cancer therapies. Ever since the first coherent studies using various sensitizers, the selectivity challenge has been recognized and addressed by several different approaches. Generally, two major solutions have been

proposed: (1) active targeting via tumor-specific recognition units (targeting devices) such as antibodies, peptides or fragments thereof, and (2) passive targeting which essentially takes advantage of the enhanced permeation and retention (EPR) effect (see Figure 1) [1].

In this brief overview, the term "carrier system" is used for all combinations of targeting devices, linkers and photosensitizer(s). Thus, an antibody-sensitizer conjugate with its active targeting mode as well as a nanoparticlebased sensitizer complex with its passive targeting mode are both carrier systems.

Active targeting generally implies that the attachment of the sensitizer does not detrimentally affect the activity of the targeting device towards the tumor. Clearly, if the sensitizer(s) dominate(s) an active-targeting carrier system, chances are high that the selectivity will not be



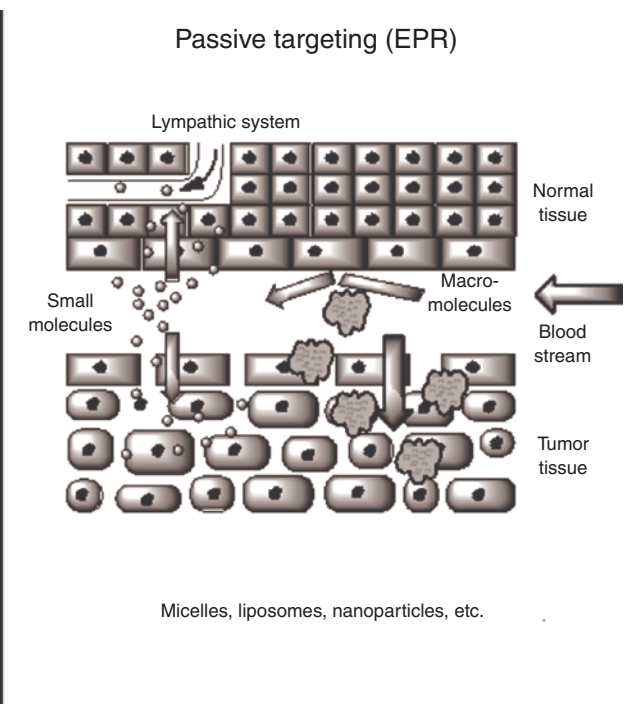


Figure 1: Schematic representation of active targeting (left). Difference in small and large (>40 kDa) molecule uptake – passive targeting (right). EPR, enhanced permeation and retention.

high. As a consequence, changes in the recognition unit, either by covalent bonds, or by electrostatic or hydrophobic interactions, should be avoided. But, in terms of efficiency, it is desirable to use as high a ratio of sensitizer to recognition unit as possible.

2 Solution approach

Within the last 30-40 years, many attempts have been made to generate active-targeting carriers that utilize various recognition units; only those with antibodies will be mentioned here briefly. As linkers, polymers such as polyvinyl alcohol, γ-polyglutamic acid, or modified poly-L-lysine were attached to the antibodies [1]. Sensitizers were then covalently bound to these polymers, completing the carrier systems. It should be pointed out that many more studies were made but that most of them, although successful in cell experiments, apparently never led to a breakthrough in PDT. We considered a slightly different approach, i.e. not employing polymers with their multitude of conformations but rather dendrimers as multiplying motifs. In particular, fullerene seemed to be an excellent candidate as it allowed, as a dendritic core, the attachment of up to 12 substituents in a simple manner. Thus, we prepared fullerene adducts with up to 24 sensitizers – our choice was pyropheophorbide-a – as reference compounds and an antibody conjugate with 10 dye moieties (see Figure 2 for a selection of these molecules). In a proof-of-priniciple, we showed that the antibody conjugate did indeed selectively bind to cell with the respective antigene [2].

Detailed photophysical investigations with all conjugates [3, 4] showed that extensive resonance energy transfer and excitonic coupling significantly lowered singlet

oxygen quantum yields, Φ_Δ . The decrease of Φ_Δ essentially correlated with the number of sensitizers attached to the core. At this point it became clear why previous approaches were not as successful as hoped and that just putting as many sensitizers as possible on a carrier system is not a good strategy. This observation also applies to passive-targeting systems, maybe even more so as the internal energy dissipation can also include the cores, such as nanoparticles.

Fortunately, these obstacles may be overcome if the sensitizers are released from the carrier once they reach the target tissue. By separating the dyes, they will regain their full power as singlet oxygen sensitizers. For example, given the slightly acidic conditions in tumor cells, hydrolysis of ester or amide moieties is possible – although, given the size of the whole complex, enzyme-catalyzed processes may be rather slow. At the moment, we are working on carrier systems that take on the one hand advantage of the EPR effect and on the other hand, possess covalent bonds that can be cleaved by tumor-specific stimuli such as pH changes. Also, external stimuli for bond cleavage such as heat or radiation are conceivable which - similar to internal tumor mechanisms – would allow for intravenous application of the carrier systems. Clearly, the whole system must stay fully intact until it reaches the target tissue.

3 Conclusion

In summary, the accumulated knowledge of the work done on carrier systems, the deeper understanding of the EPR mechanism, the development of photophysical characterization and chemical synthetic techniques in recent years now demand intelligent carrier systems to be further developed. High selectivity, high efficiency, and

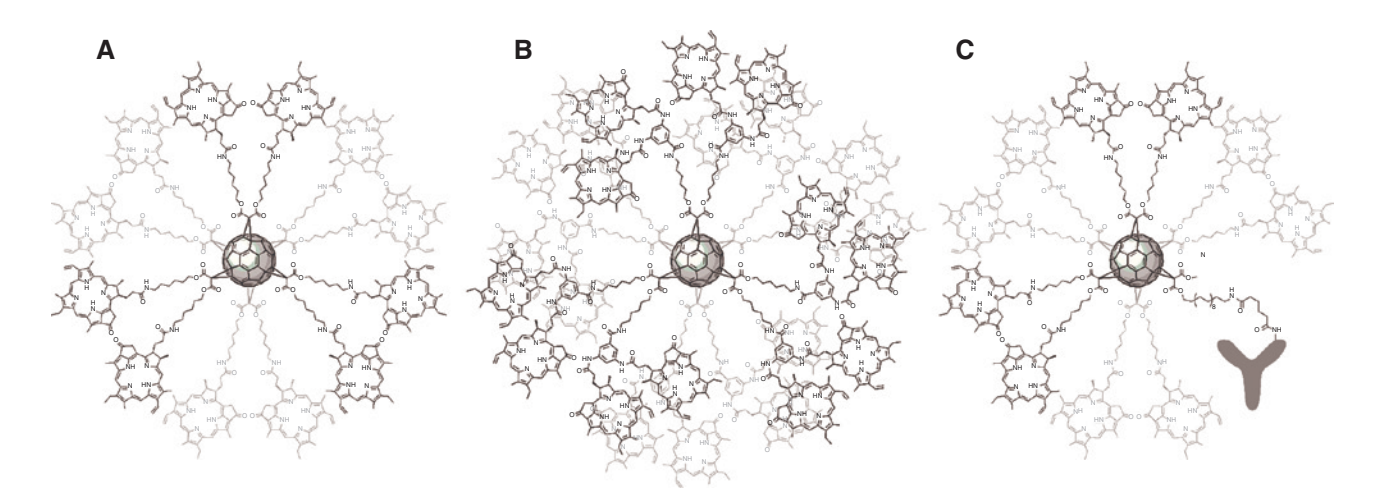


Figure 2: (A) C_{60} -conjugates with 12 pyropheophorbide-a moieties [3], (B) conjugate with 24 dyes [4] and (C) schematic representation of a C_{60} -pyropheophorbide-a rituximab® carrier system [2].

high activity versus tumors in PDT are the milestones that need to be achieved.

References

- [1] Jux N, Röder B. Targeting strategies for tetrapyrrole-based photodynamic therapy of tumors. In: Kadish KM, Smith KM, Guilard R, editors. Handbook of porphyrin science. With Applications to Chemistry, Physics, Materials Science, Engineering, Biology and Medicine - Volume 4: Phototherapy, Radioimmunotherapy and Imaging. Singapore: World Scientific; 2010, p. 325-402.
- [2] Rancan F, Helmreich M, Mölich A, Ermilov EA, Jux N, Röder B, Hirsch A, Böhm F. Synthesis and in vitro testing of a pyropheo-

- phorbide-a-fullerene hexakis adduct immunoconjugate for photodynamic therapy. Bioconjug Chem 2007;18(4): 1078-86.
- [3] Helmreich M, Ermilov EA, Meyer M, Jux N, Hirsch A, Röder B. Dissipation of electronic excitation energy within a C₆₀ [6:0]-hexaadduct carrying 12 pyropheophorbide a moieties. J Am Chem Soc 2005;127(23):8376-85.
- [4] Ermilov EA, Helmreich M, Jux N, Röder B. Novel pyropheophorbide fullerene conjugates as part of modular carrier systems in PDT and as promising units in artificial photosynthesis. In: Arnold SV, editor. Chemical physics research trends -Horizons in world physics. Volume 252. New York: Nova Science Publishers; 2007, p. 215-46.

[2.02] A novel drug carrier targeting uPAR for tumor imaging and treatment

Ke Zheng¹, Rui Li², Zhuo Chen² and Mingdong Huang^{1,2,*}

¹Department of Chemistry, Fuzhou University, Fuzhou, China

²State Key Laboratory of Structural Chemistry and Danish-Chinese Centre for Proteases and Cancer, Fujian Institute of Research on the Structure of Matter, Chinese Academy of Sciences, Fuzhou, Fujian, China

*Corresponding author: Prof. Mingdong Huang, mhuang@fjirsm.ac.cn

Abstract: Cell receptor, uPAR, is widely considered as a tumor marker. We prepared a novel tumor targeting drug carrier (ATF-HSA) by fusing human serum albumin (HSA) with a uPAR inhibitory peptide (amino-terminal fragment of urokinase, ATF) and successfully loaded a photosensitizer, mono-substituted β-carboxy phthalocyanine zinc (CPZ), into ATF-HSA by a novel strategy to form a molecular complex (ATF-HSA:CPZ). ATF-HSA:CPZ was demonstrated to be an effective photosensitizer showing remarkable anti-tumor effect and, at the same time, faster liver clearance compared to other types of photosensitizers. Moreover, ATF-HSA:CPZ showed much higher (100×) fluorescence compared to a control and was demonstrated to be able to track the location of xenografted tumor.

Keywords: urokinase receptor; amino-terminal fragment of urokinase; human serum albumin; phthalocyanine zinc; tumor targeting.

1 Introduction

Urokinase-type plasminogen activator (uPA) and its receptor (uPAR) are important components of the plasminogen activation system [1] which generates active enzyme (plasmin) and leads to the degradation of fibrin clot, the extracellular proteins, and the activation of metallomatrix proteins [2].

Many studies suggest that the levels of uPA and uPAR expression are substantially higher in invasive, malignant cancer cells than in either most healthy cells or benign tumors [2–4]. High level of uPAR on cell surface can bind to circulating uPA and concentrates the uPA proteolytic activity onto pericellular space. Tumor cells hijack this uPAR/uPA system for the purpose of tumor cell migration and metastasis. Thus, uPAR is widely advocated as a surface marker for tumors, and is an important target for tumor therapy and tumor imaging [1, 2]. One peptidyl inhibitor of uPAR conjugated with a radioactive isotope is used in a clinical trial as a positive emission tomography (PET) tracer to identify tumors with aggressive phenotype [5]. Amino-terminal fragment of urokinase (ATF) is the primary receptor binding region of uPA to uPAR, and can be used as a potent inhibitor of uPAR [6].

Human serum albumin (HSA) is the most abundant plasma protein and plays many important physiological roles. HSA can bind to many endogenous and exogenous substances, e.g. fatty acids, bilirubin, heavy metal ions and many kinds of drugs [7], and has been used as a drug carrier for delivery and for improving the pharmacokinetic profile of drugs [8]. In this study, we constructed the fusion protein ATF-HSA by merging ATF together with HSA to enhance tumor targeting ability of HSA as a drug carrier.

Photodynamic therapy (PDT) is an increasingly valuable therapeutic modality for a range of tumors. In the process of photodynamic therapy, photosensitizers (PSs) are activated by light of a specific wavelength, and in the presence of tissue oxygen, singlet oxygen is produced to kill tumor cells [9]. Phthalocyanine is a second generation photosensitizer, and has unique advantages, such as near-infrared absorption at 680 nm, and allowing deeper tissue penetration compared to the first generation PSs

[9]. However, phthalocyanine-type PSs do not have tumor targeting capability, and tend to have a prolonged retention in normal tissues [10, 11].

2 Methods and results

To enhance the tumor retention of phthalocyanine and to improve its clearance rate from the body, we loaded a PS, mono-substituted β-carboxy phthalocyanine zinc (CPZ), non-covalently into ATF-HSA, forming a molecular complex ATF-HSA:CPZ. We demonstrated that only one CPZ molecule was embedded inside ATF-HSA at the fatty acid binding site 1 of HSA.

Phthalocyanine tends to form heavy aggregates in aqueous solvents, but such an aggregation of CPZ molecules was minimized in our preparation. Compared with free CPZ, CPZ in ATF-HSA:CPZ was mainly in monomeric form (UV absorption peak at 680 nm) and its fluorescence was enhanced ~100 fold compared to a water soluble phthalocyanine (ZnPc-5K) [11], which is an important property for optical imaging application. The hydrodynamic radius of ATF-HSA:CPZ was 7.5 nm close to that of HSA (6.5 nm), which is different from albumin nanoparticles (~200 nm) in previous studies [12].

The PS-loaded ATF-HSA:CPZ did indeed bind to uPAR with high potency, indicating that the loading of CPZ did not perturb the receptor binding property of ATF-HSA. In non-small cell lung carcinoma cells (H1299) and human breast cancer cells (MDA-MB-231), both with uPAR overexpression on the surface of cells, ATF-HSA:CPZ had higher cell uptake than HSA:CPZ, which demonstrated the receptor-mediated targeting effect in vitro. In addition, we carried out the tumor targeting studies in vivo using a fluorescent molecular tomography FMT 2500TM instrument (PerkinElmer, Waltham, MA, USA) which can achieve three-dimensional imaging and precise quantification on living mice. ATF-HSA:CPZ and HSA:CPZ were injected into H22 tumor-bearing Kunming mice at a dose of 80 nmol/ kg. The mice were then imaged at different time points in a noninvasive manner on the FMT instrument by the fluorescence of ATF-HSA:CPZ and HSA:CPZ. The result showed that HSA:CPZ targeted the tumor, presumably through an enhanced permeability and retention effect and/or some albumin receptor. Furthermore, ATF-HSA:CPZ had a tumor retention ~2-3 fold higher than HSA:CPZ, demonstrating the ATF-mediated tumor targeting effect. Then photodynamic anti-tumor experiments were carried out on H22 tumor-bearing Kunming mice at 80 nmol/kg injection dose and 50-J/cm² illumination (3 min once a day) for 7 days. Both ATF-HSA:CPZ-treated and HSA:CPZ-treated groups displayed a significantly reduced tumor growth

rate compared to the control. Consistent with the result of tumor targeting study, ATF-HSA:CPZ had a more potent photodynamic anti-tumor effect compared to HSA:CPZ. The tumor size of ATF-HSA:CPZ-treated group was reduced by 2-fold compared to that of the HSA:CPZ-treated group.

Our biodistribution study showed that both ATF-HSA:CPZ and HSA:CPZ were accumulated mainly in the liver and kidney but much less in other organs/tissues after injection. The results showed that both ATF-HSA:CPZ and HSA:CPZ were eliminated from ~2 μM to ~150 nM in liver and from \sim 0.5 μ M to \sim 80 nM in kidney in 7 days. They were cleared faster than other phthalocyanines. This is likely to be related to the incorporation of monomeric CPZ inside ATF-HSA or HSA.

3 Conclusion

In summary, a molecular complex, ATF-HSA:CPZ, was prepared by a novel strategy. ATF-HSA:CPZ was demonstrated to be an effective probe for tumor imaging and have remarkable anti-tumor effect. Moreover, both ATF-HSA:CPZ and HSA:CPZ had faster liver and kidney clearance.

References

- [1] Blasi F, Carmeliet P. uPAR: a versatile signalling orchestrator. Nat Rev Mol Cell Biol 2002;3(12):932-43.
- [2] Smith HW, Marshall CJ. Regulation of cell signalling by uPAR. Nat Rev Mol Cell Biol 2010;11(1):23-36.
- [3] Lester RD, Jo M, Montel V, Takimoto S, Gonias SL. uPAR induces epithelial-mesenchymal transition in hypoxic breast cancer cells. J Cell Biol 2007;178(3):425-36.
- [4] Madsen CD, Ferraris GM, Andolfo A, Cunningham O, Sidenius N. uPAR-induced cell adhesion and migration: vitronectin provides the key. J Cell Biol 2007;177(5):927-39.
- Persson M, Madsen J, Østergaard S, Jensen MM, Jørgensen JT, Juhl K, Lehmann C, Ploug M, Kjaer A. Quantitative PET of human urokinase-type plasminogen activator receptor with 64Cu-DOTA-AE105: implications for visualizing cancer invasion. J Nucl Med 2012;53(1):138-45.
- [6] Yang L, Sajja HK, Cao Z, Qian W, Bender L, Marcus AI, Lipowska M, Wood WC, Wang YA. uPAR-targeted optical imaging contrasts as theranostic agents for tumor margin detection. Theranostics 2013;4(1):106-18.
- [7] Elsadek B, Kratz F. Impact of albumin on drug delivery New applications on the horizon. J Control Release 2012;157(1): 4-28.
- [8] Kratz F. Albumin as a drug carrier: design of prodrugs, drug conjugates and nanoparticles. J Control Release 2008;132(3): 171-83.
- [9] Castano AP, Demidova TN, Hamblin MR. Mechanisms in photodynamic therapy: part one-photosensitizers, photochemistry and cellular localization. Photodiagnosis Photodyn Ther 2004;1(4):279-93.
- [10] Smirnova ZS, Oborotova NA, Makarova OA, Orlova OL, Polozkova AP, Kubasova IY, Luk'yanets EA, Meerovich GA,

- Zimakova NI, Kuz'min SG, Vorozhtsov GN, Baryshnikov AY. Efficiency and pharmacokinetics of photosense: a new liposomal photosensitizer formulation based on aluminum sulfophthalocyanine. Pharm Chem J 2005,39(7):341-4.
- [11] Chen Z, Zhou S, Chen J, Deng Y, Luo Z, Chen H, Hamblin MR, Huang M. Pentalysine beta-carbonylphthalocyanine zinc: an
- effective tumor-targeting photosensitizer for photodynamic therapy. ChemMedChem 2010;5(6):890-8.
- [12] Bae S, Ma K, Kim TH, Lee ES, Oh KT, Park ES, Lee KC, Youn YS. Doxorubicin-loaded human serum albumin nanoparticles surface-modified with TNF-related apoptosis-inducing ligand and transferrin for targeting multiple tumor types. Biomaterials 2012;33(5):1536-46.

[2.03] Upconversion nanoprobe as a theranostic agent for deep-seated photodynamic therapy

Wenkai Fang, Lijuan Liu, Aiguo Zhou and Yanchun Wei*

MOE Key Laboratory of Laser Life Science and Institute of Laser Life Science, College of Biophotonics, South China Normal University, Guangzhou 510631, China

*Corresponding author: Assoc. Prof. Yanchun Wei, weiyanchun@scnu.edu.cn

Abstract: The limited therapeutic depth and the difficult dosage determination of photodynamic therapy (PDT) restrict its clinical application to topical lesions. Novel near-infrared nanoprobes, which were constructed with upconversion nanoparticles (UCNPs) and photosensitizers (PSs), were studied as a theranostic agent for deepseated PDT. In our study, by cooperation of UCNP and PS, one part of the light energy was transferred from UCNP to PS for deep-seated PDT; another part of the energy was transformed to emit red light for imaging. The nanoprobes showed considerable potential for both deep-seated tumor treatment and therapeutic monitoring.

Keywords: tumor; photodynamic therapy; singlet oxygen; upconversion nanoprobe.

1 Introduction

Photodynamic therapy (PDT) is a cancer treatment modality involving a combination of light, photosensitizer (PS), and molecular oxygen. Upon irradiation with an appropriate light, the PS is excited and transfers its energy to the surrounding molecular oxygen to generate cytotoxic reactive oxygen species (ROS) [1]. This leads to selective and irreversible destruction of diseased tissues, without damaging adjacent healthy ones.

Despite the many advantages of PDT over current treatments (e.g. surgery, radiation therapy, and chemotherapy), PDT still has yet to gain general clinical acceptance.

The first reason is that PSs often need to be excited with a visible band light causing limited therapeutic depth which clinically restricts its treatment to topical lesions [2]. There is an "optical window" of tissue from 700 to 1100 nm, where tissue has maximum transparency to light [3]. So the therapeutic depth of PDT would be greatly improved if the excitation light lies within this window.

The delivery process of PS is another major challenge in PDT. Majority of currently available PSs are hydrophobic by nature and their intrinsic tumor specificity is less than optimal. Numerous approaches have been proposed to achieve not only stable aqueous dispersion but also site-specific delivery of therapeutic agents. Therefore, biocompatible delivery vehicles are often used.

The third reason is that the used dosage of PDT is difficult to determine. Understanding both the PDT dose and the threshold dose and giving a proper treatment are important [4]. But to determine PDT dosage for planning the PDT effect is difficult with any of the three players involved in PDT: PS, light and oxygen due to the complicated interplay among them, although the correlation of treatment response to the total light dose in PDT has shown varying success [5]. However, to optimize the biological effect, accurate dosimetry needs to be implemented.

2 Materials and methods

To overcome these limitations, upconversion nanoparticles were used in our study due to its intrinsic advantages. We explored the functions of upconversion nanoparticles as a drug carrier and energy donor in PDT.

Upconversion is an anti-Stokes process that involves long-wavelength radiation, usually near-infrared (NIR) at 800 or 980 nm [6], being converted to a shorter wavelength such as ultraviolet or visible radiation (Figure 1). Upon radiation of NIR, upconversion nanoparticles (UCNPs) emit visible light that can be used to excite PS to generate ROS. Modified with PSs, these upconversion nanoparticles have the potential of increasing the limited therapeutical depth of current PDT techniques [7].

3 Results

In our research, we constructed a nanoprobe (UCNP-Ppa-RGD) for NIR-PDT. The nanoprobe uses NaYF,:Yb/

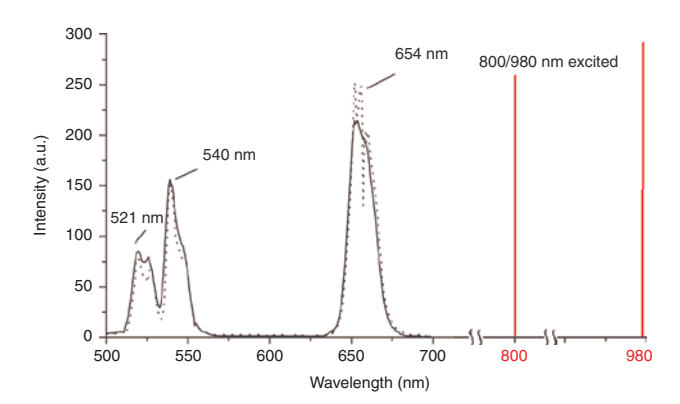


Figure 1: Emission spectra of upconversion nanoparticles excited with near-infrared light.

Er upconversion nanoparticles that are wrapped by O-carboxymethyl chitosan, and were co-modified with c(RGDyK) and pyropheophorbide-a [8] to result in the UCNP-Ppa-RGD nanoparticle. We demonstrated its targeting specificity and singlet oxygen generation upon NIR irradiation (980 nm); we also explored the PDT efficacy and therapeutical depth *in vitro* and *in vivo*. The results showed a strong targeting specificity for integrin $\alpha v\beta$ 3-positive tumor and an effective treatment outcome [9, 10].

However, in this application only the energy of the red light band of UCNP was utilized. And although the green emission can be used for imaging, it is not so effective because of the poor tissue transmission. More critically, the treatment dosage of PDT could not be determined. Further work is still required to improve the excitation efficiency and the imaging availability.

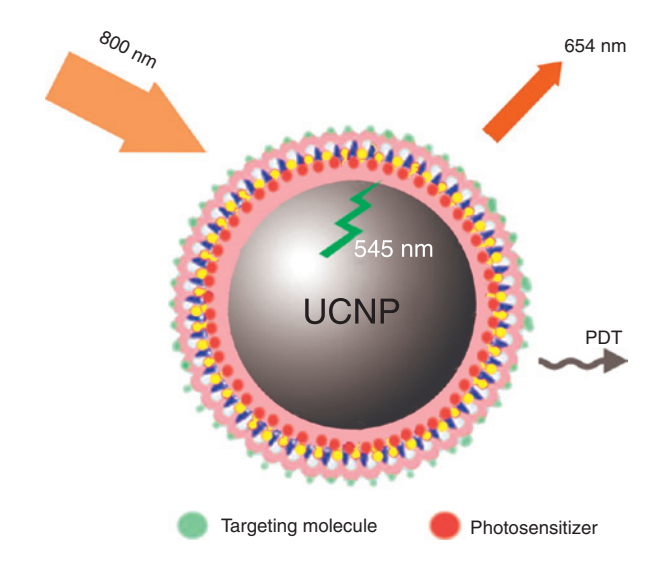


Figure 2: Near-infrared upconversion nanoprobe for monitoring photodynamic therapy.

Several methods have been reported to predict the therapy dosage [5, 11, 12], but their application is limited by their intrinsic shortcomings. Based on these points, we further improved the nanophotosensitizer by selecting other kinds of UCNPs and providing monitoring capability. The newly designed probes with NaYF₄:Yb/Er/Nd can be excited with 808 nm laser, which has a very low absorption of water, to achieve a much deeper tissue penetration. In this research, the energy of the emission at the 540 nm band was used for exciting PS, and the energy at 650 nm was used for real-time therapeutic effect monitoring based on the change of the tissue optical parameters attributed to PDT (Figure 2). This work has been submitted to report as a very feasible strategy to realize a monitoring for PDT.

4 Conclusion

In conclusion, our study aimed to develop a tumor-targeting PS based on upconversion nanoparticle for NIR fluorescent imaging and deep-tissue PDT. The composite nanoparticle was proved to be convenient and controllable for applications. The drug delivery, the tumor localization, and the tumor treatment effect can all be monitored in situ. With the real-time monitoring and dosimetry, any potential side effects of the treatment will be reduced. All of these results suggest that the highly tumor-specific NIR-nanoparticles are advantageous as a photodynamic imaging reagent for tumor localization and as a therapeutic agent for the treatment of large or deeply seated tumors. The proposed technique combines several wellestablished individual concepts into one novel integrated procedure, significantly improving both the tumor diagnosis and treatment capability.

Acknowledgments: This research is supported by the Key Program of the National Natural Science Foundation of China (Grant number: '613300033'), the Guangdong Natural Science Foundation (Grant number: '2015A030313394'), and the Science and Technology Planning Project (Grant number: '2014A020212738') of Guangdong Province, China.

References

- [1] Ding J, Zhao J, Cheng K, Liu G, Xiu D. *In vivo* photodynamic therapy and magnetic resonance imaging of cancer by TSPP-coated Fe₃O₄ nanoconjugates. J Biomed Nanotechnol 2010;6(6):683–6.
- [2] Liu B, Farrell TJ, Patterson MS. Comparison of photodynamic therapy with different excitation wavelengths using a dynamic model of aminolevulinic acid-photodynamic therapy of human skin. J Biomed Opt 2012;17(8):088001-1.
- [3] Guo W, Chen N, Tu Y, Dong C, Zhang B, Hu C, Chang J. Synthesis of Zn-Cu-In-S/ZnS core/shell quantum dots with inhibited blue-

- shift photoluminescence and applications for tumor targeted bioimaging. Theranostics 2013;3(2):99-108.
- [4] Farrell TJ, Wilson BC, Patterson MS, Olivo MC. Comparison of the in vivo photodynamic threshold dose for photofrin, monoand tetrasulfonated aluminum phthalocyanine using a rat liver model. Photochem Photobiol 1998;68(3):394-9.
- [5] Johansson A, Johansson T, Thompson MS, Bendsoe N, Svanberg K, Svanberg S, Andersson-Engels S. In vivo measurement of parameters of dosimetric importance during interstitial photodynamic therapy of thick skin tumors. J Biomed Opt 2006;11(3):34029.
- [6] Wang Y, Ji L, Zhang B, Yin P, Qiu Y, Song D, Zhou J, Li Q. Upconverting rare-earth nanoparticles with a paramagnetic lanthanide complex shell for upconversion fluorescent and magnetic resonance dual-modality imaging. Nanotechnology 2013;24(17):175101.
- [7] Idris NM, Gnanasammandhan MK, Zhang J, Ho PC, Mahendran R, Zhang Y. In vivo photodynamic therapy using upconversion nanoparticles as remote-controlled nanotransducers. Nat Med 18(10):1580-5.

- [8] Sengee GI, Badraa N, Shim YK. Synthesis and biological evaluation of new imidazolium and piperazinium salts of pyropheophorbide-a for photodynamic cancer therapy. Int J Mol Sci 2008;9(8):1407-15.
- [9] Zhou A, Wei Y, Wu B, Chen Q, Xing D. Pyropheophorbide A and c(RGDyK) comodified chitosan-wrapped upconversion nanoparticle for targeted near-infrared photodynamic therapy. Mol Pharm 2012;9(6):1580-9.
- [10] Aiguo Z, Wei Y, Qun C, Xing D. In vivo near-infrared photodynamic therapy based on targeted upconversion nanoparticles. J Biomed Nanotechnol 2015;11(11): 2003-10.
- [11] Wei Y, Song J, Chen Q. In vivo detection of chemiluminescence to monitor photodynamic threshold dose for tumor treatment. Photochem Photobiol Sci 2011;10(6):1066-71.
- [12] Wei Y, Xing D, Luo S, Yang L, Chen Q. Quantitative measurement of reactive oxygen species in vivo by utilizing a novel method: chemiluminescence with an internal fluorescence as reference. J Biomed Opt 2010;15(2):027006.

Session 3: Photosensitizers and targeting carrier systems (II)

[3.01] Carbon dots: efficient photodynamic therapy agents with high singlet oxygen generation

Jiechao Ge and Pengfei Wang*

Key Laboratory of Photochemical Conversion and Optoelectronic Materials, Technical Institute of Physics and Chemistry, Chinese Academy of Sciences, Beijing 100190, China

*Corresponding author: Prof. Pengfei Wang, wangpf@mail.ipc.ac.cn

Abstract: Clinical applications of current photodynamic therapy (PDT) agents are often limited by their low singlet oxygen (102) quantum yields, as well as by photobleaching and poor biocompatibility. Recently, we have prepared a new PDT agent based on carbon dots that can produce ¹O₂ via a multistate sensitization process, resulting in a quantum yield of ~1.3, the highest reported for PDT agents.

Keywords: photodynamic therapy; singlet oxygen quantum yields; carbon dots.

1 Background

Carbon dots (C-dots) have recently emerged as important nanomaterials and have received much attention for their unique properties, such as high water solubility, surface modification flexibility, low toxicity, excellent biocompatibility, and high photostability [1]. To date, a wide range of synthetic approaches, including top-down and bottom-up methods, have been pursued to produce C-dots. The topdown methods are primarily based on the post-treatment of nanographene broken off from large graphene sheets. The bottom-up method involves the synthesis of graphene moieties containing a certain number of conjugated carbon atoms or solution chemistry methods in which the C-dots are formed from molecular precursors [2]. However,

the application of C-dots in PDT from the current synthesis methods remains unexplored.

2 Materials and methods

In this paper, we present highly water-dispersible, positive charged, and sulfur and nitrogen doped C-dots in large quantities using a hydrothermal method with polythiophene derivatives as the carbon source [3].

3 Results

The C-dots exhibit a broad absorption in the ultravioletvisible region and a strong emission peak at 680 nm. We demonstrated that the C-dots exhibit good biocompatibility and excellent ¹O₂ generation capability with a quantum yield of ~1.3. Moreover, in vitro and in vivo studies suggest that the C-dots can be applied as a PDT agent for the simultaneous imaging and highly efficient treatment of cancer.

References

- [1] Baker SN, Baker GA. Luminescent carbon nanodots: emergent nanolights. Angew Chem Int Ed Engl 2010;49(38):6726-44.
- [2] Lim SY, Shen W, Gao Z. Carbon quantum dots and their applications. Chem Soc Rev 2015;44(1):362-81.
- [3] Ge J, Lan M, Zhou B, Liu W, Guo L, Wang H, Jia Q, Niu G, Huang X, Zhou H, Meng X, Wang P, Lee CS, Zhang W, Han X. A graphene quantum dot photodynamic therapy agent with high singlet oxygen generation. Nat Commun 2014;5:4596.

[3.02] Photodynamic therapy based on upconversion nanoconstructs

Deyan Yin, Weidong Gao, Sisi Cui and Yueqing Gu*

Department of Biomedical Engineering, School of Engineer, China Pharmaceutical University Nanjing, Jiangsu Province, China

*Corresponding author: Prof. Yueging Gu, guyueqingsubmission@hotmail.com

Abstract: Although photodynamic therapy (PDT) has been approved by many countries for numerous clinical cancer treatments, two major challenges still persist: 1) the limited penetration of excitation light in tissue, and 2) the poor tumor-selectivity of the photosensitizer. To address these issues, we have developed a multifunctional nanoconstruct consisting of upconversion nanoparticles

(UCNPs) that transform near-infrared (NIR) light into visible light, and a photosensitizer, zinc(II) phthalocyanine (ZnPc), for in vivo deep tissue PDT triggered by NIR light. The results indicate that the multifunctional nanoconstruct is a promising PDT agent for deep-seated tumor treatment and demonstrates a new paradigm for enhancing PDT efficacy.

Keywords: upconversion nanoparticles; chitosan; folate; singlet oxygen; photodynamic therapy.

1 Introduction

Photodynamic therapy (PDT) is a treatment modality based on the photochemical reactions mediated by the interaction of photosensitizers (PSs) with specific light and oxygen. PDT induces cell death through intracellular generation of reactive oxygen species (ROS), which are produced by energy transition from the excited PS to molecular oxygen. Although PDT is a minimally invasive therapeutic modality approved by many countries for numerous clinical cancer treatments, some challenges still persist, including limited penetration depth of the excitation light, poor water solubility of PSs, and significant photosensitivity to sunlight. The upconversion luminescence mechanism provides a potential strategy to overcome some drawbacks of current PDT. The excitation light of upconversion nanoparticles (UCNPs) is in the near-infrared (NIR) region, which is a transparent window in the tissue and permits a deeper tissue penetration than visible light. Li and Zhang [1] first reported the representative application of NaYF, UCNPs in biomedicine by introducing the upconversion luminescence mechanism into PDT.

2 Materials and methods

To improve the optical properties of NaYF, UCNPs, we prepared hydrophilic hexagonal phase NaYF, UCNPs as PS carriers for in-vivo PDT. In addition, most of the current PSs are hydrophobic, requiring solubilization in biological buffers through polymer and silica-based UCNPs for PDT in deep tissues. Amphiphilic chitosan, which self-assembles into core-shell nanoparticles, has been widely used for targeted drug delivery in cancer therapy due to its good biocompatibility and biodegradability. Amphiphilic chitosan could

significantly improve the water solubility of hydrophobic drugs and prolong the blood circulation time in vivo for better therapeutic efficacy. Meanwhile, the hydrophilic branches of amphiphilic chitosan enhance its water solubility and stability in physiological solution. Thus, chitosanmodified UCNP is an ideal drug carrier for hydrophobic PSs. The co-localization of UCNP and PSs encapsulated in chitosan-modified nanoparticles limits the toxicity of PSs and enhances the PS excitation efficiency. In our study, hydrophilic UCNPs were first prepared by coating amphiphilic chitosan (N-succinvl-N'-octyl chitosan, SOC) on the surface of hydrophobic oleic acid-capped NaYF, UCNPs (OA-UCNPs). Hydrophobic PS zinc(II)phthalocyanine (ZnPc) was loaded into the SOC-coated UCNPs (SOC-UCNPs) via hydrophobic interactions to form a novel drug delivery system for in vivo deep tissue PDT triggered by NIR light (Figure 1).

3 Results

The ZnPc-loaded SOC-UCNPs exhibited good dispersibility, excellent optical properties and good photostability. Under NIR light irradiation, the measurement of singlet oxygen production indicated that ZnPc effectively generated singlet oxygen induced by the emission from the UCNPs. Cell viability assays showed the low cytotoxicity of the UCNPs after surface modification. In vitro and in vivo therapeutic investigation demonstrated the prominent PDT effects of ZnPc-loaded SOC-UCNPs upon NIR light irradiation. Furthermore, NIR imaging of indocvanine green derivative-loaded SOC-UCNPs after intratumoral injection indicated the high retention of SOC-UCNPs only at the tumor site. Histological examination confirmed the negligible toxicity of ZnPc-loaded SOC-UCNPs on other organs. All the results demonstrate the promising potential of using SOC-UCNPs as new PS carriers for PDT of cancer and other diseases in deep tissues [2].

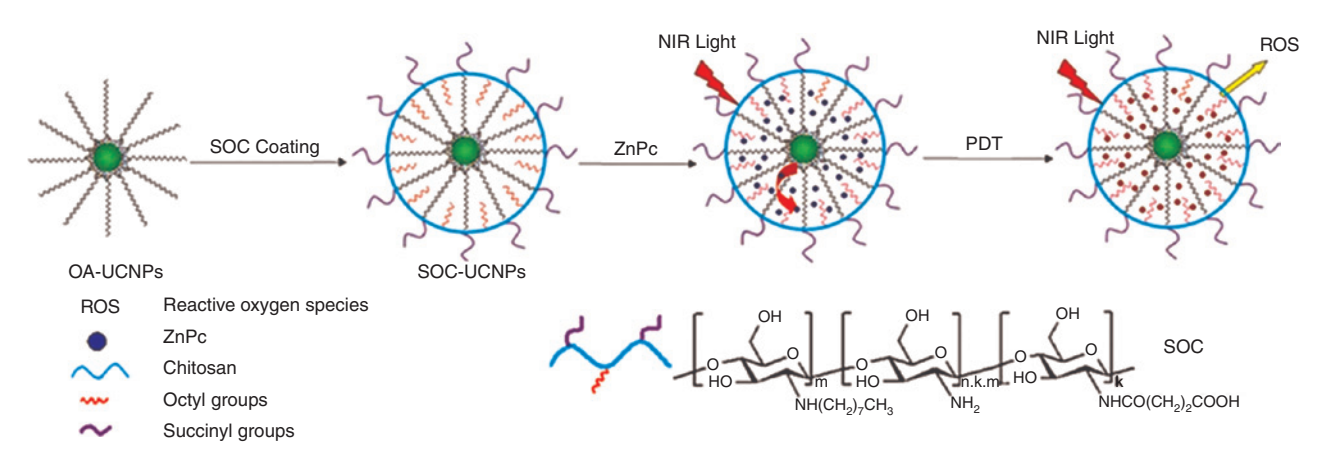


Figure 1: Schematic of the synthesis of ZnPc-loaded chitosan-modified upconversion nanoparticles (SOC-UCNPs).

4 Discussion

Diverse UCNP-based PDT agents have been developed for in vivo cancer treatment. However, only a few of them have been utilized for in vivo PDT treatment through intratumoral injection. This inefficient route of administration was needed to obtain higher PDT efficiency and fewer side effects because of the limited tumor specificity and selectivity of previously reported UCNPs. Unfortunately, local injection of PDT agents does not disperse the nanoparticles uniformly in the tumor and this technique is less efficient for tumors in deep tissue. Since the passive targeting of UCNP-based PDT nanoparticles is not adequate for in vivo PDT treatment through systemic administration, the modification of active targeting ligands to the nanocomplexes is urgently needed to increase local concentration of PSs in tumors and avoid side effects. Biomolecular recognition moieties such as cyclic arginine glycine aspartic acid (RGD) peptide and folic acid (FA) are usually conjugated to UCNPs for the targeted PDT of cancer cells. Tumor-targeted UCNP-based PDT agents can effectively increase the accumulation of the nanoparticles and improve PDT efficiency in deep-seated tumors. Very recently, Idris et al. [3] first reported the use of targeted upconversion nanoparticles for PDT of subcutaneous tumors, but their treatment programs need long time exposure (2 h) to laser light due to the limited PS loading of silica-coated UCNPs (<0.6 kg/l), which might induce photodamage to the tissues. In our work, we applied the FA-modified chitosan (FASOC) to coat UCNPs PSs to constitute a PDT system for deep-tissue treatment. The tumor-targeted FASOC-modified upconversion nanoconstruct (FASOC-UCNP) loaded with ZnPc is designed to selectively accumulate in tumors and to activate the adjacent ZnPc, producing photodynamic therapeutic effects after NIR irradiation (Figure 2).

This study aims to treat deep-seated tumors by using a tumor-targeted, UCNP-based PDT nanoconstruct. A high loading of PS to UCNP-based nanoconstructs is typically a prerequisite for efficient in vivo PDT treatment through Förster resonance energy transfer (FRET). In this study, we constructed FASOC-coated UCNPs as ZnPc carriers with a high drug loading capacity (~10%) through hydrophobic interaction. Compared with the reported UCNP-based PDT system, FASOC-UCNP nanoconstructs possess an improved loading capacity for hydrophobic ZnPc molecules. However, the higher loading capacity of ZnPc does not guarantee a better PDT efficiency because there is an optimal loading concentration for ZnPc. Excess ZnPc (250 µg/ml) in the nanoconstructs could not be entirely photoactivated during PDT, and the large number of ZnPc may form aggregates in the FASOC-UCNPs in aqueous media. These conditions would decrease ROS production by increasing the likelihood of deleterious processes such as triplet-triplet annihilation and self-quenching. Thus, the optimal loading of ZnPc (150 µg/ ml) in the FASOC-UCNP was utilized in the subsequent invivo experiments. A similar result of PS-dependent singlet oxygen production from UCNP-PS complexes has been reported by other researchers. To maximize ROS production from FASOC-UCNP-ZnPc, ZnPc loading should be controlled to avoid aggregation. In addition, owing to the hydrophobic property and planar structure of ZnPc, it can be efficiently encapsulated in the nanoconstruct with minimal leakage (<20%) even after 50 h incubation at various pH values (5.7, 7.4 and 8.0), which maximized FRET efficiency from UCNP to ZnPc. The good stability of the FASOC-UCNP-ZnPc nanoconstruct makes it an excellent UCNP-based PDT system for nonsuperficial tumors. Furthermore, the targeting ability of the FASOC-UCNP-ZnPc nanoconstruct was demonstrated in vitro

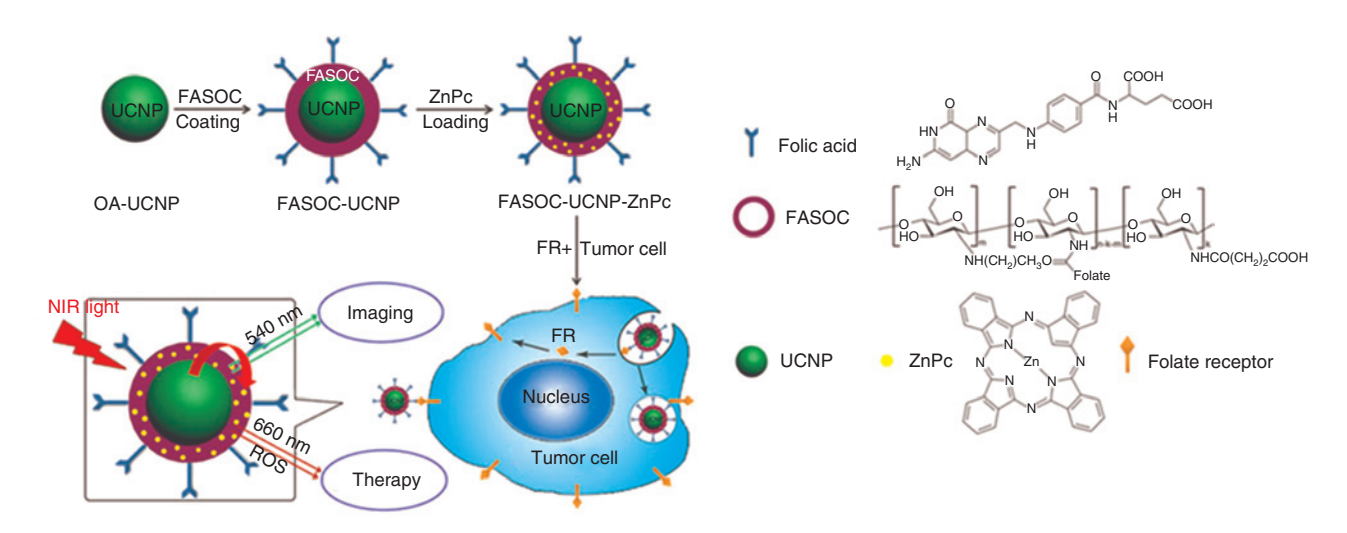


Figure 2: Schematic of the synthesis of FASOC-UCNP-ZnPc nanoconstruct and folate-mediated binding of tumor cells with folate receptor expression.

and in vivo. The enhanced intracellular uptakes of FASOC-UCNP-ZnPc by folic acid receptor (FR)-positive tumor cells (Bel-7402 and MDA-MB-231) were significantly higher than that in FR-negative A549 tumor cells. This increased uptake is attributed to FR-mediated endocytosis, which is evidenced by FR-blocking experiment in FR-positive cancer cells. In our experiment, a high concentration of free folic acid (1 mm) can effectively inhibit the uptake of folate-modified complexes in FR-positive cells. Similar findings have been reported for FRmediated tumor targeting of different drugs or nanomaterials in cancer cells and in vivo using FR blocking experiments. The *in-vivo* biodistribution of the UCNP-based nanoconstruct with or without FA modification further confirmed the high tumor targeting ability of FASOC-UCNP in tumor bearing mice. This result suggests that conjugating FA ligands with SOC coating significantly improved the active tumor-targeting of FASOC-UCNP to FR-overexpressed tumors (Bel-7402 and S180). In general, the main mechanism associated with the killing of cancer cells by PDT is the activation of PSs by light irradiation, which generates cytotoxic ROS that directly destroy the tumor cells. It has been demonstrated that PDT has two ways to kill cells, defined as type-I and type-II mechanisms. The type-I mechanism involves hydrogen-atom abstraction or electron-transfer reactions between the PS and a substrate to yield free radicals and radical ions, which can interact with molecular oxygen to either generate ROS (such as superoxide anions and hydroxyl radicals) or can cause irreparable biological damage. The type-II mechanism results from an energy transfer between the PS and the molecular oxygen to produce singlet oxygen. Dichlorofluorescindiacetate and 1,3-diphenylisobenzofuran probes can detect lethal cytotoxic ROS (not only singlet oxygen) production inside cells and in solution, allowing its use to report the potential PDT efficacy of the nanoconstructs. Unlike visible light, PDT triggered by NIR light enables the feasibility of deep-tissue PDT treatment. Significant light attenuation of 72% and 95% was observed through 1-cm adipose tissue using the same power density (0.2 W/cm²) at 980 and 660 nm excitation, respectively. Our in vitro results suggest that UCNP-based PDT induced by deep-penetrating 980 nm light produces more ROS than 660 nm light in the cancer cells covered by a 1-cm pork tissue.

5 Conclusion

In vivo PDT treatments for deep-seated tumors demonstrated that NIR light-triggered PDT based on the nanoconstructs possessed remarkable therapeutic efficacy with tumor inhibition ratio up to 50% compared with conventional visible light-activated PDT with a noticeably reduced tumor inhibition ratio of 18%. Although in vivo results indicate 660 nm light-induced PDT possesses better therapeutic efficacy for subcutaneous tumors, NIR-induced PDT using FASOC-UCNP-ZnPc demonstrates superior treatment of simulated 1-cm deep tumors. These results demonstrate the considerable advantages of tumor-selective UCNPbased PDT induced by NIR light over traditional PDT for internal tumors and prompt further explorations of these nanoconstructs for targeted drug delivery and deep-tissue PDT of other related diseases [4, 5].

References

- [1] Li Z, Zhang Y. An efficient and user-friendly method for the synthesis of hexagonal-phase NaYF,:Yb, Er/Tm nanocrystals with controllable shape and upconversion fluorescence. Nanotechnology 2008;19(34):345606.
- [2] Cui S, Chen H, Zhu H, Tian J, Chi X, Qian Z, Achilefu S, Gu Y. Amphiphilic chitosan modified upconversion nanoparticles for in vivo photodynamic therapy induced by near-infrared light. I Mater Chem 2012;22(11):4861-73.
- [3] Idris NM, Gnanasammandhan MK, Zhang J, Ho PC, Mahendran R, Zhang Y. In vivo photodynamic therapy using upconversion nanoparticles as remote-controlled nanotransducers. Nat Med 2012;18(10):1580-5.
- [4] Cui S, Yin D, Chen Y, Di Y, Chen H, Ma Y, Achilefu S, Gu Y. In vivo targeted deep-tissue photodynamic therapy based on nearinfrared light triggered upconversion nanoconstruct. ACS Nano 2013;7(1):676-88.
- [5] Cui S, Chen H, Qian Z, Chen WR, Gu Y. Folate receptor-mediated tumor-targeted upconversion nanocomplex for photodynamic therapy triggered by near-infrared light. Proc SPIE 2013;8582:85820A. doi: 10.1117/12.2003246.

[3.03] New triplet photosensitizers showing strong absorption of visible light and long-lived triplet excited states

Jianzhang Zhao*

State Key Laboratory of Fine Chemicals, School of Chemical Engineering, Dalian University of Technology, E-208 West Campus, 2 Ling Gong Rd., Dalian 116024, China

*Corresponding author: Prof. Jianzhang Zhao, zhaojzh@dlut.edu.cn

Abstract: Triplet photosensitizers are used for photodynamic therapy (PDT). The conventional triplet photosensitizers used in PDT studies are limited to porphyrin derivatives and analogues. Very few new triplet photosensitizers have been reported. Recently we prepared a series of new triplet photosensitizers which are potential candidates

for PDT studies. These new triplet photosensitizers included transition metal complexes (Pt, Ir, Ru, Re, etc.), and organic compounds. We devised new molecular structure design methods, such as an intramolecular spin converter for preparation of heavy atom-free triplet photosensitizers, and photosensitizers based on Förster resonance energy transfer (FRET) effect, so that photosensitizers exhibiting broadband visible light-absorbing properties can be obtained.

Keywords: Bodipy; FRET; photochemistry; transition metal complex; triplet state.

1 Introduction

Triplet photosensitizers (PSs) are crucial for photodynamic therapy (PDT) studies [1]. Conventional triplet PSs are limited to the porphyrin derivatives or analogues [2]. However, these compounds suffer from certain drawbacks, such as difficulties in preparaton, isolation/purification, and modification of the molecular structures to improve the photophysical or biological properties. On the other hand, it is difficult to design new triplet PSs because the intersystem crossing (ISC) property of organic compounds is difficult to predict for heavy atom-free triplet PSs.

2 Investigations and results

In order to address the above challenges in the area of triplet PSs, we developed a few new molecular designing methods for preparation of triplet PSs [2]. These methods include: 1) Direct metalation for preparation of visible light-harvesting transition metal complexes [3]; 2) Matched energy levels for the visible light-harvesting antenna (ligand) and the coordination center, so that energy transfer from the visible light-absorbing ligand to the coordination center ensured [4, 5]; 3) using spin converter, e.g. C₆₀, for design heavy atom-free triplet PSs [6]; and 4) using Förster resonance energy transfer (FRET) for preparation of broadband visible light absorbing triplet PSs [7, 8]. Attaching a visible light-harvesting chromophore into a transition metal complex will result in strong absorption of visible light for the complex. However, it does not necessarily mean the harvested photoexcitation energy can be efficiently funneled to the triplet excited state manifold. In order to address this problem, we propose the direct metalation concept that directly attaches the transition metal to the π -conjugation core of the ligand. Thus the heavy atom effect and the ISC can be maximized. Following this molecular designing method, we prepared a Bodipy-based binuclear Pt(II) complexes (Pt-1, Figure 1), for which room temperature phosphorescence of the Bodipy ligand was observed [3].

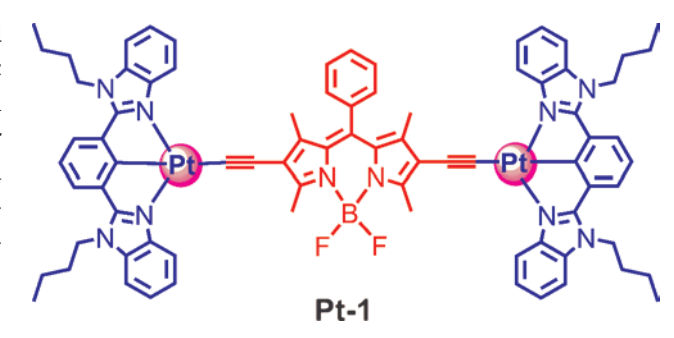


Figure 1: Red-absorbing Pt(II) complex Pt-1.

3 Results

The room temperature (RT) phosphorescence of Pt-1 indicated efficient ISC, which is unprecedented for Bodipy containing transition metal complexes.

Pt-1 shows strong absorption in the red spectra range, the RT phosphorescence is at 770 nm. The triplet excited state lifetime is up to 128.4 μ s. The complex was used in triplet-triplet annihilation upconversion. The excitation is at 632 nm, and the upconverted emission is at 450 nm. Pt-1 may be a promising candidate for PDT studies.

We also propose to use of a visible light-harvesting ligand with a matched energy level to that of the coordination center, so that the photoexcitation energy harvested by the ligand can be efficiently funneled to the coordination center. Therefore the photoexcitation energy can be efficiently transformed into the triplet excited state energy, otherwise the photoexcitation energy may be trapped on the ligand.

Following this method, we prepared visible light-harvesting Ir(III) and Ru(II) complexes (Figure 2). Ir-1 gives strong absorption at approx. 470 nm, and the triplet excited state lifetime is up to 75 µs. These complexes were

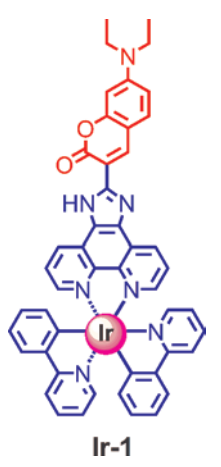


Figure 2: Ir(III) complex Ir-1 showing strong absorption of visible light and long triplet state lifetime.

used for triplet-triplet-annihilation upconversion, but the PDT effect of these complexes was not studied [5].

It is still a challenge to design a heavy atom-free organic triplet photosensitizer because the ISC property is difficult to predict in this case. In order to design heavy atom-free triplet PSs, we propose to use the concept of spin converter. A spin converter is a chromophore which undertakes efficient ISC upon photoexcitation. C₆₀ is one example, for which the ISC is close to unit. However, the visible light-harvesting ability of C_{60} is very weak, thus C_{60} is not an ideal triplet photosensitizer.

In order to address this drawback, we propose attaching a visible light-absorbing chromophore to C_{60} as the antenna and singlet energy donor. C_{60} is the singlet energy acceptor and the spin converter. Photoexcitation into the visible lightharvesting antenna will finally lead to the formation of the triplet excited state of C60. Following this method, we prepared a series of heavy atom-free triplet PSs based on C60 as the spin converter and Bodipy as the visible light-harvesting antenna (Figure 3) [6]. These dyads are efficient heavy atomfree triplet PSs and have been used for triplet-triplet-annihilation upconversion. The advantage of these dyads is the absorption wavelength that can be easily tuned with using different visible light-absorbing antennas.

Another major challenge in the area of triplet PSs is that most of the triplet PSs are on the profile of single chromophore, thus there is only one major absorption band for these conventional triplet PSs in the visible spectral region. In order to address this drawback, we propose to prepare broadband visible light-absorbing triplet photosensitizers based on the FRET effect (Figure 4) [2]. FRET has been widely used in singlet excited state manifold,

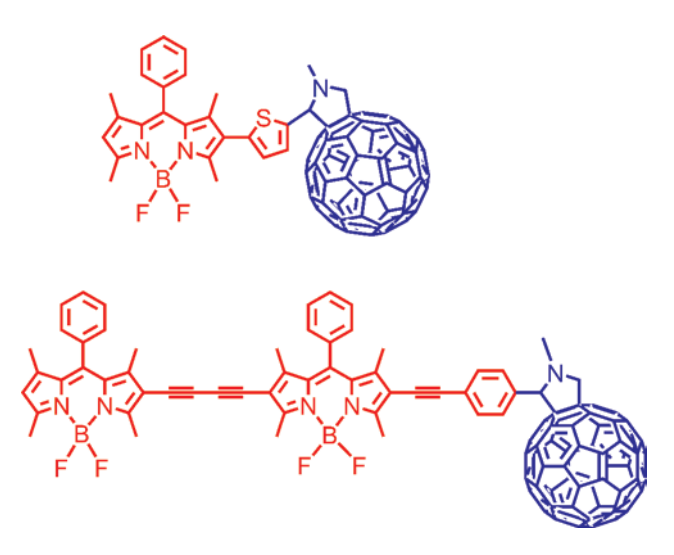


Figure 3: Visible light-harvesting C₆₀-Bodipy dyads as heavy atomfree triplet photosensitizers.

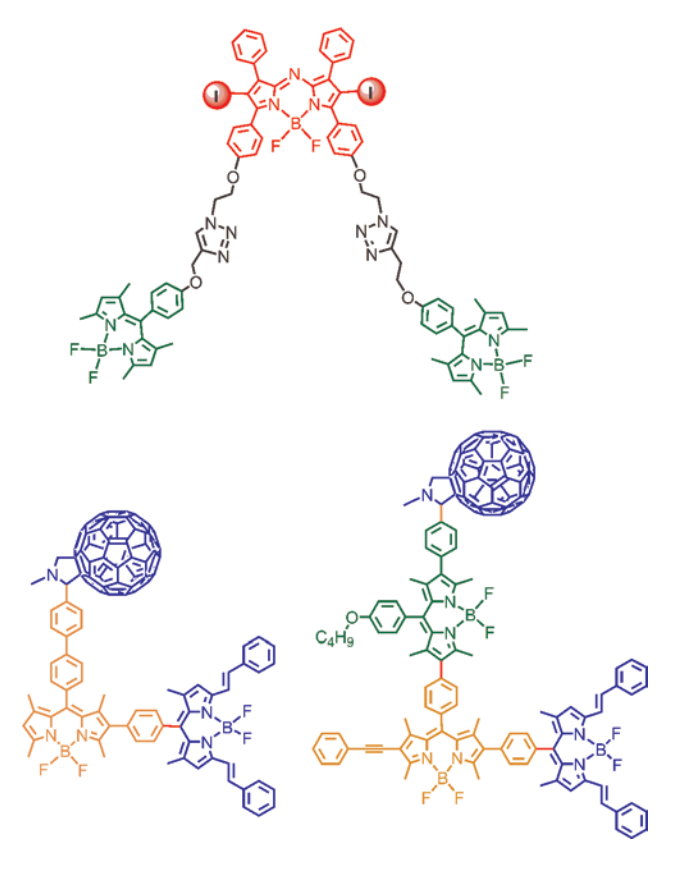


Figure 4: Broadband visible light-absorbing organic triplet photosensitizers.

but it has been rarely used in the triplet state manifold. Following this method we prepared series of new triplet PSs which show broadband visible light absorption, and long-lived triplet excited states (Figure 4). These novel triplet PSs may be promising PDT reagents for which white light can be used to reduce the treatment time and these compounds are ideal for PDT with white-light light emitting diodes as a light source [7, 8].

References

- [1] Kamkaew A, Lim SH, Lee HB, Kiew LV, Chung LY, Burgess K. BODIPY dyes in photodynamic therapy. Chem Soc Rev 2013;42(1):77-88.
- [2] Zhao J, Wu W, Sun J, Guo S. Triplet photosensitizers: from molecular design to applications. Chem Soc Rev 2013;42(12):5323-51.
- Wu W, Zhao J, Guo H, Sun J, Ji S, Wang Z. Long-lived roomtemperature near-IR phosphorescence of BODIPY in a visiblelight-harvesting N \(\cappa C \(\cappa N \) Pt(II)-acetylide complex with a directly metalated BODIPY chromophore. Chemistry 2012;18(7):1961-8.
- Wu W, Ji S, Wu W, Shao J, Guo H, James TD, Zhao J. Ruthenium(II)polyimine-coumarin light-harvesting molecular arrays: design rationale and application for triplet-triplet-annihilation-based upconversion. Chemistry 2012;18(16):4953-64.
- Sun J, Wu W, Guo H, Zhao J. Visible-light harvesting with cyclometalated Iridium(III) complexes having long-lived 3IL excited

- states and their application in triplet–triplet-annihilation based upconversion. Eur J Inorg Chem 2011;2011(21): 3165–73.
- [6] Wu W, Zhao J, Sun J, Guo S. Light-harvesting fullerene dyads as organic triplet photosensitizers for triplet-triplet annihilation upconversions. J Org Chem 2012;77(12):5305–12.
- [7] Guo S, Ma L, Zhao J, Küçüköz B, Karatay A, Hayvali M, Yaglioglub HG, Elmali A. BODIPY triads triplet photosensitizers
- enhanced with intramolecular resonance energy transfer (RET): broadband visible light absorption and application in photooxidation. Chem Sci 2014;5(2):489–500.
- [8] Huang L, Cui X, Therrien B, Zhao J. Energy-funneling-based broadband visible-light-absorbing Bodipy-C₆₀ triads and tetrads as dual functional heavy-atom-free organic triplet photosensitizers for photocatalytic organic reactions. Chemistry 2013;19(51):17472–82.

[3.04] Novel phthalocyanine-based anticancer and antifungal photosensitizers: synthesis and structure-activity relationships

Wenliang Lan, Dongmei Zhao, Biyuan Zheng, Meirong Ke and Jiandong Huang* *College of Chemistry, Fuzhou University, Fuzhou, China* *Corresponding author: Prof. Jiandong Huang, jdhuang@fzu.edu.cn

Abstract: This short report summarized the structure-activity relationships of a series of phthalocyanines substituted with different functional groups at axial or peripheral positions reported previously by us. The effects of the type, number, and position of substituents as well as center ions, e.g. Si(IV) and Zn(II), have been discussed on the photophysical and photochemical properties, and photodynamic activities.

Keywords: phthalocyanine; photosensitizer; photodynamic therapy; anticancer; antifungus.

1 Introduction

Due to the desirable photophysical and photochemical properties, phthalocyanines (Pcs) have emerged to be most promising photosensitizers for photodynamic therapy (PDT) [1]. In recent years, we have synthesized and reported a series of Pcs as shown in Figure 1, including silicon(IV) phthalocyanines (SiPcs) {1–20} and zinc(II) phthalocyanines (ZnPcs) {21–37}, which are substituted with different functional groups, such as hydrophilic quanternary ammonium, carboxyl, sulfonate, amphiphilic triethylene glycol chain, and hydrophobic adamantine, for anticancer and antifungal PDT [2–16]. To rationally design more efficient compounds, here we briefly summarize their structure-activity relationships.

2 Results

As shown in Table 1, the Q-band absorption ranges from 672 nm to 686 nm in N,N-dimethylformamid (DMF) for the SiPcs. Generally, the SiPcs substituted with aryloxy derivatives {1–4 and 15} exhibit a red-shift relative to the analogues substituted with alkoxy groups {5–14 and 16–20}. For the ZnPcs, the α -tetra-substituted compounds show Q-bands at 686–700 nm, which are significantly red-shifted

compared to the corresponding β-tetra-substituted analogues. The Q-bands of quaternized SiPcs show a slightly red-shift (3-5 nm) compared with that of the corresponding counterparts. On the contrary, the quaternized ZnPc {31} shifts the Q-band to the blue compared with its counterpart {**30**}. The SiPcs {**1**, **3**, **5**}, and {**10**}, which contain the amine moieties close to the Pc ring, show extremely low fluorescence quantum yields $(\Phi_{\rm p})$ values as a result of photoinduced electron transfer (PET) effect of amino groups, while the Φ_{r} values are greatly increased for the corresponding quaternized compounds {2, 4, 6, and 11}. However, the PET effect is not observed obviously on the ZnPcs. Generally, the ZnPcs present higher singlet oxygen quantum yields (Φ_{λ}) than the SiPcs as shown in Table 1. The PET effect can also be significantly observed on singlet oxygen generation efficiency for the SiPcs. On the whole, the α -tetra-substituted ZnPcs show higher Φ but lower $\Phi_{\scriptscriptstyle E}$ than the corresponding β -tetra-substituted compounds, suggesting that the α -substituted analogues should have more efficient intersystem crossing.

As shown in Table 2, the *in vitro* photodynamic anticancer activities of these Pcs greatly depend on the substituents. The SiPc {17} substituted with uridines exhibits a very high photoactivity against HepG2 cells with an IC $_{50}$ value, defined as the dye concentration required to kill 50% of the cells, down to 6 nm, which can be attributed to its high cellular uptake and non-aggregated nature [9]. The photocytotoxicity of SiPcs can be enhanced dramatically after quaternization (e.g. {1} vs. {2}, and {5} vs. {6}). It is worth mentioning that the octa-sulfonated ZnPc {29} exhibits a high selectivity toward tumor tissue by targeting tumor-associated macrophages [13]. Moreover, incorporating the tetra-sulfonated ZnPc {28} with layered double hydroxide (LDH) could afford a novel tumor-pH-activatable nanophotosensitizer with an IC $_{50}$ value as low as 0.053 µm [12].

	N N N N N N N N N N N N N N N N N N N		-0-\\\\\\\\\\\\\\\\\\\\\\\\\\\\\\\\\\\	R	N R	α -tetra-substituted, R =		
			1-0~N	N	/ \ / \.		N N R	
SiPc		11 ^[5]	-0\\\\\\\\\\\\\\\\\\\\\\\\\\\\\\\\\\\\	R				
R=		12 ^[5]	-0	β-tetra	β-tetra-substituted, R =		-O-CH2CH2COOH	
1 ^[2]	1-0-(N-N-N-O)	13 ^[6]	1-0-43	32 ^[10]	=0 - COOC ₄ H ₉	24 ^[11]	N- Boc	
2 ^[2]	}-O-{\\\\\\\\\\\\\\\\\\\\\\\\\\\\\\\\\\\	14 ^[6]	1-0~~	33 ^[10]	-О-СООН	25 ^[11]	O N N- Boc	
3 ^[3]	1-0-NH O	15 ^[7]	N NH ₂ N N CF ₃	34 ^[10]	-O-CH ₂ CH ₂ COOH	26 ^[11]	√ _O N NH	
4 ^[3]	1-0-NH ₂	16 ^[8]	O O N NH ₂	35[11]	N N N N N N N N N N N N N N N N N N N	27 ^[11]	~0~0~N_NH	
5 ^[4]	-ONO	17 ^[9]	O NHO	00[15]	NN NN CNH	28 ^[12]	-O -SO ₃ Na	
6 ^[4]	-OO	18 ^[9]	I-O O NH	36 ^[15]	N Z N	29 ^[13]	SO ₃ Na	
7 ^[5]	1-0-NH	19 ^[9]	O N NH ₂	37 ^[15]	ON N N N N N N N N N N N N N N N N N N	30 ^[14]	-N_N_N_N_N_N_N_N_N_N_N_N_N_N_N_N_N_N_N_	
8 ^[5]	-0 - N -	20 ^[9]	ON NH2	Ò	O'N'N O'NO	31 ^[14]	-N'-	

Figure 1: Structure of phthalocyanines {1–37}.

Table 1: Photophysical and photochemical data for phthalocyanines in N,N-dimethylformamid.

Pc	λ_{max} (nm)	$\boldsymbol{\Phi}_{_{\mathrm{F}}}$	$\Phi_{\!\scriptscriptstyle\Delta}$	Pc	λ_{max} (nm)	$\boldsymbol{\Phi}_{_{\mathrm{F}}}$	$\Phi_{\!\scriptscriptstyle\Delta}$	Pc	λ_{max} (nm)	$\boldsymbol{\Phi}_{_{\mathrm{F}}}$	$\Phi_{\!\scriptscriptstyle \Delta}$
1	680	0.02	0.15	14	673	0.50	0.40	27	700	0.11	0.69
2	685	0.22	0.49	15	686	0.46	0.38	28	692	0.15	0.72
3	679	0.01	0.05	16	676	0.33	0.31	29	696	0.14	0.82
4	680	0.10	0.18	17	678	0.37	0.44	30	700	0.13	0.77
5	674	0.03	0.04	18	676	0.29	0.46	31	696	0.12	0.77
6	678	0.45	0.45	19	677	0.36	0.42	32	675	0.31	0.64
7	672	0.23	0.25	20	676	0.30	0.67	33	674	0.25	0.63
8	673	0.29	0.23	21	687	0.24	0.76	34	679	0.23	0.58
9	676	0.47	0.40	22	686	0.14	0.68	35	678	0.27	0.54
10	673	0.08	0.07	23	695	0.16	0.70	36	685	0.10	0.74
11	678	0.39	0.41	24	700	0.12	0.64	37	699	0.03	0.54
12	673	0.36	0.49	25	699	0.13	0.77				
13	672	0.46	0.43	26	700	0.11	0.56				

 $[\]Phi_{\!\scriptscriptstyle P}$, fluorescence quantum yield; $\Phi_{\!\scriptscriptstyle \Delta}$, oxygen quantum yield; Pc, phthalocyanine; $\lambda_{\scriptscriptstyle \max}$, wavelength at maximum absorption.

Table 2: IC₅₀ values of phthalocyanines against different cancer cells.

Pc	IC ₅₀ (μм)	Cancer cells	Pc	IC ₅₀ (μм)	Cancer cells	Pc	IC ₅₀ (μм)	Cancer cells
1	>2.5	B16	16	0.078	HepG2	36	0.08	HepG2
2	0.033	B16	17	0.006	HepG2	37	3.31	HepG2
5	1.02	B16	18	0.051	HepG2	22	3.05	MGC803
6	0.30	B16	19	0.400	HepG2	23	3.78	MGC803
3	5.50	HT29	20	0.080	HepG2	33	3.29	MGC803
4	0.015	HT29	28	1.27	HepG2	34	5.30	MGC803
15	0.500	HepG2	29	3.78	HepG2	29	0.28	J774A.1

IC_{so}, dye concentration required to kill 50% of the cells; Pc, phthalocyanine.

Cancer cell lines: B16, melanoma carcinoma cells; HT29, human colorectal carcinoma cells; HepG2, human hepatocellular carcinoma cells; MGC803, human gastric carcinoma cells; J774A.1, mouse macrophages.

Table 3: Comparison of IC_{on} values of phthalocyanines against *C. albicans* [5, 11, 14, 16].

Pc	2	6	7	8	9	10	11	12	30	31	35
IC ₉₀ (μм)	61	66	88	85	19	54	49	>100	15.59	1.46	9

IC, dye concentration required to kill 90% of the cells; Pc, phthalocyanine.

The photodynamic antifungal activities of some Pcs against Candida albicans are shown in Table 3. The SiPcs containing amine moieties exhibit the IC₀₀ values (defined as the dye concentration required to kill 90% of the cells) of 19-88 µM, while the quaternized cationic compounds show obviously enhanced antifungal activities due to their higher Φ_{Λ} values. Interestingly, the dodeca-cationic ZnPc {31} exhibits a high as well as selective photocytotoxicity towards C. albicans with an IC₉₀ value as low as 1.46 um [14].

Acknowledgments: This work was supported by the National Nature Science Foundation of China (Grant numbers: '21172037', '21301031' and '21473033').

References

- [1] Dolmans DE, Fukumura D, Jain RK. Photodynamic therapy for cancer. Nat Rev Cancer 2003;3(5):380-7.
- [2] Jiang XJ, Huang JD, Zhu YJ, Tang FX, Ng DK, Sun JC. Preparation and in vitro photodynamic activities of novel axially substituted silicon (IV) phthalocyanines and their bovine serum albumin conjugates. Bioorg Med Chem Lett 2006;16(9):2450-3.
- [3] Huang JD, Jiang XJ, Shen XS, Tang QQ. Synthesis and photobiological properties of novel silicon (IV) phthalocyanines axially modified by paracetamol and 4-hydroxyphenylacetamide. Porphyrins Phthalocyanines 2009;13(12):1227-32.
- [4] Zhu YJ, Huang JD, Jiang XJ, Sun JC. Novel silicon phthalocyanines axially modified by morpholine: Synthesis, complexation with serum protein and in vitro photodynamic activity. Inorg Chem Commun 2006;9(5):473-7.
- [5] Zheng BY, Jiang XJ, Lin T, Ke MR, Huang JD. Novel silicon (IV) phthalocyanines containing piperidinyl moieties: synthesis

- and in vitro antifungal photodynamic activities. Dyes Pigments 2015;112:311-6.
- [6] Shen XM, Jiang XJ, Huang CC, Zhang HH, Huang JD. Highly photostable silicon (IV) phthalocyanines containing adamantane moieties: synthesis, structure, and properties. Tetrahedron 2010;66(46):9041-8.
- [7] Shen XM, Jiang XJ, Zhu YJ, Zhang HH, Huang JD. Spectral properties, photodynamic anticancer activity and the interaction with albumin of silicon phthalocyanine axially modified by pyrimidine derivatives. Guang Pu Xue Yu Guang Pu Fen Xi 2013;33(8):2148-52. [Article in Chinese].
- [8] Shen XM, Zheng BY, Zhang HH, Huang JD. Synthesis and photodynamic anticancer activity of silicon phthalocyanine axially modified by nucleoside derivatives. Guang Pu Xue Yu Guang Pu Fen Xi 2013;33(10):2731-5. [Article in Chinese].
- [9] Shen XM, Zheng BY, Huang XR, Wang L, Huang JD. The first silicon(IV) phthalocyanine-nucleoside conjugates with high photodynamic activity. Dalton Trans 2013;42(29):10398-403.
- [10] Ke MR, Huang JD, Weng SM. Comparison between non-peripherally and peripherally tetra-substituted zinc (II) phthalocyanines as photosensitizers: Synthesis, spectroscopic, photochemical and photobiological properties. J Photochem Photobiol A 2009;201(1):23-31.
- [11] Zheng BY, Zhang HH, Ke MR, Huang JD. Synthesis and antifungal photodynamic activities of a series of novel zinc (II) phthalocyanines substituted with piperazinyl moieties. Dyes Pigments 2013;99(1):185-91.
- [12] Li XS, Ke MR, Huang W, Ye CH, Huang JD. A pH-responsive layered double hydroxide (LDH)-phthalocyanine nanohybrid for efficient photodynamic therapy. Chemistry 2015;21(8):3310-7.
- [13] Li XS, Ke MR, Zhang MF, Tang QQ, Zheng BY, Huang JD. A non-aggregated and tumour-associated macrophage-targeted photosensitiser for photodynamic therapy: a novel zinc(II) phthalocyanine containing octa-sulphonates. Chem Commun (Camb) 2015;51(22):4704-7.

- [14] Li XS, Guo J, Zhuang JJ, Zheng BY, Ke MR, Huang JD. Highly positive-charged zinc(II) phthalocyanine as non-aggregated and efficient antifungal photosensitizer. Bioorg Med Chem Lett 2015;25(11):2386-9.
- [15] Chen XW, Ke MR, Li XS, Lan WL, Zhang MF, Huang JD. Synthesis, supramolecular behavior, and in vitro photodynamic
- activities of novel zinc(II) phthalocyanines "side-strapped" with crown ether bridges. Chem Asian J 2013;8(12):3063-70.
- [16] Zheng BY, Lin T, Yang HH, Huang JD. Photodynamic inactivation of Candida albicans sensitized by a series of novel axially di-substituted silicon (IV) phthalocyanines. Dyes Pigments 2013;96(2):547-53.

Session 4: Photodynamic inactivation of microorganisms

[4.01] Photodynamic inactivation of multi-resistant bacteria

Tim Maisch*

Department of Dermatology, Antimicrobial photodynamic and cold plasma research unit, University Medical Center, Regensburg, Germany

*Corresponding author: PD Dr. Tim Maisch, tim.maisch@klinik.uni-regensburg.de

Abstract: In 2014, experts of the World Health Organization were alarmed about the worldwide antibiotic resistance. Antibiotic resistance is currently one of the most important clinical challenges and not longer only a prediction. Therefore new approaches such as the photodynamic principle to fight against multi-resistant bacteria are necessary. This review summarizes the talk about photodynamic inactivation of multi-resistant bacteria given at the Sino-German Symposium on "Singlet molecular oxygen and photodynamic effects". Taken together the most promising environmental and clinical applications of the antibacterial photodynamic principle are: (i) photodynamic active surfaces; (ii) decolonization of methicillin-resistant Staphylococcus aureus (MRSA) on skin, (iii) treatment of diseases of the oral cavity e.g. caries, parodontitis, or endodontitis and (iv) superinfected burn wounds.

Keywords: singlet oxygen; decolonization; antibiotic resistance; MRSA; photodynamic antimicrobial chemotherapy (PACT).

1 Antibiotic resistance worldwide

During the Sino-German Symposium on "Singlet molecular oxygen and photodynamic effects" the newspaper Metropolitan Beijing [1] highlighted the fact that the use of antibiotics in pork in China is soaring. Half of the world's production of pigs (600 millions) is produced in China annually. Four times as many antibiotics per pound of meat are used in the raising of pigs as in cattle [1]. In fact, exactly the same antibiotics that one can buy in a pharmacy are those used to keep animals healthy. This could lead to the spread of drug-resistant bacteria from animal to farmer and consumer, and pose a significant threat to public health. Furthermore the unrestricted sale of antibiotics in developing countries, inappropriate prescription of antibiotics, insufficient doses and duration of antibiotic treatment, and overuse of antibiotics in livestock farming could additionally lead to the beginning of new multi-resistant superbugs that are not harmful to immunocompromised humans alone [2]. The worldwide prevalence of methicillin-resistant Staphylococcus aureus (MRSA) demonstrates that high levels of resistance can be found in all regions of the world [3]. In 1995, Norrby [4] stated that Vancomycin is active against all MRSA strains. Actually, 13 cases of Vancomycin-resistant S. aureus isolates have been observed in the USA since 2002 [5]. However MRSA is not the worst-case scenario, because Carbapenem-resistant Enterobacteriaceae has become resistant to all, or nearly all available antibiotics [5]. The strain KPC-OXA 48/181 is defined as "pan-resistant" bacteria that repels every single kind of antibiotic.

Therefore a new approach such as the antibacterial photodynamic principle is of interest to combat multiresistant bacteria. So far it has already been accepted that photodynamic antimicrobial chemotherapy (PACT) is an efficient antimicrobial approach to kill both antibioticsensitive and multi-resistant bacteria [6–8].

2 Decolonization of MRSA

Successful eradication of MRSA from intact skin entails of a 5-day standard decolonization regimen as follows: (i) mupirocin ointment twice daily, (ii) oral rinsing with 0.2% chlorhexidine solution 3 times daily, and (iii) daily body washing with 4% chlorhexidine solution [9]. Up to 10 decolonization courses are needed for successful MRSA eradication depending on the number of sites initially colonized by MRSA. Buehlmann et al. [9] showed that MRSA decolonization was only highly effective in patients who completed the full decolonization treatment course. However decolonization of MRSA by the photodynamic principle is possible. Maisch et al. [10] investigated the antimicrobial photodynamic efficacy of XF73, a two-fold positively charged porphyrine derivative, against MRSA applied on ex vivo porcine skin. Depending on the XF73 concentration (10 µM), incubation time (minimum 15 min) and light dose (15.2 mW/cm², 12.7 J/cm²), a 99.9% of MRSA eradication was possible which highlights the potential of PACT to use it as a sustentative approach for the skin decolonization of MRSA.

3 Type-II photosensitizer

Oxidative stress provoked by superoxide anions, hydrogen peroxide or hydroxyl radicals are general stress factors in bacterial life. All these ROS are also mostly generated by the type-I mechanism of PACT. Therefore bacteria can evade such stress inducing molecules by expressing enzymes such as catalase, peroxidase and superoxide dismutase. So far, detoxification of the highly reactive singlet oxygen (type-II mechanism) by pathogenic bacteria via specific quenching systems is not available. Therefore in order to optimize PACT efficacy, Cieplik et al. [11] from our group investigated a new generation of a type-II photosensitizer, SAPYR, based on a 7-perinaphthenone structure [11, 12]. SAPYR shows a singlet quantum yield of 0.99, therefore reacting almost quantitatively according to the photodynamic type-II mechanism. A polymicrobial biofilm can be expressed by Enterococcus faecalis, Actinomyces naeslundii, and Fusobacterium nucleatum were inactivated after a single treatment by light-activated SAPYR (600 mW/cm²; 120 s) with an efficacy of ≥99.99%.

4 Photodynamic active surfaces

One further new application of PACT is the use of photodynamic active surfaces. Here the photosensitizer is immobilized (convalently linked) in the surface material (e.g. polyurethan). Polyurethan is gas permeable, an essential prerequisite so that a sufficient amount of oxygen reaches the photosensitizer in the coating material. After light activation of the photodynamic active surface singlet oxygen is generated and can diffuse to the bacteria attached to the surface. There is no direct contact between the photosensitizer and the bacteria. The process works as long as light activates the system, preventing bacteria from settling at the surface and growing. Felgenträger et al. [13] from our group demonstrated that singlet oxygen is generated in a porphyrin-doped polymeric surface coating, which facilitates a photodynamic killing of >99.9% within an irradiation time of 30 min using an incoherent light source. No leakage of the porphyrin derivative was measured from the coating material into the aqueous surroundings which demonstrates that no direct contact between the photosensitizer and the respective bacteria is necessary. Singlet oxygen diffuses from the photodynamic active coating material into air leading to oxidative damage of the bacteria attached to the surface.

5 Application of PACT in the oral cavity

Several different PACT systems using phenothiazinebased photosensitizers have been used in the clinic for dental plaque-related diseases and infections [14]. These PACT systems have several advantages:

- Bacteria can be eradicated quickly (within seconds or minutes).
- The development of resistance in the target bacteria is unlikely.
- Disruption of the normal microflora can be avoided.
- Clinical outcomes can be improved by PACT as an auxiliary approach.

However as well as the above mentioned advantages of PACT, there are also some disadvantages:

- The overall photodynamic killing efficacy is not convincing in vivo.
- So far no real benefit has been proved in vivo even to the point of view that the clinical outcome is juged to be heterogenous.
- It is questionable that the right photosensitizers are used in vivo.

6 Summary and outlook

PACT is a multi-target process that means no specific bacterial target is required for the attack of the oxidative burst induced by the light-activated photosensitizer. In contrast to this, antibiotics act very specific (key hole principle). Therefore PACT is practical in parallel to antibiotic treatment even if antibiotics work takes several days [8]. So far, PACT is not only active against bacteria, but also against fungi, virus and parasites. PACT can destroy biofilms, inactivate virulence factors and exhibits a therapeutic window. Overall, PACT is a new antimicrobial platform to support the current standard antimicrobial treatments to inactivate multiple pathogens.

- [1] Metropolitan Beijing. Hogwash Experts alarmed about the soaring use of antibiotics in pork. http://www.globaltimes.cn/ content/914121.shtml [Accessed on July 22, 2015].
- World Health Organization. Antimicrobial resistance: global [2] report on surveillance 2014. http://www.who.int/drugresistance/documents/surveillancereport/en/ [Accessed on July 22, 2015].
- [3] Voss A, Doebbeling BN. The worldwide prevalence of methicillin-resistant Staphylococcus aureus. Int J Antimicrob Agents 1995;5(2):101-6.
- [4] Norrby SR. Emerging antibiotic resistance in gram-positive bacteria: return to the pre-antibiotic era? HKMJ 1995;1:129-35.
- [5] U.S. Department of Health and Human Services. Antibiotic resistance threats in the United States, 2013. http://www.cdc. gov/drugresistance/pdf/ar-threats-2013-508.pdf [Accessed on July 22, 2015].
- [6] Wainwright M. Photodynamic antimicrobial chemotherapy (PACT). J Antimicrob Chemother 1998;42(1):13-28.
- Maisch T. A new strategy to destroy antibiotic resistant microorganisms: antimicrobial photodynamic treatment. Mini Rev Med Chem 2009;9(8):974-83.

- [8] Kharkwal GB, Sharma SK, Huang YY, Dai T, Hamblin MR. Photodynamic therapy for infections: clinical applications. Lasers Surg Med 2011;43(7):755-67.
- [9] Buehlmann M, Frei R, Fenner L, Dangel M, Fluckiger U, Widmer AF. Highly effective regimen for decolonization of methicillin-resistant *Staphylococcus aureus* carriers. Infect Control Hosp Epidemiol 2008;29(6):510–6.
- [10] Maisch T, Bosl C, Szeimies RM, Love B, Abels C. Determination of the antibacterial efficacy of a new porphyrin-based photosensitizer against MRSA ex vivo. Photochem Photobiol Sci 2007;6(5):545-51.
- [11] Cieplik F, Späth A, Regensburger J, Gollmer A, Tabenski L, Hiller KA, Bäumler W, Maisch T, Schmalz G. Photodynamic biofilm inactivation by SAPYR – an exclusive singlet

- oxygen photosensitizer. Free Radic Biol Med 2013;65: 477–87.
- [12] Späth A, Leibl C, Cieplik F, Lehner K, Regensburger J, Hiller KA, Bäumler W, Schmalz G, Maisch T. Improving photodynamic inactivation of bacteria in dentistry: highly effective and fast killing of oral key pathogens with novel tooth-colored type-II photosensitizers. J Med Chem 2014;57(12):5157–68.
- [13] Felgenträger A, Maisch T, Späth A, Schröder JA, Bäumler W. Singlet oxygen generation in porphyrin-doped polymeric surface coating enables antimicrobial effects on *Staphylococcus aureus*. Phys Chem Chem Phys 2014;16(38):20598–607.
- [14] Cieplik F, Tabenski L, Buchalla W, Maisch T. Antimicrobial photodynamic therapy for inactivation of biofilms formed by oral key pathogens. Front Microbiol 2014;5:405.

[4.02] New triarylmethanes enabling selective photodynamic inactivation against bacteria over mamallian cells

Ke Li, Qianxiong Zhou and Xuesong Wang*

Key Laboratory of Photochemical Conversion and Optoelectronic Materials, Technical Institute of Physics and Chemistry, Chinese Academy of Sciences, Beijing 100190, China

*Corresponding author: Prof. Xuesong Wang, xswang@mail.ipc.ac.cn

Abstract: The photodynamic antimicrobial chemotherapy (PACT) is facing a great challenge, i.e. how to find a therapeutic window *in vivo* where bacteria but not human cells are killed. Several new triarylmethanes have been examined to address this issue. We modified commercial triarylmethanes with protonatable groups, and studied their photodynamic inactivation capabilities against *Escherichia coli* cells and human lung carcinoma A549 cells. It was found that our new triarylmethanes are able to selectively inactivate *E. coli* cells over A549 cells upon visible light irradiation. It seems, that multivalent cationic photosensitizers are promising PACT candidates for selective inactivation against bacteria.

Keywords: photodynamic therapy; inactivation of bacteria; triarylmethane.

1 Introduction

The rapidly increasing emergence of antibiotic resistance among pathogenic bacteria has encouraged the development of alternative antibacterial therapeutics that may not lead to resistance. In this regard, photodynamic antimicrobial chemotherapy (PACT) is drawing more and more attention as a promising solution to this issue. PACT follows the same mechanism of photodynamic therapy (PDT). The interplay of a photosensitizer, light at a suitable wavelength and singlet oxygen ($^{1}O_{2}$) has given rise to the generation of reactive oxygen species (ROS), such as $^{1}O_{2}$, superoxide anion radical and hydroxyl radical, which in turn lead to the damage of biomaterials, including DNA, protein, enzyme, as well as lipid membranes. The

multiple-targeting character makes it difficult for bacteria to develop resistance toward PACT.

2 Objective

For clinical application, PACT still faces a major challenge, i.e. how to find a phototherapeutic window to selectively kill bacteria but leave mammalian cells unaffected. So far, nearly all PACT agents can also effectively kill mammalian cells. To address this issue, we should at first find the difference between bacteria and mammalian cells. Similar to the cell wall of bacteria, the cytoplasmic membrane of mammalian cells are also negatively charged. However, the magnitude of transmembrane potentials is much smaller in mammalian cells than in bacteria. Moreover, unlike bacteria, acidic phospholipids are sequestered in the inner leaflets of the mammalian cell membranes, leading to much a lower negative charge density on the cell surface. These differences may be utilized to develop PACT agents of high selectivity. We surmised that a photosensitizer bearing more positive charges might be more hydrophilic and therefore more difficult to be taken up by mammalian cells, but would still have a strong binding affinity toward bacteria by virtue of electrostatic attraction.

3 Materials and methods

To test this idea, we designed and synthesized a series of new triarylmethanes as shown in Figure 1 and examined their photodynamic activities, using *Escherichia coli* and human lung carcinama A549 cells as models for bacteria and mamallian cells, respectively. Due to the protonation

Figure 1: Chemical structures of the examined triarylmethanes: crystal violet (CV), monopiperazine modified crystal violet (MPCV), dipiperazine modified crystal violet (DPCV), ethyl violet (EV) and aliphatic amine-modified ethyl violet (AEV).

of the tertiary aliphatic amine group(s) in neutral aqueous solutions, monopiperazine modified crystal violet (MPCV), dipiperazine modified crystal violet (DPCV), and aliphatic amine-modified ethyl violet (AEV) can be regarded as the bivalent or trivalent catinoic derivatives of the commercially available triarylmethanes crystal violet (CV) and ethyl violet (EV). Upon modification by protonatable group(s), the oil/water partition coefficients of MPCV, DPCV, and AEV underwent a remarkable decrease with respect to CV and EV, indicating the enhancement in hydrophilicity for the three new triarylmethanes. In spite of this, the three new triarylmethanes exhibit absorption spectra very similar to their parent dye molecules.

4 Results

We first examined the binding/uptake behaviors of these triarylmethanes. For A549 cells, the binding/uptake followed the order CV>>MPCV>DPCV. This is in good agreement with the rule that the more hydrophilic a photosensitizer is the less effective it will be taken up by mammalian cells. In the case of *E. coli*, the binding/uptake ability of MPCV is just a little bit lower than that of CV, and that of DPCV is even larger than CV. Obviously, electrostatic attraction between bivalent or trivalent cationic dve molecules and highly negatively charged *E. coli* play an important role.

In contrast to porphyrin-type dyes, triarylmethanes do not generate 10, upon irradiation but hydroxyl radicals instead. As a result, we used electron paramagnetic resonance technique to evaluate the ROS generation using 5,5-dimethyl-1-pyrroline-N-oxide as spin trapping agent of hydroxyl radicals. It was found that MPCV and AEV can generate hydroxyl radicals more efficiently than

Finally, we compared the PACT/PDT activities of these triarylmethanes. The photoinactivation ability of MPCV is found to be much stronger than that of CV. For example, at 5 µM and 20 min irradiation, the colony-forming units reduction by MPCV was 5 log units, while it was only 3 log units using CV. A similar result was also observed comparing AEV to EV. This can be attributed to the improved electrostatic attraction of the bivalent cationic molecules with bacteria. The enhanced hydroxyl radical generation also plays a role. DPCV showed the lowest photoinactivation potential to E. coli, which may be due to its high bleaching propensity. In sharp contrast, the PDT activities of MPCV and AEV toward A549 cells were found to be much lower than their parent dye molecules, mainly due to their greatly diminished uptake by the mammalian cells.

5 Conclusion

In summary, by introducing protonatable group(s) into the structures of commercial triarylmethanes, we obtained new multivalent cationic PACT agents, which showed enhanced inactivation activities against bacterial cells but reduced PDT activities towards mammalian cells [1]. The strategy we utilized could be extended to other types of photosensitizers to develop more efficient and selective antimicrobial agents.

Reference

[1] Li K, Lei W, Jiang G, Hou Y, Zhang B, Zhou Q, Wang X. Selective photodynamic inactivation of bacterial cells over mammalian cells by new triarylmethanes. Langmuir 2014;30(48):14573-80.

[4.03] PDT in oral diseases of microbial origin: The challenge of oral biofilm

Silvia Cristina Nuñez*

Centro de Lasers e Aplicações, IPEN-CNEN/SP, Av. Lineu Prestes, 2242, São Paulo, SP 05508-000, Brazil *Corresponding author: Dr. Silvia Cristina Nuñez, silvianunez@uol.com.br

Abstract: Oral infectious diseases are comprised of several different conditions caused by bacteria, fungi and viruses. Due to the present threat of microbial resistance,

dental professionals are looking for different antimicrobial approaches to treat oral infections. In this context, antimicrobial photodynamic therapy (aPDT) could be an important technique providing efficient treatment against all types of microorganisms. The technique involves the use of light sources that can reach all areas of the oral cavity and photosensitizers that have been proven effective against microorganisms in this environment. With consistent research, aPDT could provide an efficient antimicrobial approach for dentistry.

Keywords: oral disease; biofilm; photodynamic therapy; photoinactivation; microbial resistance; dental infections.

1 Introduction – Status quo

The role of dental infections in systemic health has been investigated from the focal infection theory presented in the early 20th century up until the present date. Improved microbiological techniques have allowed the identification of oral microorganisms at different sites in the body, and advances in bacterial identification methods, mostly culture independent approaches as 16S rRNA gene sequencing, have greatly contributed to the studies in this field [1].

The link between oral diseases and systemic healthy is not definitive for a lot of diseases, but plausible biological mechanisms including direct infection and/or the presence of low grade chronic inflammatory markers in the blood stream have made researchers link diseases such as rheumatoid arthritis and the oral health status [2]. So far, enough evidence has been produced to support the link between periodontal disease and cardiovascular disease and diabetes [3].

Chronic infections are rarely caused in the majority of the cases by planktonic microorganisms, microbial biofilm being the main cause of the disease. Biofilm is a microbially derived sessile community, characterized by cells that are attached to a surface. They are embedded in an extracellular polymeric matrix produced by the cells, the matrix is a highly hydrated, predominantly anionic exopolymer matrix and the cells in this habitat exhibit an altered phenotype and gene transcription pattern. Biofilm is a nutrient-sufficient ecosystem and these sessile microbes differ from their planktonic counterparts [4]. Due to the developmental challenges and interactions among species inside the biofilm, the cells become very resistant to traditional therapies with antibiotics and/or antifungal drugs [4]. Of late considerable research efforts have been made to develop effective antimicrobial approaches that can overcome the microbial resistance, as for many researchers, the microbial resistance can be considered the major global healthcare issue of the 21st century [5].

Oral diseases are mainly caused by microorganisms and are always in the form of biofilms; some examples are dental cavities, periodontal disease, endodontic abscess, peri-implantitis, oral candidiasis, and oral herpes infection. According to Peterson and Ogawa [6] more than 90% of the population worldwide at the age of 35-44 years has some degree of periodontal disease, conforming to the World Health Organization approach [6]. In addition to the high incidence of oral infections, the oral cavity is considered to be a reservoir of microbial resistant microorganisms [7] and dentists seem to be responsible for around 10% of all the antibiotics prescribed in the world [8]. Putting these facts together, it would be highly desirable to have an alternative antimicrobial approach to treat oral infections that could overcome and not promote the selection of resistance among microorganisms.

In this context antimicrobial photodynamic therapy (aPDT) is a promising alternative approach.

2 Antimicrobial photodynamic therapy

2.1 State of the art

Photodynamic therapy is a therapeutic approach that combines a chemical compound known as a photosensitizer (PS) and light to produce oxidative stress at the target area. aPDT has been studied intensively in the last few years, and substantial evidence has been collected to prove its efficiency against a broad spectrum of microbes including bacteria [9, 10], fungi [11, 12] and viruses [13] in vitro. For topical aPDT, as it is performed in the oral cavity, the PS can be directly delivered to the target and the light source can be focused on a certain point without significant obstacles, with the added bonus that the dye concentrations and light fluences that kill microorganisms are lower than those required to kill host cells or damage tissues [14].

Some clinical research has showed the potential of aPDT to treat oral infections, even in the presence of resistant bacteria [15], and also a good clinical outcome has been reported on the treatment of oral fungal infection in immunocompromised patients [16].

2.2 Further development steps

Despite the good results, aPDT has to produce consistent and predictable results to become a standard therapeutic modality for dental infection treatment. The need for improved PS to work on the oral cavity, where blood and saliva will interact with the PS and suitable light sources that will allow professionals to reach all the oral sites, are important developmental fields in oral aPDT. A PS such as methylene blue, a substance that is already approved by regulatory agencies in Europe and America, is already used in the oral cavity, but has to be further improved [17]. Alternatively it would be even better if a PS were to be specifically designed to be effective against oral biofilm.

3 Outlook

Oral aPDT is a reasonable, easy to perform therapy that presents enough compliance to be used in the oral cavity. With further research effort, it may become the first choice treatment for localized oral infections leaving antimicrobial prescriptions reserved for widespread infections where light and PS are not an option.

References

- [1] Parahitiyawa NB, Jin LJ, Leung WK, Yam WC, Samaranayake LP. Microbiology of odontogenic bacteremia: beyond endocarditis. Clin Microbiol Rev 2009;22(1):46-64.
- [2] Hashimoto M, Yamazaki T, Hamaguchi M, Morimoto T, Yamori M, Asai K, Isobe Y, Furu M, Ito H, Fujii T, Terao C, Mori M, Matsuo T, Yoshitomi H, Yamamoto K, Yamamoto W, Bessho K, Mimori T. Periodontitis and Porphyromonas gingivalis in preclinical stage of arthritis patients. PLoS One 2015;10(4):e0122121.
- [3] Cullinan MP, Seymour GJ. Periodontal disease and systemic illness: will the evidence ever be enough? Periodontol 2000 2013;62(1):271-86.
- [4] Donlan RM, Costerton JW. Biofilms: survival mechanisms of clinically relevant microorganisms. Clin Microbiol Rev 2002;15(2):167-93.
- [5] Alanis AJ. Resistance to antibiotics: are we in the post-antibiotic era? Arch Med Res 2005;36(6):697-705.
- [6] Petersen PE, Ogawa H. Strengthening the prevention of periodontal disease: the WHO approach. J Periodontol 2005;76(12):2187-93.
- [7] Roberts AP, Mullany P. Oral biofilms: a reservoir of transferable, bacterial, antimicrobial resistance. Expert Rev Anti Infect Ther 2010;8(12):1441-50.

- [8] Poveda Roda R, Bagan JV, Sanchis Bielsa JM, Carbonell Pastor E. Antibiotic use in dental practice. A review. Med Oral Patol Oral Cir Bucal 2007;12(3):E186-92.
- Usacheva MN, Teichert MC, Biel MA. Comparison of the methylene blue and toluidine blue photobactericidal efficacy against gram-positive and gram-negative microorganisms. Lasers Surg Med 2001;29(2):165-73.
- [10] Miyabe M, Junqueira JC, Costa AC, Jorge AO, Ribeiro MS, Feist IS. Effect of photodynamic therapy on clinical isolates of Staphylococcus spp. Braz Oral Res 2011;25(3):230-4.
- [11] de Souza SC, Junqueira JC, Balducci I, Koga-Ito CY, Munin E, Jorge AO. Photosensitization of different Candida species by low power laser light. J Photochem Photobiol B 2006;83(1):34-8.
- [12] Lyon JP, Moreira LM, de Moraes PC, dos Santos FV, de Resende MA. Photodynamic therapy for pathogenic fungi. Mycoses 2011:54(5):e265-71.
- [13] Wainwright M, Baptista MS. The application of photosensitisers to tropical pathogens in the blood supply. Photodiagnosis Photodyn Ther 2011;8(3):240-8.
- [14] Mitra S, Haidaris CG, Snell SB, Giesselman BR, Hupcher SM, Foster TH. Effective photosensitization and selectivity in vivo of Candida Albicans by meso-tetra (N-methyl-4-pyridyl) porphine tetra tosylate. Lasers Surg Med 2011;43(4):324-32.
- [15] Garcez AS, Nuñez SC, Hamblim MR, Suzuki H, Ribeiro MS. Photodynamic therapy associated with conventional endodontic treatment in patients with antibiotic-resistant microflora: a preliminary report. J Endod 2010;36(9):1463-6.
- [16] Scwingel AR, Barcessat AR, Núñez SC, Ribeiro MS. Antimicrobial photodynamic therapy in the treatment of oral candidiasis in HIV-infected patients. Photomed Laser Surg 2012;30(8):429-32.
- [17] Nuñez SC, Yoshimura TM, Ribeiro MS, Junqueira HC, Maciel C, Coutinho-Neto MD, Baptista MS. Urea enhances the photodynamic efficiency of methylene blue. J Photochem Photobiol B 2015:150:31-7.

[4.04] Photodynamic inactivation - An alternative strategy to combat sub-aerial biofilms

Annegret Preuß* and Beate Röder

Humboldt-Universität zu Berlin, Department of Physics, Photobiophysics Group, Newtonstraße 15, 12489 Berlin, Germany *Corresponding author: Dr. Annegret Preuß, apreuss@physik.hu-berlin.de

Abstract: Microorganisms, like bacteria, fungi and algae grow in biofilms on surfaces and provoke problems for human health, environment, and building fabrics. Conventional biocides and antibiotics are outdated because of the fast rising number of multi-resistant microorganisms and the environmental toxicity that they lead to. The photodynamic effect, originally used in photodynamic therapy has recently been introduced for the photodynamic inactivation (PDI) of microorganisms. We were able to show that PDI is a promising strategy to combat biofilm forming microorganisms and even the highly resistant conidia of mold fungi by attacking their cell walls from outside of the cells.

Keywords: photodynamic inactivation; singlet oxygen; biofilm; bacteria; mold fungi.

1 Introduction

Photodynamic inactivation (PDI) is an alternative strategy to combat microorganisms [1]. Especially the rising number of multi-resistant pathogens, such as methicillin-resistant Staphylococcus aureus (MRSA), makes alternative biocides a very important and pressing field of current research [2, 3]. The photodynamic effect is also widely used in photodynamic therapy (PDT), which has a broad field of application in human medicine e.g. in dermatology, oncology, and ophthalmology [4, 5]. Due to our long experience in the field of PDT research [5–9], it was a logical step to test whether singlet oxygen generating photosensitizers can be also used against microorganisms.

In addition to multi-resistant pathogens, environmental relevant microorganisms and their suppression is a very important field of research. Various microorganisms like mold fungi, green algae, and cyanobacteria provoke problems for human health, environment, and building fabrics leading to large economic losses [10]. As a result, many different biocides are discharged into the environment to combat them. Unfortunately the biocides themselves provoke new environmental and human health problems. Therefore the first sufficient results in PDI against pathogen bacteria makes the environmental relevant microorganisms a new and very interesting target for photodynamic treatment [11].

A particular challenge in the fight against environmental relevant microorganisms, growing on surfaces is their organization into biofilms. Biofilms are the most frequent form of microbial growth. The three-dimensional structure of the biofilms, their high diversity and the production of extracellular substances strongly increase the microorganism's resistance to environmental influences.

2 Own studies

Even though the diversity of microorganisms is extensive, they all have one characteristic in common. All microorganisms are protected by cell walls, and the integrity of the cell wall is essential for their reproduction. This fact had led to the idea that biofilm growth could be prevented by oxidative stress to the cell walls from outside of the cells, using photodynamic drugs immobilized in surfaces.

2.1 Photoinactivation of Escherichia coli

To proof the concept of PDI without intracellular uptake of the drug, a study was carried out with two different photosensitizers [12]. The two photosensitizers are cationic 5,10,15,20-tetrakis(N-methyl-4-pyridyl)-21H,23H-porphine (TMPyP) and the non-charged chlorine e6. Both compounds show a high singlet oxygen quantum yield; therefore they are high-potential photosensitizers. *Escherichia coli* (SURE2), a multi-resistant gram negative strain, was used as model organism for this study.

It could be shown by fluorescence lifetime imaging that none of the two compounds was taken up into the bacterial cells. Nevertheless, TMPyP shows a phototoxic effect to *E. coli*. In contrast to the cationic TMPyP, the none-charged chlorine e6 did not show any phototoxicity to the bacteria. In this study we could show, that it is possible to inactivate microorganisms by PDI without intracellular uptake of the photosensitizer. The second

outcome of these experiments was the observation that none-charged photosensitizer molecules, even if they are well-known photosensitizers for human cancer cells, have no phototoxic effect to microorganisms.

2.2 Photoinactivation of mold fungi

Mold fungi are a very frequently part of sub-aerial biofilms. They cause respiratory and skin diseases. Moreover, they can cause allergies and produce toxins which are carcinogenic, teratogenic or otherwise toxic. Thus they are an important focus of interest in our PDI research. Mold fungi are survivalist because of their highly resistant conidia. In another study [13], we could show the high potential of PDI to inhibit the growth of the mold fungi mycelium and fortunately even to inactivate the conidia. The investigated photosensitizers were developed and synthesized by the group of Zeev Gross at the Technion in Haifa, Israel. The four different corroles are two cationic and two anionic compounds. One cationic and one anionic corrole contained antimony as the central atom. As a new and very promising strategy, the other two corroles were modified with phosphorus as a central atom.

First of all we could show that all four compounds, the cationic and the anionic corroles were able to inhibit the growth of three different mold fungi: Aspergillus niger, Cladosporium cladosporoides, and Penicillium purpurgenum. Especially noteworthy was the success as PDI drugs of the cationic phosphor corroles. We could show that the cationic corroles were able to inactivate the mold fungi conidia. The inactivation of the conidia alone was enough to prevent the recovery of mold fungi after the PDI treatment. With this experiment we could prove the concept of PDI on mold fungi and their conidia and show cationic phosphor corroles to be a potential none-dark toxic photodynamic fungicides. Especially having phosphorus as a central atom is a powerful alternative to the toxic antimony for further application in the environment.

2.3 Photodynamic treatment of native biofilms

Following our preliminary studies on bacteria, mold fungi and green algae our final interest was the photodynamic treatment of native biofilms. Our first step away from the investigation of monocultures of lab grown organisms to the complex system of native sub-aerial biofilms was the harvest of outdoor biofilms and the cultivation of these microorganisms under reproducible conditions.

Our approx. 10-year old building of the Department of Physics is made of concrete, glass, steel and bamboo. All of these materials located on the outer walls are covered with biofilms (see Figure 1).

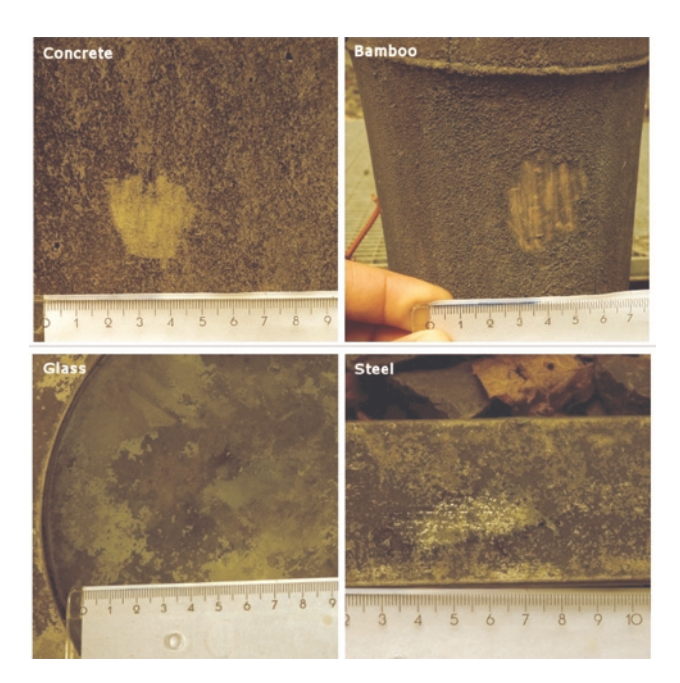


Figure 1: Sub-aerial biofilms growing on different materials on outdoor walls, images are taken after the harvest of microorganisms at concrete, bamboo, glass (bottom lamps), and steel.

These biofilms were the source of our collection of environmentally relevant biofilm-forming microorganism mixtures. Biofilms were scratched from the material using a spatula and suspended in Bold's basal medium (BBM) containing 5% Tween80 to suspend even very hydrophobic conidia. After homogenization the suspension was stored at -20°C for further investigation.

Cultivation of these microorganisms in different culture media, such as lysogeny broth agar plates, malt agar plates, and BBM agar plates showed very different results in the composition of microorganisms, as well as cultivation of microorganisms' probes harvested from different materials or from the same location and material but in different seasons in the same culture media. This illustrated the difficulty of reproducible cultivation of the native biofilm forming microorganisms. Nevertheless, we are currently working on methods for reproducible cultivation and study of biofilms.

First experiments to investigate PDI as a weapon against biofilm formation in surfaces were done in our group using wall paints containing cationic photosensitizers such as TMPyP and toluidine blue (TBO) (see Figure 2).

These first experiments showed a huge reduction in the growth of the microorganisms on the wall paints containing photosensitizers compared to the reference (wall paint without photosensitizer under illumination)

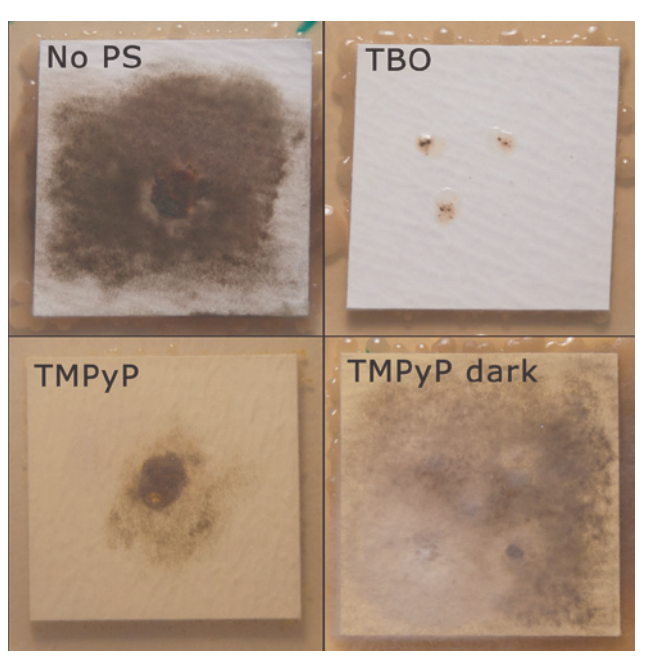


Figure 2: Photo- and dark toxicity of toluidine blue (TBO) and cationic 5,10,15,20-tetrakis(N-methyl-4-pyridyl)-21H,23H-porphine (TMPyP) in wall paint on a mixture of biofilm forming microorganisms. No PS: Reference without photosensitizer (PS), TBO: wall paint with 0.1% TBO, TMPyP: wall paint with 0.1% TMPyP, TMPyP dark: dark control with TMPyP but grown in darkness. The wall paint was applied to a 1-mm thick filter paper which was placed on 10% malt agar plates. 10 µl of the microorganism suspension were placed on the wall paint und incubated for 3 weeks in 12-h illumination/darkness cycles. Illumination by day light bulb of ~5 mW/cm².

and to the dark control (wall paint with photosensitizers incubated in darkness).

3 Conclusion

Our research results led to our optimistic conclusion that PDI using immobilized cationic photosensitizers is a promising strategy to prevent biofilm formation on surfaces. We hope that further investigations will help to realize the development of photoactive self-disinfectant surfaces as an alternative to the polluting and the harmful use of biocides.

- [1] Hamblin MR, Jori G, editors. Photodynamic inactivation of microbial pathogens: medical and environmental applications. Comprehensive series in photochemistry and photobiology. Cambridge: RSC Publishing; 2011.
- [2] Arias CA, Murray BE. Antibiotic-resistant bugs in the 21st century - A clinical super-challenge. N Engl J Med 2009;360(5):439-43.
- [3] Rice LB. Federal funding for the study of antimicrobial resistance in nosocomial pathogens: no ESKAPE. J Infect Dis 2008;197(8):1079-81.

- [4] Moan J, Peng Q. An outline of the history of PDT. In: Patrice T, editor. Photodynamic therapy. Comprehensive series in photochemical & photobiological sciences. Cambridge: RSC Publishing; 2003, p. 1-18.
- [5] Röder B. Photodynamic therapy. In: Meyers RA, editor. Encyclopedia of analytical chemistry: applications, theory, and instrumentation. Chichester: John Wiley & Sons; 2006, p. 1-20.
- [6] Chen K, Preuss A, Hackbarth S, Wacker M, Langer K, Röder B. Novel photosensitizer-protein nanoparticles for photodynamic therapy: photophysical characterization and in vitro investigations. J Photochem Photobiol B 2009;96(1):66-74.
- [7] Hackbarth S, Schlothauer J, Preuss A, Röder B. New insights to primary photodynamic effects - Singlet oxygen kinetics in living cells. J Photochem Photobiol B 2010;98(3):173-9.
- [8] Wacker M. Chen K. Preuss A. Possemever K. Roeder B. Langer K. Photosensitizer loaded HSA nanoparticles. I: preparation and photophysical properties. Int J Pharm 2010;393(1-2):253-62.

- [9] Preuss A, Chen K, Hackbarth S, Wacker M, Langer K, Röder B. Photosensitizer loaded HSA nanoparticles II: in vitro investigations. Int J Pharm 2011;404(1-2):308-16.
- [10] Pohl J, Saltsman I, Mahammed A, Gross Z, Röder B. Inhibition of green algae growth by corrole-based photosensitizers. J Appl Microbiol 2015;118(2):305-12.
- [11] Pohl J. Preuß A, Röder B. Photodynamic inactivation of microorganisms. In: Nonell S, Flors C, editors. Singlet oxygen: applications in biosciences and nanosciences. Cambridge: RSC Publishing; 2015.
- [12] Preuss A, Zeugner L, Hackbarth S, Faustino MA, Neves MG, Cavaleiro JA, Roeder B. Photoinactivation of Escherichia coli (SURE2) without intracellular uptake of the photosensitizer. J Appl Microbiol 2013;114(1):36-43.
- [13] Preuß A, Saltsman I, Mahammed A, Pfitzner M, Goldberg I, Gross Z, Röder B. Photodynamic inactivation of mold fungi spores by newly developed charged corroles. J Photochem Photobiol B 2014;133:39-46.

[4.05] Photodynamic inactivation of phototrophic microorganisms

Judith Pohl and Beate Röder*

Humboldt-Universität zu Berlin, Department of Physics, Photobiophysics Group, Newtonstraße 15, 12489 Berlin, Germany *Corresponding author: Prof. Dr. Beate Röder, roeder@physik.hu-berlin.de

Abstract: Phototrophic microorganisms as primary colonizers play a key role in formation of biofilms on outdoor surfaces. The biodeterioration of said surfaces arising from those biofilms motivates research for means of biofilm inhibition without impact on surrounding ecosystems. Photodynamic inactivation has a high potential as an alternative antimicrobial agent, its light-induced mechanism making it especially suited for inhibition of phototrophic microorganisms. Recent advances in this field - including the first successful applications on green algae and mixed fresh water cultures - are reported here.

Keywords: photodynamic inactivation; singlet oxygen; green algae; biofilms; phototrophic microorganisms.

1 Introduction

Microorganisms growing and forming biofilms on manmade surfaces play a significant role in distribution of infections and biodeterioration of said surfaces. Amongst those microorganisms, the phototrophic ones have a key role for formation of biofilms on outdoor surfaces; since due to their autotrophic growth they are primary colonizers, starting the formation of biofilms and facilitating growth of other microorganisms. Since it was shown in 2000 that biofilms have a devastatingly stimulating effect on biodeterioration of construction materials, numerous efforts are devoted to their removal

or the reduction of their growth. Well established means as the mechanical removal or the use of biocides come with side effects like high costs coupled with fast recurrence of the biofilms or the involved environmental risks respectively [1–3].

At the same time, biofilms show higher resistances towards every facet of change in environmental factors such as humidity, nutritional factors or chemical compounds such as antibiotics or biocides, thus making their removal an even bigger challenge [3-5]. Photocatalytic or other light-induced mechanisms are promising as means against phototrophic microorganisms especially, because those as well rely on light for their growth. Photoactive surfaces comprised of semiconductors like TiO, which are based on generation of hydrogen peroxide upon illumination are already commercially available as coatings of building materials [6, 7]. Unfortunately, with long time weathering they revealed shortcomings [8, 9] and their functional principle suggests these resulting from generation of NO, species during degeneration of microorganisms on these surfaces, which may then act as fertilizers for successive microorganisms [10-12].

2 Photodynamic inactivation

Photodynamic inactivation, relying on the photodynamic effect for generation of singlet oxygen, also has high potential as countermeasure against phototrophic microorganisms. Especially the availability of light and oxygen on growth sites of phototrophic organisms makes it suitable for this purpose. The absence of reported resistances against singlet oxygen - as opposed to hydrogen peroxide - gives this method another advantage. Most remarkably, until now only few efforts have been made to adopt photodynamic inactivation for inhibition of phototrophic organisms. This may partially be due to the presence of molecules like carotenoids which act as quenchers for singlet oxygen naturally produced during photosynthesis. These then also pose the risk of diminishing the effects of singlet oxygen intracellularly produced by photosensitizers.

Despite this availability of intracellular quenchers, a successful photodynamic inactivation of green algae was reported recently. Using cationic metallocorroles, Pohl et al. [13] demonstrated a significant photosensitizationinduced reduction of biomass in incubated samples after 4 days of discontinuous illumination in a 12 h:12 h rhythm. The reduction of biomass continued over a time span of 18 days, resulting in bleaching of the algae and no recurrence of cell growth. Moreover, those results were compared to the ones obtained by incubation with similar anionic metallocorroles, which only resulted in small reduction of growth rates in the green algae. This is in accordance to the work previously published by Drábková et al. [14], suggesting cationic photosensitizers to be more suitable for inactivation of phototrophic microorganisms.

Following this line of evidence, the effect of multi cationic porphyrins on green algae as well as a mixed phototrophic freshwater culture (sampled from a fish tank at the Physics Department of Humboldt-Universität zu Berlin) was investigated using the protocol described in [13]. Surprisingly, the course of the biomass in green algae samples showed only meager reduction of the growth rate with no reduction of biomass. However, administered to the mixed freshwater culture, the same photosensitizers demonstrated cytostatic properties [15]. This result suggests mixed phototrophic cultures to be more sensitive towards photodynamic inactivation. A possible explanation for the effect observed lies in the symbiotic dependencies often occurring in biofilms. Targeting of influential bottleneck organisms in microbial communities may thus be a powerful strategy for inhibition of phototrophic cultures. Though further investigations concerning the cause of the results are necessary, clearly this also makes it impossible to predict effects of photodynamic inactivation on mixed cultures based on data obtained from monocultures.

3 Conclusion and outlook

Despite recent breakthroughs in the field of photodynamic inactivation of phototrophic microorganisms, investigations are still at the beginning. The method of photodynamic inactivation shows high potential as an alternative treatment not only against phototrophic microorganisms but also against all biofilms occurring on outdoor surfaces. Therefore, this initial research should be followed by further investigations towards the means of photosensitization of phototrophic organisms, the preparation of model cultures for mixed biofilms as well as the effects arising from use of these mixed cultures.

- [1] Aminov RI. The role of antibiotics and antibiotic resistance in nature. Environ Microbiol 2009;11(12):2970-88.
- [2] Warscheid T, Braams J. Biodeterioration of stone: a review. Int Biodeter Biodegr 2000;46(4):343-68.
- Young ME, Alakomi HL, Fortune I, Gorbushina AA, Krumbein WE, Maxwell I, McCullagh C, Robertson P, Saarela M, Valero J, Vendrell M. Development of a biocidal treatment regime to inhibit biological growths on cultural heritage: BIODAM. Environ Geol 2008;56(3-4):631-41.
- [4] Flemming HC, Wingender J, Griebe T, Mayer C. Physicochemical properties of biofilms. In: Evans LV, editor. Biofilms: recent advances in their study and control. Amsterdam: Harwood Academic Publishers; 2005, p. 19-34.
- [5] Davies DG. Biofilm dispersion. In: Flemming HC, Wingender J, Szewzyk U, editors. Biofilm highlights. Berlin and Heidelberg: Springer-Verlag; 2011, p. 1-28.
- [6] Hashimoto K, Irie H, Fujishima A. TiO, photocatalysis: a historical overview and future prospects. Jpn J Appl Phys 2005;44(12):8269-85.
- [7] Fujishima A, Zhang X, Tryk DA. Heterogeneous photocatalysis: From water photolysis to applications in environmental cleanup. Int J Hydrogen Energ 2007;32(14):2664-72.
- [8] Gladis F, Schumann R. A suggested standardised method for testing photocatalytic inactivation of aeroterrestrial algal growth on TiO2-coated glass. Int Biodeter Biodegr 2011;65(3):415-22.
- [9] Gladis F, Schumann R. Influence of material properties and photocatalysis on phototrophic growth in multi-year roof weathering. Int Biodeter Biodegr 2011;65(1):36-44.
- [10] Dalton JS, Janes PA, Jones NG, Nicholson JA, Hallam KR, Allen GC. Photocatalytic oxidation of NO, gases using TiO,: a surface spectroscopic approach. Environ Pollut 2002;120(2):415-22.
- Donaldson MA, Berke AE, Raff JD. Uptake of gas phase nitrous [11] acid onto boundary layer soil surfaces. Environ Sci Technol 2014;48(1):375-83.
- Kebede MA, Scharko NK, Appelt LE, Raff JD. Formation of nitrous acid during ammonia photooxidation on TiO, under atmospherically relevant conditions. J Phys Chem Lett 2013;4(16):2618-23.
- [13] Pohl J, Saltsman I, Mahammed A, Gross Z, Röder B. Inhibition of green algae growth by corrole-based photosensitizers. J Appl Microbiol 2015;118(2):305-12.
- [14] Drábková M, Marsálek B, Admiraal W. Photodynamic therapy against cyanobacteria. Environ Toxicol 2007;22(1):112-5.
- Pohl J, Jux N, Röder B. Private communication and unpublished results.

[4.06] Staphylococcus aureus and Pseudomonas aeruginosa

Ying Wang, Yucheng Wang, Sumin Wu, Xuesong Wang, Jiyong Yang, Yanping Luo and Ying Gu* Department of Laser Medicine, Chinese People's Liberation Army General Hospital, Beijing 100853, China *Corresponding author: Prof. Ying Gu, guyinglaser@sina.com

Abstract: *Staphylococcus aureus* and *Pseudomonas aeruginosa* are typical Gram-positive and Gram-negative bacteria, respectively. In the last two decades, they were the most common multidrug-resistant bacteria both in hospitals and community. One reason is attributed to the abuse of antibiotics. The other one is the formation of biolfilm. In this study, we investigated the effectiveness of photodynamic inactivation (PDI) mediated by three Ru(II) polypyridine complexes against four isolates of clinical methicillin-resistant *Staphylococcus aureus* (MRSA) and four isolates of *Pseudomonas aeruginosa* (one wild strain and three clinical isolated strains).

Keywords: photodynamic inactivation (PDI); methicillinresistant *Staphylococcus aureus* (MRSA); *Pseudomonas aeruginosa*; biolfilm.

1 Background

Photosensitizer-mediated antimicrobial photodynamic therapy (PDT) appears to be a promising approach for treating multidrug-resistant bacteria. Many studies had shown that PDT presents selective toxicity to microbe over eukaryocyte. In the past three years, we cooperated with Prof. Wang Xuesong from the Chinese Academy of Sciences to select potential antimicrobal photosensitizers. In this report, we present our results with three Ru(II) complexes; the surrounding ligands are showed in [1]. The three complexes (1, 2, 3) has a high singlet oxygen quantum yield. Photosensitizers with cationic and amphipathic properties are thought to be easy to bind with bacteria. The aim of this study was to quantify the antimicrobial PDT effect of Ru(II) complexes against multidrug-resistant Staphylococcus aureus (MRSA) and Pseudomonas aeruginosa, and to observe the ultrastructure changes induced by PDT.

2 Methods and results

Firstly, the killing effect on planktonic cultures using the dilution-plate method was examined. Then, the ultrastructure changes induced by PDT were observed using electron microscope. Finally, the eradication effect on biofilm was explored.

MRSA is the most common multidrug resistant strain among *S. aureus*. Four clinical isolates of MRSA (MRSA-1, MRSA-2, MRSA-3 and MRSA-4) were used in this study.

They were all collected from sputum specimen of patients. Their sensitivity to commonly used antibiotics was tested using the paper disc diffusion method. The results are shown in [1]. The sensitivity of four *P. aeruginosa* strains (one wild strain – PAO1, and three clinical isolates) was also tested. The results showed that they are all multidrugresistant strains.

According to the absorption spectra and molar extinction coefficients of these three complexes, 457 nm was used for the excitation of complex 2 and complex 3, and 532 nm used for the excitation of complex 1. In the PDT group, cell suspensions were incubated with photosensitizer of different concentrations for 30 min in 48-well plate. Illumination for 10 min was then performed with the plate covered at a power density of 40 mW/cm². Colony-forming unit (CFU) assays were used to determine the viability of bacteria. The results showed that no detectable reduction in cell viability was induced in control groups (P-L-). This result of PDT groups showed that for complex 2 and complex 3 (Figure 1), bacterial viability decreased with photosensitizer concentrations increasing, while for complex 1, when photosensitizer concentration increased to 25 μM and 50 μM, the bacterial viability did not increase.

The minimal bactericidal concentration (MBC) was calculated to compare the killing effect of these three complexes. MBC of complex 2 and complex 3 were similar. The

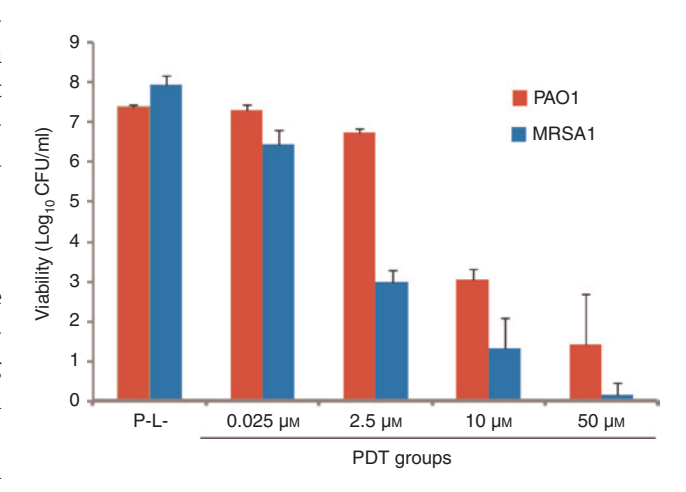


Figure 1: The killing effect of Ru3 (complex 3) on planktonic MRSA-1 and planktonic PAO1, one wild strain of *P. aeruginosa*.

killing effect of complex 2 and complex 3 is significantly stronger than that of complex 1.

To analyze the reason, complex 3 has the highest singlet oxygen quantum yield and molar extinction coefficient among the three complexes. There is a dppn ligand [1], which can insert unto the phospholipid biolayer of cell membrane and stabilize the binding to bacteria. While complex 1 has the lowest singlet oxygen quantum yield and molar extinction coefficient, and less easily be bind with bacteria.

To further determine the PDT efficacy for other strains, MRSA-2, MRSA-3 and MRSA-4 were also tested. The PDT activity of complex 3 was assessed and compared with that of methylene blue (MB), which is the gold standard photosensitizer for antimicrobal PDT. The experimental conditions were the same as those described above. After treatment, samples without dilution were spotted (10 µl/spot) on Mueller-Hinton agar and grown overnight. Colonies from the three strains can almost be completely inactivated at 2.5 µM. However, for MB, complete inactivation was not achieved even at 25 µM.

The killing effect result of complex 3 on planktonic P. aeruginosa showed that the MBC of complex 3 for the four P. aeruginosa isolates is 10 μM, which is higher than the MBC of complex 3 for MRSA. This suggests that MRSA is more sensitive than *P. aeruginosa*.

The transmission electron microscope picture of S. aureus is also shown in [1]. The cell envelope is intact and smooth in control group. Immediately after PDT, the cell envelope became irregular, and vesicles were found to protrude mainly from surface. About 30 min after PDT, cell surfaces were even less well-defined, and leakage of cellular content was observed.

For P. aeruginosa, the outer wall and inner plasma membrane of control sample are intact and the electron density is evenly distributed. Immediately after PDT, incontinuous cell envelope can be seen, both inner membrane and outer wall were damaged. The damage of the inner membrane permits the leakage of the cytoplasm, which is seen as bubble formation on the surface of outer membrane. For a severe damage, the cytoplasm was released from the cell and the whole cell ended up "burst". These results are published in [2].

To further investigate the effect of PDT on the structures of biofilms, SEM studies were carried out. Ru3-PDT can eradicate the biofilms of MRSA [1] and P. aeruginosa [3]. The size of aggregates and the number of adherent bacteria significantly reduced. According to the ultrastructure changes observed in this study, we presume that the membrane of cells was possibly the superior target in PDT process. Reactive oxygen species disturb the structural integrity, permeability, physiological function, etc.

3 Conclusion

Based on the present results, we concluded Ru(II) complexes; especially Ru3 are potential candidates for the effective photodynamic control of multidrug resistant S. aureus and P. aeruginosa. PDT induces bacterial death by damaging cell membrane.

Acknowledgments: The study was supported by Nature Science Foundation of China (Grant numbers: '81171633' and '21172228') and Nature Science Foundation of Beijing (Grant number: '4132079').

- [1] Wang Y, Zhou Q, Wang Y, Ren J, Zhao H, Wu S, Yang J, Zhen J, Luo Y, Wang X, Gu Y. In vitro photodynamic inactivation effects of Ru(II) complexes on clinical methicillin-resistant Staphylococcus aureus planktonic and biofilm cultures. Photochem Photobiol 2015;91(1):124-33.
- [2] Wu S, Wang Y, Zhen J, Wang Y, Gu Y. Antibacterial activity of Ru photosensitizer: An in vitro study on Pseudomonas aeruginosa strains. Chin J Laser Med Surg 2014;23(1):1-57.
- Wu S, Wang Y, Gu Y. Photodynamic antibacterial activity on [3] Pseudomonas aeruginosa in planktonic and biolfilm culture in vitro. Chin J Laser Med Surg 2014;23(2):59-63.

Session 5: Enhancement of singlet oxygen generation

[5.01] Development of smart photosensitizers for photodynamic therapy

Pui-Chi Lo^{1,2}, Xiong-Jie Jiang¹, Janet T. F. Lau¹, Hui He¹, Mei-Rong Ke¹ and Dennis K. P. Ng^{1,*}

¹Department of Chemistry, The Chinese University of Hong Kong, Shatin, N.T., Hong Kong

²Department of Biomedical Sciences, City University of Hong Kong, Tat Chee Avenue, Kowloon, Hong Kong

*Corresponding author: Prof. Dennis K. P. Ng, dkpn@cuhk.edu.hk

Abstract: Being a crucial component in photodynamic therapy, photosensitizers have been studied extensively with a view to enhancing their tumor selectivity and photodynamic activity. As an innovative and promising approach, "smart" photosensitizers that can be selectively activated by tumor-associated stimuli have recently been reported. We have been inspired by this strategy and extended our study of phthalocyanine-based photosensitizers to incorporate a control unit for their photophysical and photobiological properties. This article highlights our recent endeavor in developing pH-and thiol-responsive photosensitizers toward targeted photodynamic therapy.

Keywords: photodynamic therapy; photosensitizers; phthalocyanines; singlet oxygen.

1 Introduction

Photodynamic therapy (PDT) has emerged as a treatment modality for cancer and some other noncancerous conditions [1]. It involves the combined action of three individually nontoxic components, namely a photosensitizer, light of appropriate wavelength, and oxygen to generate cytotoxic reactive oxygen species (ROS). These species, predominantly singlet oxygen, eradicate tumors by multiple mechanisms, including killing malignant cells by apoptosis and/or necrosis, shutting down tumor vasculature, and stimulating the host immune system [2]. To date, only a few photosensitizers have been clinically approved for oncologic indication and they still suffer from some disadvantages such as weak absorptions in the body's therapeutic window (650-800 nm), sustained skin photosensitivity, and long drug-to-light intervals (48–96 h). As a result, there has been considerable interest in exploring various strategies to improve their therapeutic efficacy [3].

Inspired by the activatable fluorescent probes for bioanalytes, "smart" photosensitizers that can be selectively activated by tumor-associated stimuli have received much current attention [4]. In these systems, the photosensitizers are either self-quenched due to aggregation or deactivated by the neighboring quenchers.

Upon interaction with the stimuli, such as the acidic and reducing environment of tumors, cancer-related proteases, or mRNAs that have high tumor specificity, the photosensitizers are disaggregated or detached from the quenchers, resulting in restoration of their fluorescence and photosensitizing properties. This approach can therefore minimize the damage to normal tissues. As part of our continuing interest in the development of efficient phthalocyanine-based photosensitizers [5], we have extended the study to their activatable analogues, focusing on those which are responsive toward acids and thiols, which can mimic the acidic and reducing environment of malignant tissues.

2 Methods and results

As the first series of these photosensitizers, silicon(IV) phthalocyanines with two axial amine-containing substituents were prepared, of which the electronic absorption,

Figure 1: Chemical structures of pH-responsive photosensitizers 1–3.

fluorescence, and photosensitizing properties could be modulated by pH [6, 7]. Compounds 1 and 2 (Figure 1) exhibited the most desirable changes in the pH range of 6.0-7.4, which can roughly differentiate the tumor and normal tissue environments. Their intracellular fluorescence intensity and efficiency in generating singlet oxygen and superoxide radical were greatly enhanced at lower pH, mainly due to protonation of the amino groups which inhibited the intramolecular photoinduced electron transfer process. Compound 3 (Figure 1) is another pH-responsive photosensitizer, which is composed of a

self-quenched phthalocyanine dimer [8]. It can be activated in an acidic environment (pH=5.0-6.5) as a result of cleavage of the ketal linker and separation of the phthalocyanine units, resulting in enhanced fluorescence emission and ROS production, both in solution and in vitro.

By using ferrocenyl moieties as quenchers, we also prepared the hydrazone-linked conjugate 4 (Figure 2) [9]. Its fluorescence intensity increased by 6-fold when the pH decreased from 7.4 to 4.5 in phosphate buffered saline (PBS), and by 10-fold when the pH decreased from 7.4 to 5.0 inside MCF-7 human breast cancer cells, using

Figure 2: Chemical structures of activatable photosensitizers 4-7.

nigericin to temporary equilibrate the intracellular and extracellular pH. The results indicated the occurrence of hydrolytic cleavage of the hydrazone bonds under an acidic condition and that the detachment of the ferrocenyl quenchers restored the fluorescence emission. By using a disulfide instead of hydrazone linker, a related conjugate 5 (Figure 2) was also prepared, which was responsive toward dithiothreitol (DTT) [10]. Apart from the enhancement in fluorescence emission and singlet oxygen production, the in vitro photodynamic activity of this compound was also promoted by DTT. The IC_{ro} value, defined as the dye concentration required to kill 50% of the cells, against MCF-7 cells decreased from 124 nm to 50 nm when the cells were pre-incubated with 4 mm of DTT.

As an extension of this work, a novel dual activatable analogue was also synthesized [9]. Having both an acid-labile hydrazone linker and a DTT-cleavable disulfide linker, compound 6 (Figure 2) functioned as a dual pHand redox-responsive photosensitizer. Its fluorescence intensity, singlet oxygen generation efficiency, intracellular fluorescence, and in vitro photodynamic activity were enhanced in a slightly acidic environment (pH=4.5-6.0) or in the presence of DTT (in mm range). The greatest enhancement could be attained when both of these two conditions occurred. The activation of this compound was also demonstrated in tumor-bearing nude mice. The intratumoral fluorescence of 6 was greatly increased within 10 h after injection, while that of a noncleavable control was negligible, showing that the fluorescence of 6 could also be restored inside the tumor. In addition, this compound could also effectively inhibit the growth of tumor upon illumination.

Recently, we have also reported another simple vet very efficient activatable photosensitizer (compound 7, Figure 2) [11]. This compound can be prepared readily by treating 2-hydroxy zinc(II) phthalocyanine with 2,4-dinitrobenzenesulfonyl chloride in the presence of triethylamine. Upon interaction with glutathione (GSH), the 2,4-dinitrobenzenesulfonyl quencher is detached from the phthalocyanine. Its fluoresence emission and ROS generation are greatly enhanced in PBS and inside MCF-7 cells. Similarly, the fluorescence activation has also been

demonstrated in vivo. On the basis that the intracellular GSH level is in the mm range and tumor tissues generally have an elevated GSH concentration compared with normal tissues, this GSH-activated system serves as a promising tumor-selective photosensitizer.

3 Conclusion

In summary, we have reported a number of activatable phthalocyanine-based photosensitizers and demonstrated their pH- and thiol-responsive bahavior. The results show that they are promising candidates which could be modified further toward targeted PDT.

- [1] Dolmans DE, Fukumura D, Jain RK. Photodynamic therapy for cancer. Nat Rev Cancer 2003;3(5):380-7.
- Castano AP, Mroz P, Hamblin MR. Photodynamic therapy and anti-tumour immunity. Nat Rev Cancer 2006;6(7):535-45.
- Lim CK, Heo J, Shin S, Jeong K, Seo YH, Jang WD, Park CR, Park SY, Kim S, Kwon IC. Nanophotosensitizers toward advanced photodynamic therapy of cancer. Cancer Lett 2013:334(2):176-87.
- [4] Lovell JF, Liu TW, Chen J, Zheng G. Activatable photosensitizers for imaging and therapy. Chem Rev 2010;110(5):2839-57.
- [5] Ng DK. Phthalocyanine-based photosensitizers: more efficient photodynamic therapy? Future Med Chem 2014;6(18):1991-3.
- [6] Jiang XJ, Lo PC, Tsang YM, Yeung SL, Fong WP, Ng DK. Phthalocyanine-polyamine conjugates as pH-controlled photosensitizers for photodynamic therapy. Chemistry 2010;16(16): 4777-83.
- [7] Jiang XJ, Lo PC, Yeung SL, Fong WP, Ng DK. A pH-responsive fluorescence probe and photosensitiser based on a tetraamino silicon(IV) phthalocyanine. Chem Commun (Camb) 2010;46(18):3188-90.
- [8] Ke MR, Ng DK, Lo PC. A pH-responsive fluorescent probe and photosensitiser based on a self-quenched phthalocyanine dimer. Chem Commun (Camb) 2012;48(72):9065-7.
- [9] Lau JT, Lo PC, Jiang XJ, Wang Q, Ng DK. A dual activatable photosensitizer toward targeted photodynamic therapy. J Med Chem 2014;57(10):4088-97.
- [10] Lau JT, Jiang XJ, Ng DK, Lo PC. A disulfide-linked conjugate of ferrocenyl chalcone and silicon(IV) phthalocyanine as an activatable photosensitiser. Chem Commun (Camb) 2013;49(39):4274-6.
- [11] He H, Lo PC, Ng DK. A glutathione-activated phthalocyaninebased photosensitizer for photodynamic therapy. Chemistry 2014;20(21):6241-5.

[5.02] Multifunctional nanoprobes for targeted imaging and photodynamic therapy of gastric cancer

Daxiang Cui*

Institute of Nano Biomedicine and Engineering, Key Laboratory for Thin Film and Microfabrication Technology of the Ministry of Education, Department of Instrument Science and Engineering, National Center for Translational Medicine, Shanghai Jiao Tong University, 800 Dongchuan Road, Shanghai 200240, China

*Corresponding author: Prof. Daxiang Cui, dxcui@sjtu.edu.cn

Abstract: Gastric cancer is the second most common cancer in China, and is the second leading cause of cancerrelated death worldwide. Successful development of safe and effective nanoprobes for targeted imaging and photodynamic therapy (PDT) of gastric cancer has become a hotspot [1]. Here, three types of gold nanoparticles such as gold nanorods, gold nanoprisms, and gold nanoclusters were prepared, and conjugated with chlorin e6 (Ce6) and folic acid. The resulting folic acid-Ce6-conjugated gold nanorods, folic acid-Ce6-conjugated gold nanoprisms and folic acid-Ce6-conjugated gold nanoclusters were used for in vitro and in vivo targeted imaging and PDT of gastric cancer. Results showed that the prepared three types of nanoprobes could bind with gastric cancer cell line MGC803 specifically, and exhibited photodynamic therapeutic effects, inducing cell apoptosis, markedly inhibiting growth of gastric cancer cells. In-vivo experiment results showed that the three types of gold nanoprobes could target gastric cancer, and realized targeted fluorescent imaging, photoacoustic imaging and PDT, especially gold nanoclusters can enhance Ce6 photodynamic therapeutic efficacy, and could be excreted from kidney, owns good biocompatibility. In conclusion, the prepared three types of gold nanoprobes could be used for targeted imaging and PDT of gastric cancer, and exhibit clinical translation prospect.

Keywords: gold nanorods; gold nanoprisms; gold nanoclusters; Ce6; fluorescent imaging; photodynamic therapy.

Reference

[1] Zhang C, Li C, Liu Y, Zhang J, Bao C, Liang S, Wang Q, Yang Y, Fu H, Wang K, Cui D. Gold nanoclusters-based nanoprobes for simultaneous fluorescence imaging and targeted photodynamic therapy with superior penetration and retention behavior in tumors. Adv Funct Mater 2015;25(8):1314-25.

[5.03] Plasmonic nanostructures: New photosensitizers or plasmonic photocatalysts

Zhang Hui^{1,2}, Liu Wenqi^{1,2}, Tao Wen^{1,2} and Xiaochun Wu^{1,*}

¹CAS Key Laboratory of Standardization and Measurement for Nanotechnology, National Center for Nanoscience and Technology, Beijing 100190, China

²University of the Chinese Academy of Sciences, Beijing 100049, China

*Corresponding author: Prof. Dr. Xiaochun Wu, wuxc@nanoctr.cn

Abstract: Recently, noble metal nanoparticles (NMPs) have been demonstrated as a new kind of photosensitizers (PSs). However, in comparison with traditional PSs, the exact photosensitization mechanism is still elusive. As is known that plasmon-enhanced photocatalysis has been observed from many different NMPs. It therefore raises an interesting question of how to understand their activation of molecular oxygen.

Keywords: photosensitizers; noble metal nanostructures; plasmon; photocatalysts.

1 Introduction

Owing to the tailorable near-infrared (NIR) localized surface plasmon resonance (LSPR) features of gold nanostructures, such as nanorods (NRs), cages, gold coated SiO₃ spheres, they have attracted significant attention in disease diagnosis and treatment, such as LSPRenhanced imaging and photothermal therapy.

In 2011, the research group led by Hwang [1] found that upon excitation of LSPR, noble metal nanoparticles (gold, Au; silver, Ag; platinum, Pt; and palladium, Pd) are able to generate singlet oxygen (${}^{1}O_{2}$). The ${}^{1}O_{2}$ generation has been demonstrated directly by 10, phosphorescence, or indirectly by ¹O₂ probes or ¹O₂ specific reactions. Later, the same group further reported that sensitization and formation of singlet oxygen is strongly dependent on the shapes of gold and silver nanostructures [2]. For instance, silver decahedrons and triangular nanoplates exposed {111} facets can generate 10, but not Ag nanocubes. In contrast, Au

nanoparticles (NPs) show the opposite trend. These studies indicate that activation of molecular oxygen is closely related to the material composition and exposed facets. Recently, the same researchers further demonstrated the AuNRs photodynamic therapy (PDT) in destructing B16F0 melanoma tumor cells in mice. Apart from producing $^1\mathrm{O}_2$ (type II-like PS), noble metal nanoparticles (NMPs) are reported to act as type I-like PS as they are observed to generate OH free radical upon LSPR excitation. Considering the high tunability in size, shape, composition and structure, noble metal nanostructures may become a new kind of highly attractive PS and find a place in the PDT.

2 Materials and methods

Using AuNRs as templates we have synthesized a series of noble metal nanostructures with NIR plasmonic responses, and investigated their catalytic activities in dark [3, 4]. Using 9,10-anthracenediyl-bis(methylene) dimalonic (ABD) as singlet oxygen probe, we observed

its enhanced photo-oxidation in the presence of Au and Pd, indicating the generation of $^{1}O_{2}$ [5]. Herein, we demonstrated this "sensitization" process for Pt nanodots. In order to have NIR plasmonic response, they were epitaxially deposited on the AuNR, denoted as Au@Pt nanodots on rod (NDRs), see Figure 1A.

3 Results

The obtained nanostructure has an obvious longitudinal surface plasmon resonance band around 790 nm. Upon LSPR excitation, the temperature of the reaction solutions increases due to photothermal effect (Figure 1B). Thermal treatment leads to slight increase in ABD degradation (Figure 1C); 3.2% at 44°C for 0.05 nm NDRs. In contrast, plasmonic excitation produces much more ABD degradation. It causes 14.3% reduction from pure plasmonic effect for the same NDRs concentration, indicating plasmonenhanced reactivity for Pt dots (Figure 1D). Additionally, an obvious dose-effect relationship is observed (Figure 1E).

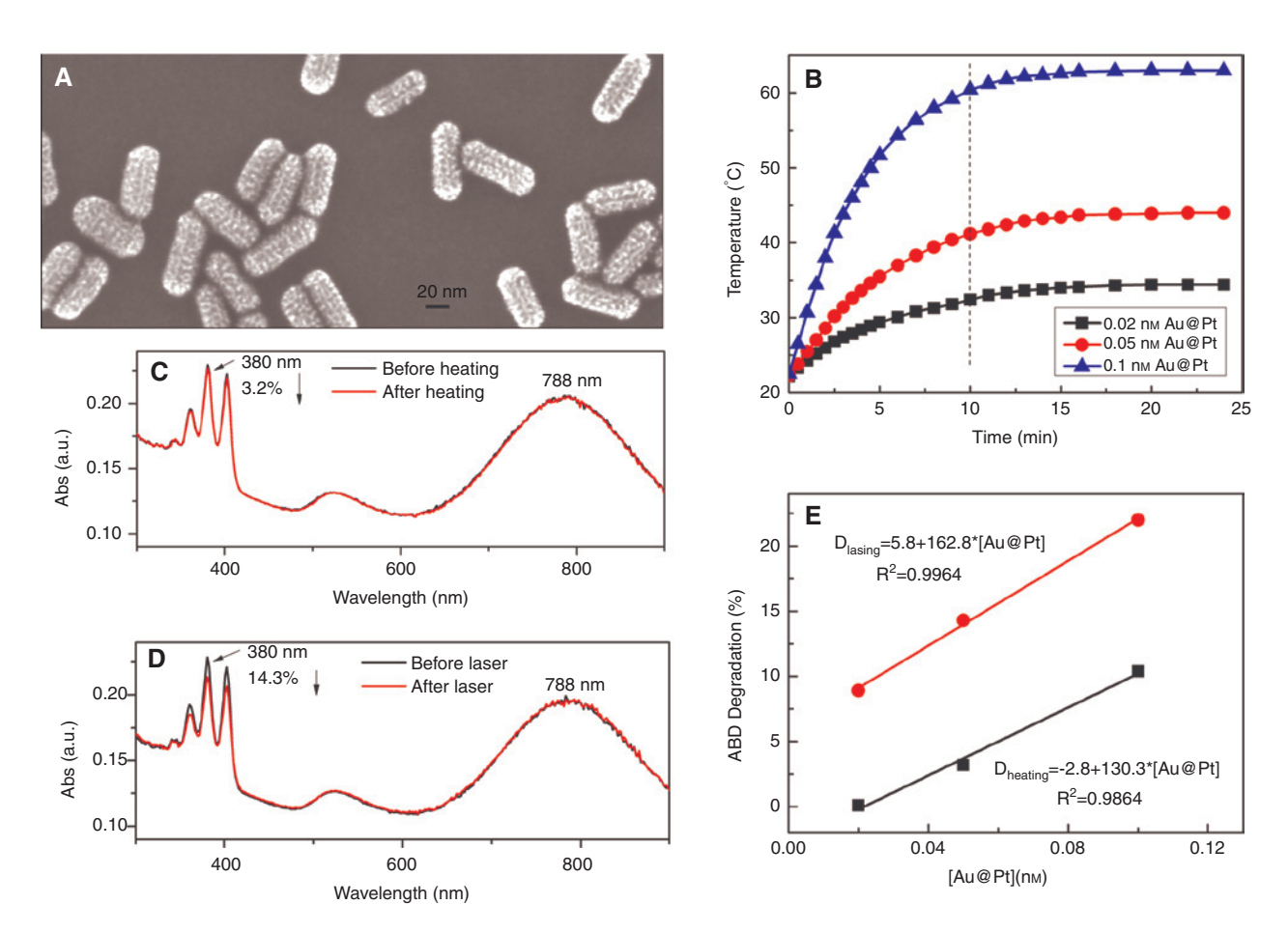


Figure 1: SEM image of Au@Pt NDRs (A), temperature rising curves of the NDR at three different concentrations (B) and effect of the NDRs on ABD (100 μ M) degradation: (C) 10 min thermal treatment, (D) 10 min irradiation with a continuous wave 808 nm laser, (E) effect of the NDR concentration. For (D), the sample is kept at the temperature after 10 min irradiation obtained from temperature rising curves in order to get pure plasmonic effect.

4 Conclusion

Generally, the generation of reactive oxygen species from plasmonic nanostructures upon LSPR excitation is understood as follows: Noble metal nanostructures first produce hot electrons upon light absorption. The hot electrons are then rapidly injected into molecluar oxygen and produce superoxide radical. At one hand, superoxide radicals themselves can initiate redox reactions. On the other hand, the hot holes of the excited nanostructures may capture electrons from superoxide radicals and this process can produce ¹O₂. The latter process is similar to the ¹O₂ generation from TiO₂ or ZnO particles upon irradiation. However, using electron spin resonance (ESR) method, we did not succeed in obtaining meaningful signals either for OH free radical or for ¹O₂ by using their corresponding ESR probes (BMPO for OH free radical and 4-oxo-TEMP for ¹O₂). Only a very weak signal is detected and shows no doseeffect relationship. It thus makes the identification of ¹O₂ and OH free radical as active oxygen species ambiguous. Based on the current research progress, we are sure about the plasmon-enhanced reactivity from NMPs. The exact active species from molecular oxygen activation cannot be identified unambiguously at the moment. We feel that it is

better to understand this phenomenon from the viewpoint of plasmonic photocatalysis.

Acknowledgment: The work was supported by National Natural Science Foundation of China (Grant number: '21173056').

References

- [1] Vankayala R, Sagadevan A, Vijayaraghavan P, Kuo CL, Hwang KC. Metal nanoparticles sensitize the formation of singlet oxygen. Angew Chem Int Ed Engl 2011;50(45):10640-4.
- [2] Vankayala R, Kuo CL, Sagadevan A, Chen PH, Chiang CS, Hwang KC. Morphology dependent photosensitization and formation of singlet oxygen by gold and silver nanoparticles and its application in cancer treatment. J Mater Chem B 2013;1: 4379-87.
- [3] Hou S, Hu X, Wen T, Liu W, Wu X. Core-shell noble metal nanostructures templated by gold nanorods. Adv Mater 2013:25(28):
- [4] Li J, Liu W, Wu X, Gao X. Mechanism of pH-switchable peroxidase and catalase-like activities of gold, silver, platinum and palladium. Biomaterials 2015;48:37-44.
- [5] Liu W, Zhang H, Wen T, Yan J, Hou S, Shi X, Hu Z, Ji Y, Wu X. Activation of oxygen-mediating pathway using copper ions: finetuning of growth kinetics in gold nanorod overgrowth. Langmuir 2014;30(41):12376-83.

[5.04] Localized electric field of plasmonic nanoplatform enhanced photodynamic tumor therapy

Yiye Li^{1,#}, Tao Wen^{2,#}, Ruifang Zhao¹, Xixi Liu^{1,3}, Tianjiao Ji¹, Hai Wang¹, Xiaowei Shi²,

Jian Shi¹, Jingyan Wei³, Yuliang Zhao¹, Xiaochun Wu^{2,*} and Guangjun Nie^{1,*}

¹CAS Key Laboratory for Biomedical Effects of Nanomaterials and Nanosafety, National Center for Nanoscience and Technology, Beijing 100190, China

²CAS Key Laboratory of Standardization and Measurement for Nanotechnology, National Center for Nanoscience and Technology, Beijing 100190, China

³College of Pharmaceutical Science, Jilin University, Changchun 130021, China

*Yiye Li and Tao Wen contributed equally to this work.

*Corresponding authors: Prof. Xiaochun Wu, wuxc@nanoctr.cn and Prof. Guangjun Nie, niegj@nanoctr.cn

Abstract: Near-infrared (NIR) plasmonic nanoparticles demonstrate great potential in disease theranostic applications. Herein a nanoplatform, composed of mesoporous silica-coated gold nanorods (AuNRs), is tailor-designed to optimize photodynamic therapy (PDT) for tumor based on the plasmonic effect. The surface plasmon resonance of AuNRs was fine-tuned to overlap with the exciton absorption of indocyanine green (ICG), a NIR photodynamic dye with poor photostability and low quantum yield. Such overlap greatly increases the singlet oxygen yield of incorporated ICG by maximizing the local field enhancement, and protecting the ICG molecules against photodegradation by virtue of the

high absorption cross section of the AuNRs. The silica shell strongly increased ICG payload with the additional benefit of enhancing ICG photostability by facilitating the formation of ICG aggregates. As-fabricated AuNR@ SiO₂-ICG nanoplatform enables trimodal imaging, NIR fluorescence from ICG, and two-photon luminescence/ photoacoustic tomography from the AuNRs. The integrated strategy significantly improved photodynamic destruction of breast tumor cells and inhibited the growth of orthotopic breast tumors in mice, with mild laser irradiation, through a synergistic effect of PDT and photothermal therapy. Our study highlights the effect of local field enhancement in PDT and demonstrates

the importance of systematic design of nanoplatform to greatly enhancing the antitumor efficacy.

Keywords: gold nanorod; local field enhancement; photosensitizer; photodynamic therapy; photothermal therapy.

1 Objective

A novel plasmon-enhanced photodynamic therapy (PDT) for breast tumor is successfully designed and validated by fabricating a nanoplatform composed of mesoporous silica-coated gold nanorods (AuNRs) incorporating indocyanine green (ICG) [1], a near-infrared (NIR) photodynamic dye with poor photostability and low quantum yield [2].

2 Methods

The localized surface plasmon resonance (LSPR) peak of the AuNR core has been regulated to overlap with the exciton band of ICG, thus increasing the absorption coefficient of incorporated ICG by virtue of the localized electric field effect [3]. Such overlap also helps to protect the loaded ICG from photodegradation based on ~10⁶ higher absorbance cross section of the AuNR [4]. In addition, the formation of ICG aggregate facilitated by SiO₂ enhances photostability of incorporated ICG as well [5, 6] (Figure 1).

3 Results

The AuNR@SiO₂-ICG formulation dramatically increases singlet oxygen generation under laser excitation, relative

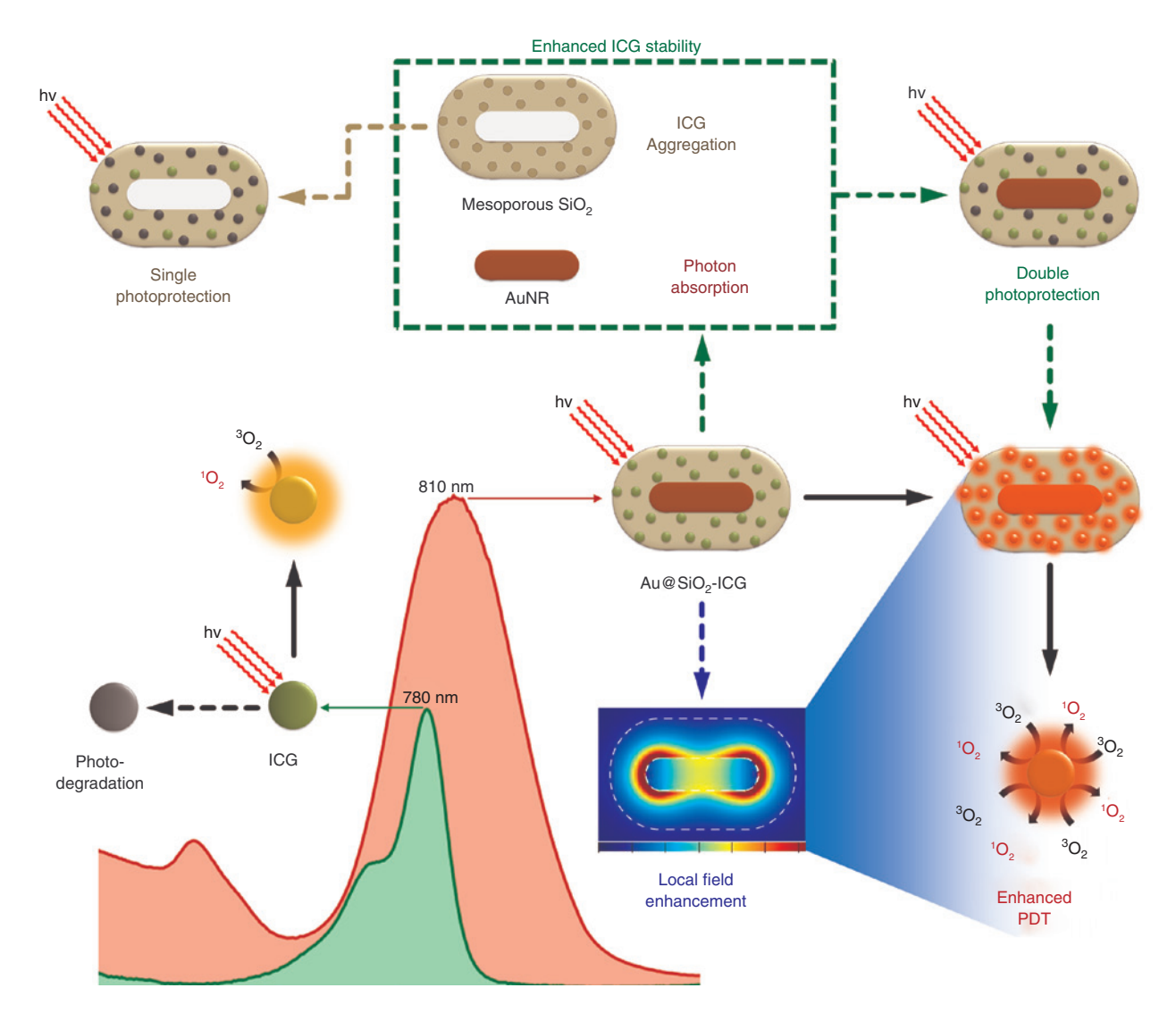


Figure 1: Design of enhanced photodynamic therapy by utilizing the surface plasmonic effect of the gold nanorods (AuNRs) to simultaneously increase the absorption coefficient and reduce photodegradation of the photodynamic dye indocyanine green (ICG). Mesoporous silica provided the second photoprotection for ICG by facilitating the formation of ICG aggregates. The double photoprotection will significantly enhance the stability of loaded-ICG in comparison with the single photoprotection of silica shell.

to free ICG, and demonstrates enhanced photodynamic destruction of human breast carcinoma cell MDA-MB-231. In addition, cellular uptake and retaining of ICG in the tumor regions is enhanced due to the stabilization and delivery of ICG provided by AuNR@SiO, nanocarrier. This was confirmed by three imaging modes (NIR fluorescence, two-photon luminescence and photoacoustic tomography) both *in vitro* and *in vivo*. Mild photothermal heating at a low laser power density was sufficient to ensure that AuNR@SiO₃-ICG induced a clear inhibition of orthotopic tumor growth through the synergistic effect of photothermal therapy and PDT.

4 Conclusion

Our study highlights a general design principle for enhancing the effectiveness of photosensitizers based on plasmon enhancement and protection, which holds great promises for cancer therapy by further development.

- [1] Li Y, Wen T, Zhao R, Liu X, Ji T, Wang H, Shi X, Shi J, Wei J, Zhao Y, Wu X, Nie G. Localized electric field of plasmonic nanoplatform enhanced photodynamic tumor therapy. ACS Nano 2014;8(11):11529-42.
- [2] Luo S, Zhang E, Su Y, Cheng T, Shi C. A review of NIR dyes in cancer targeting and imaging. Biomaterials 2011;32(29):7127-38.
- [3] Kochuveedu ST, Kim DH. Surface plasmon resonance mediated photoluminescence properties of nanostructured multicomponent fluorophore systems. Nanoscale 2014;6(10):4966-84.
- Philip R, Penzkofer A, Bäumler W, Szeimies RM, Abels C. Absorption and fluorescence spectroscopic investigation of indocyanine green. J Photoch Photobio A 1996;96(1-3): 137-48.
- [5] Holzer W, Mauerer M, Penzkofer A, Szeimies RM, Abels C, Landthaler M, Bäumler W. Photostability and thermal stability of indocyanine green. J Photoch Photobio B 1998;47(2-3):155-64.
- [6] Lee CH, Cheng SH, Wang YJ, Chen YC, Chen NT, Souris J, Chen CT, Mou CY, Yang CS, Lo LW. Near-infrared mesoporous silica nanoparticles for optical imaging: characterization and in vivo biodistribution. Adv Funct Mater 2009;19(2):215-22.

Session 6: Photodynamic therapy – General aspects

[6.01] Implementation of laser technologies in clinical photodynamic therapy

H.-Peter Berlien* and Carsten M. Philipp

Ev. Elisabeth Klinik Berlin, Zentrum Lasermedizin, Lützowstr. 24-26, 10785 Berlin, Germany *Corresponding author: Prof. Dr. H.-Peter Berlien, laserforschung.elisabeth@pgdiakonie.de

Abstract: Photodynamic therapy (PDT) is a term encompassing a collection of both curative and palliative modalities, traditionally described as treating precancerous lesions and superficial tumors using light. The list of medical fields in which PDT has managed to find a place as an accepted option for specific problems includes gastroenterology, dermatology, gynecology, ophthalmology and ENT. It is increasing importance underlined by a comparison with both traditional chemotherapy and radiotherapy, which can often significantly compromise patients' health. The therapeutic use of these well-established

therapies is accordingly limited by their toxicity. In contrast, PDT can not only show a distinct degree of tumor specificity, but also can be repeatedly applied without apparently damaging the health of the patient.

Keywords: photodynamic therapy; laser irradiation protocol; intraepithelial neoplasms; optical diagnostic.

1 Background

Historically, the traditional indication for photodynamic therapy (PDT) are malignant tumors. But with

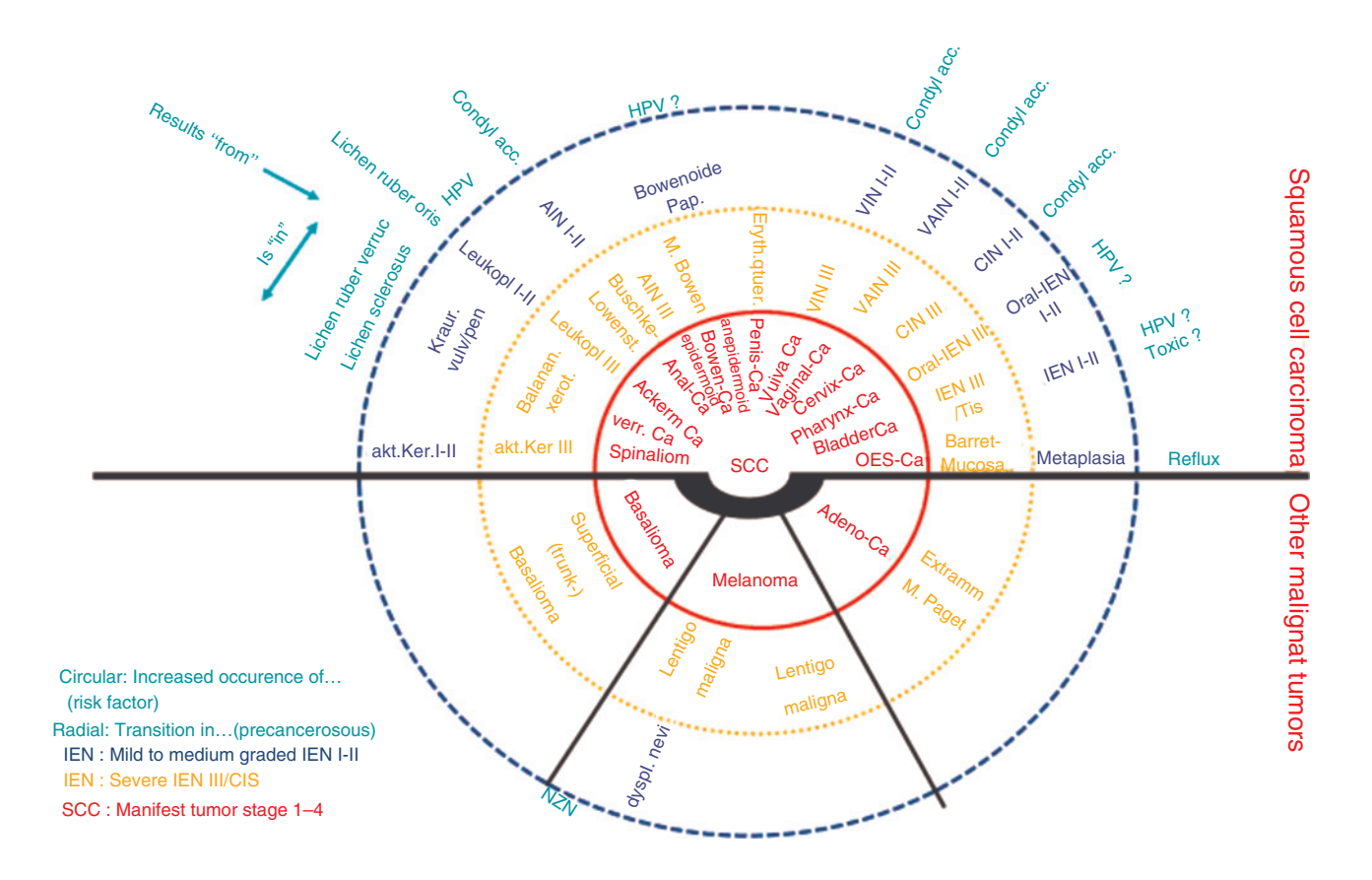


Figure 1: In the center is the squamous cell carcinoma (SCC) – overall is the human papilloma virus (HPV). In intraepithelial dysplasias is a continuing grading from grade I to III. They all have no tumor stroma and no vascularization. But the step to an invasive cancer, even an early invasive cancer, is digital. In this case no spontaneous healing is possible.

more understanding of the processes the indications for PDT increased and have changed their center of interest.

The indication in treatment of solid tumors is mainly under palliative aspects in surgical primarily not resectable tumors or local recurrences and metastasis without any other therapeutic option such as chemotherapy or radiotherapy [1]. The reason is that with a surgical R0-resection in nearly all tumor entities the best 5 year-life rates are obtainable. But in this tumor surgery another indication of PDT comes more important. After RO-resection, i.e. direct intraoperatively, a PDT is performed to irradiate the tumor bed to increase the primary radicalism without unnecessary defects. So the intention is similar to the intraoperative radiation. But one problem is the photosensitivity of the tissue to the operation or endoscopic light source. This is the reason why today only in neurosurgery the intraoperative ALA-PDT is routine.

2 New therapeutic options

With an increasing number of patients with human papilloma virus (HPV)-induced dysplasias and early detection before an invasion starts, PDT becomes a curative tool for these diseases.

Here, in strong intraepithelial dysplasias without any vascularization (IENIII/CIS) (Figure 1) topical substances are the drug of choice. But with thicker lesions the penetration of these topical substances is not safe enough and with vascularization and stroma formation the indication changes to systemic photosensitizers [2]. Here we have beside the more or less specific accumulation in

> One drug - one wavelength - one irradiation "conventional" One drug - one wavelength - two/m irradiations "recovery" One drug - one wavelength - two/m irradiations "fractionated" One drug - one wavelength - two/m cycles "boostering" One drug - two wavelengths - one irradiation "piggy-back" Two drugs - one wavelength - one irradiation "Sandwich"

Figure 2: Options for irradiation planning.

the tumor cells the secondary effect of destruction of the tumor vessels [3]. In all this cases besides the right choice of the best photosenzitizer (e.g. topical/systemic, lipo-/ hydrophilic, long-acting/short acting) the irradiation protocol is more important. Here we have options as shown in Figure 2.

But with photosensitizers which increasingly remain in the vascular system more benign indications start. The latest, but now the major indication, is at this time the age-related macula degeneration. Due to the fact that the used benzoporphyrin derivative has normally a good penetration into tissue and a low intravascular-remaining potential here a capsulation with liposomes are necessary. Because this coupling is in the blood not stable, within few minutes after application the laser activation is necessary to avoid damage of the retinal epithelium. Longer experiments started in the treatment of congenital vascular tumors like infantile hemangioma and in vascular malformation esp. port-wine stains. But even after more than 20 years research we are at this field before a broad application. The same is in the treatment of inflammatory skin diseases. The psoriasis was one of the oldest applications for PDT in non-malignant diseases but could not come to routine. At this time the most interest is now the treatment of severe acne. But comparative studies did show either severe skin photosensitivity which strained the patients more than the disease. In combination with pulsed dye laser the additional effect to laser alone is minor; so at this time it is not clear if PDT will have a real success for this indication. In treatment of warts and condylomatas without dysplasias the PDT for virus eradication could not show any success. This is easy to explain: the metabolism and proliferation in warts and non-dysplastic condylomas is better than in the surrounding

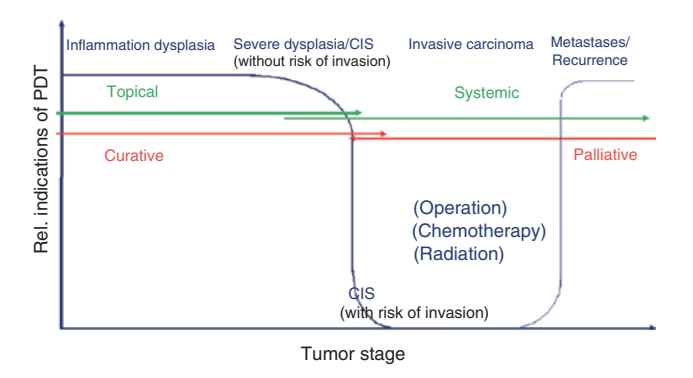


Figure 3: Indications of photodynamic therapy (PDT). Even in high-grade intraepithelial dysplasias (IEN) a PDT can be indicated. But in case of invasive cancer only surgical resection can be curative. The aim of PDT in recurrences or metastases is palliative.

tissue; so no specific effect can happen. But has the cell itself change to dysplasia the PDT again is the tool of choice (Figure 3).

References

[1] Berlien H-P. Implementation of laser technologies in clinical PDT. In: Abdel-Kader MH, editor. Photodynamic therapy: from

- theory to application. Berlin and Heidelberg: Springer-Verlag; 2014, p. 93-118.
- [2] Ziolkowska M, Philipp CM, Liebscher J, Berlien H-P. OCT of healthy skin, actinic skin and NMSC lesions. Med Laser Appl 2009:24(4):256-64.
- [3] Philipp CM, Müller U, Urban P, Berlien H-P. Potential of systemic photosensitizers for PDT of skin malignancies. Proc SPIE 2008; 6991:699119. doi: 10.1117/12.783405.

[6.02] Optical coherence tomography: A promising imaging modality for monitoring photodynamic therapy

Zhihua Ding*, Ziwei Shangguan, Yi Shen, Zhiyan Chen, Wen Bao, Yang Ni and Peng Li State Key Lab of Modern Optical Instrumentation, Department of Optical Engineering, Zhejiang University, Hangzhou 310027, China

*Corresponding author: Dr. Zhihua Ding, zh_ding@zju.edu.cn

Abstract: Novel optical coherence tomography (OCT) systems with ultralong depth range, ultrawide lateral field, and ultrahigh axial resolution are developed, which envision new medical applications. Typical applications of structural and functional OCT are presented. As a depth-resolved optical imaging modality with the merits of non-destruction, high-resolution, and high-speed, OCT is promising for the online monitoring of response to photodynamic therapy (PDT) and the assessment of therapeutic outcome.

Keywords: optical coherence tomography; vasculature imaging; photodynamic therapy; therapeutic outcome.

1 Background

Imaging in photodynamic therapy (PDT) has multiple points of significance including diagnostics, therapy guidance, monitoring, treatment assessment, and mechanistic studies [1]. The combination of imaging and PDT will provide improved research and therapeutic strategies, such as optimization and dosimetry, monitoring of response, assessment of outcome, and monitoring of oxygen. The electronic excitation of a photosensitizer (PS) can result not only in a cytotoxic effect but also in an emission of fluorescence due to relaxation of the excited singlet state PS back to the ground state. Hence, in addition to being therapeutic agents for PDT, PSs can readily serve as imaging agents that fluoresce in the visible region upon excitation with the appropriate wavelength. Such an approach based on PSs to generate fluorescence contrast is termed as photosensitizer fluorescence detection (PFD) [1]. PFD is highly successful at delineating disease margins for flat lesions, but for lesions with considerable subsurface, a more detailed picture of the underlying structure is desirable.

A variety of technologies such as X-ray computed tomography, magnetic resonance imaging, and ultrasound imaging have been developed and applied in PDT applications. However, none of them provides depthresolved resolution at micrometer scale. Currently, there are several optical methods capable of seeing the underlying structure with high resolution, those include confocal microscopy (penetration depth ~300 μm), multi-photon microscopy (penetration depth ~600–700 µm), and OCT (penetration depth \sim 1–3 mm).

2 Advantages of OCT

Three factors (speed, depth, and resolution) have made OCT an ideal imaging partner for following the detailed three-dimensional (3D) structural response to PDT in living systems. Depth range of OCT is comparable to the depth of necrosis observed in tissue. The axial resolution (~1–10 µm) is decoupled from the lateral resolution, allowing for sub-cellular, micron-resolution imaging deep in a sample. Volumetric imaging offered by OCT provides almost an order of magnitude faster than even video-rate microscopy. OCT is a non-perturbative imaging platform for PDT as the adopted light ranging from 850 nm to 1350 nm is far less energetic than those required to carry out PDT. OCT can be used to visualize a sample before, during, and after PDT without activating the PSs. OCT has been used in the conjunction with PDT as a natural partner for detecting structural alterations resulting from treatment response as well as targeting the vasculatures for on-line monitoring of vascular responses.

3 Further developments

Most recently, our group has made a further step forward in OCT instrumentations. The depth range is extended to be over 200 mm, the lateral field of view is increased to be 35 mm, and the axial resolution is improved to be 0.9 um. Novel OCT systems with these enhanced parameters definitely will open new OCT applications including PDT.

The depth ranges of typical implementations of Fourier domain OCT (FDOCT), including spectral domain OCT (SDOCT) and swept source OCT (SSOCT), are limited to several millimeters. To extend the depth range of current OCT systems, two novel systems with ultralong depth range have been developed. One is the orthogonal dispersive SDOCT (OD-SDOCT) [2, 3], and the other is the recirculated swept source (R-SS) OCT [4]. The developed OD-SDOCT system realizes the longest depth range (over 200 mm) ever achieved by SDOCT. The developed R-SS OCT achieves submicron precision within a depth range of 30 mm, holding potential in real-time contact-free on-axis metrology of complex optical systems. To ensure high-precision in determination of reflecting interfaces, the averaged spectral phase algorithm [5] is adopted. The measurement range is readily extendable if axial movement of the sample and range cascading are involved.

Aim to enhance the speed for real-time inspection, an ultrawide-field parallel SDOCT system capable of visualizing cross-sectional images of internal structures by a single shot of a two-dimensional (2D) CMOS camera is developed [6]. To achieve ultrawide-field parallel detection, one meniscus lens with negative diopter is introduced as an additional relay lens and imaging optics including sample arm, relay lenses and spectrometer are optimized as a whole for desirable imaging quality. The field of view along parallel direction is extended to 35 mm, which is to our knowledge the largest one ever reported for parallel OCT systems. The system is applied to obtain 3D volume images of a set of glass-samples, from which defects such as solid inclusion, microdeformation and bubbles are identified either on the surfaces or inside of the samples. This newly developed ultrawide-field parallel SDOCT is promising for real-time monitoring of PDT.

Utrahigh-resolution of OCT is required in applications. To this end, we are developing an ultrahigh-resolution SDOCT system using supercontinuum sources (SC). The spectra with a full width at half maximum of 230 nm centered at 665 nm are filtered from the SC and used as the broadband source for SDOCT. An axial resolution of 0.9 μm and a lateral resolution of 3.9 μm are achieved in the newly developed SDOCT system. Images of polystyrene spheres in solution with an average diameter of 5 µm and industrial abrasive papers of different types are captured by the system, demonstrating the greatly enhanced resolution as compared with conventional SDOCT systems.

This developed ultrahigh-resolution SDOCT is feasible for ultrahigh-resolution non-destructive inspection both for industrial and biomedical applications.

With custom-built novel OCT systems, two presented examples of structural OCT in ophthalmology are the morphometric measurement of Schlemm's canal [7, 8] and response monitoring of dehydration stress. Our results show that Schlemm's canal can be non-invasively imaged and measured in human eye, and the full-eye response to osmotic challenge can be characterized in vivo in mouse model, demonstrating that OCT is a potential tool in non-invasive visualization of therapeutic outcome. On the other hand, vasculature imaging is crucial to PDT because one of the key mechanisms of PDT-induced damage in the treatment of cancer is the impairment and destruction of tumor vasculature. To obtain motion contrast pertaining to blood flow in vivo, Doppler OCT [9-11] and angio-OCT [12] are developed for vasculature mapping. Typical examples of functional OCT including cerebral blood flow monitoring in rat, and complex-correlation based angiography of mouse brain are presented, confirming the feasibility of functional OCT for monitoring of PDT.

4 Conclusion

In short, OCT is ready for detecting structural and vascular alterations resulting from PDT treatment and will be a promising imaging modality complemented to the existing PFD.

- [1] Celli JP, Spring BQ, Rizvi I, Evans CL, Samkoe KS, Verma S, Pogue BW, Hasan T. Imaging and photodynamic therapy: mechanisms, monitoring, and optimization. Chem Rev 2010;110(5):2795-838.
- [2] Wang C, Ding Z, Mei S, Yu H, Hong W, Yan Y, Shen W. Ultralong-range phase imaging with orthogonal dispersive spectral-domain optical coherence tomography. Opt Lett 2012;37(21):4555-7.
- [3] Bao W, Ding Z, Li P, Chen Z, Shen Y, Wang C. Orthogonal dispersive spectral-domain optical coherence tomography. Opt Express 2014;22(8):10081-90.
- [4] Shen Y, Ding Z, Yan Y, Wang C, Yang Y, Zhang Y. Extended range phase-sensitive swept source interferometer for real-time dimensional metrology. Opt Commun 2014;318:88-94.
- [5] Yan Y, Ding Z, Shen Y, Chen Z, Zhao C, Ni Y. High-sensitive and broad-dynamic-range quantitative phase imaging with spectral domain phase microscopy. Opt Express 2013;21(22):25734-43.
- [6] Chen Z, Zhao C, Shen Y, Li P, Wang X, Ding Z. Ultrawidefield parallel spectral domain optical coherence tomography for nondestructive inspection of glass. Opt Commun 2015;341:122-30.

- [7] Shi G, Wang F, Li X, Lu J, Ding Z, Sun X, Jiang C, Zhang Y. Morphometric measurement of Schlemm's canal in normal human eye using anterior segment swept source optical coherence tomography. J Biomed Opt 2012;17(1):016016.
- [8] Wang F, Shi G, Li X, Lu J, Ding Z, Sun X, Jiang C, Zhang Y. Comparison of Schlemm's canal's biological parameters in primary open-angle glaucoma and normal human eyes with swept source optical. J Biomed Opt 2012;17(11):116008.
- [9] Meng J, Ding Z, Li J, Wang K, Wu T. Transit-time analysis based on delay-encoded beam shape for velocity vector quantification by spectral-domain Doppler optical coherence tomography. Opt Express 2010;18(2):1261-70.
- [10] Huang L, Ding Z, Hong W, Wang C, Wu T. Higher-order crosscorrelation-based Doppler optical coherence tomography. Opt Lett 2011;36(22):4314-6.
- [11] Wang C, Yang Y, Ding Z, Meng J, Wang K, Yang W, Xu Y. Monitoring of drug and stimulation induced cerebral blood flow velocity changes in rat sensory cortex using spectral domain Doppler optical coherence tomography. J Biomed Opt 2011;16(4):046001.
- [12] Li P, Ding Z, Ni Y, Xu B, Zhao C, Shen Y, Du C, Jiang B. Visualization of the ocular pulse in the anterior chamber of the mouse eye in vivo using phase-sensitive optical coherence tomography. J Biomed Opt 2014;19(9):090502.

Session 7: Photodynamic therapy – New approaches

[7.01] Vascular-targeted photodynamic therapy - Development and application

Ying Gu*, Ying Wang, Jiaying Zhang, Haixia Qiu, Naiyan Huang and Jing Zeng Department of Laser Medicine, Chinese People's Liberation Army General Hospital, Beijing 100853, China *Corresponding author: Prof. Ying Gu, guyinglaser@sina.com

Abstract: Vascular-targeted photodynamic therapy (V-PDT) is a promising treatment technique developed in the recent 20 years. It is characterized by highly targeting and precise selective destruction of the lesion vessels. V-PDT had first been successfully applied in the treatment of port wine stains (PWS) in 1991 by our team. In this article, our early basic researches and clinical studies were reviewed, and our recent progress of photosensitizer, laser equipment, monitoring techniques and clinical indications were introduced.

Keywords: vascular-targeted photodynamic therapy (V-PDT); mechanism; photobleaching; port wine stains (PWS); vascular lesions in mucosa.

1 Mechanism

The vascular targeting effect of vascular-targeted photodynamic therapy (V-PDT) for port wine stains (PWS) is based on the selective distribution of the photosensitizer in blood vessels and the precise distribution of laser in the upper layer of PWS skin [1, 2]. As illustrated in Figure 1, intravenous injection of photosensitizer leads to a high concentration difference between blood vessel and surrounding tissue. Immediately after photosensitizer injection, laser irradiation (blue to green wavelength) is carried

Port wine stains lesion

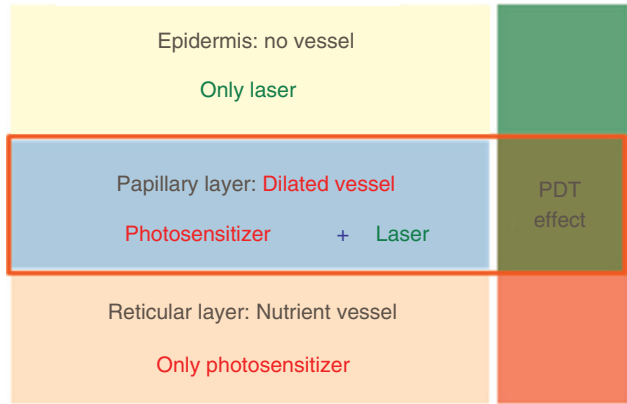


Figure 1: The mechanism of V-PDT for port wine stains.

out. Because hemoglobin has high absorption at the blue to green wavelength, laser at these wavelengths can only penetrate into the papillary layer in PWS. Photosensitizer and light coexist only in the dilated vessels in papillary layer. So PDT reaction can only take place in this layer. While in the epidermis and reticular layer, there is not enough photosensitizer or laser light to generate PDT effect. In addition, the small amount of photosensitizer in the epidermis and surrounding normal dermis which is diffused from the papillary vessels can be photobleached during laser irradiation. This photobleaching effect can further increase the selective destruction to dilated vessels.

2 Basic researches

From 1990, series of experiments at cells and animal level had been carried out by our team. Photosensitizers used were domestic hematoporphyrin derivative (HpD) and hemato porphyrin mono-methyl ether (HMME). Results showed that human vascular endothelial cells (EC) can quickly uptake the two photosensitizers, and photosensitizers' contents in EC are positively related to their incubating concentration. This indicated that EC can be the target of PDT.

In vivo study was performed in chicken comb which has abundant dilated microvasculature in the upper dermis with an overlying epidermis same to the architecture of PWS. Results demonstrated that the red combs faded completely without damaging of the overlying skin. The EC of capillary net was phototoxic damaged, walls of the capillary net were destroyed and the microvasculature was decreased dramatically. The degree of this selective photosensitive destruction was positively related to doses of photosensitizers and laser irradiations. The target damage effects of HMME-PDT and HpD-PDT were similar. Not any non-selective damage to the epidermis and other layers of skin was found in HMME-PDT group, but local damage of epidermis and connective tissue and vessels in dermis were seen in few HpD-PDT group.

3 Clinical study

The first case of clinical trial was carried out in January 1991. Results revealed that both HMME-PDT and HpD-PDT were able to treat all types of PWS and yielded similar color-faded therapeutic effects. The follow-up including 1632 lesions was made from 2 months to 9 years following treatment. No recurrence was found. Patients need avoiding strong light exposure for 30-90 days after using HpD and only 7–14 days by using HMME, respectively [3].

The impact of V-PDT on blood perfusion of PWS during and after HMME-PDT was quantitatively determined by laser Doppler flowmetry in 56 PWS patients. Results showed that the relative volume of skin blood perfusion in all treated PWS areas were obviously lower than that of them before treatment. Very close absolute values of decreased perfusion were found in all different clinical efficiency, which declared that clinical color-faded effects after HMME-PDT mainly depended on the degree of lesion and the differences of blood perfusion between normal skin and treated areas.

4 New photosensitizer

HMME (Hemoporfin) is a novel porphyrin-related secondgeneration photosensitizer developed in China. It was first synthesized by De-Yu Xu of the Second Military Medical University (Shanghai) in the 1980s. Preclinical studies demonstrate that HMME can be absorbed by EC more rapidly and easily than HpD, HMME-mediated V-PDT has fewer acute reactions, a faster healing and shorter skin photosensitivity compared with HpD [4]. After a multicenter and open-labeled phase-IIa study, our hospital and Fudan-Zhangjiang Bio-Pharmaceutical Co Ltd got the new drug certificate from our government. In 2012, China Food and Drug Administration (CFDA) had permitted its use in PWS.

5 New laser equipment

Diode-pumped solid state laser equipment for V-PDT was developed under the support of National High-Tech Research and Development Program (863 Program) with the advantage of high and stable output, uniform laser spot and long working time. This equipment has been permitted by CFDA.

6 Monitoring technique

To make optimized and individual clinical PDT protocol, the sensitivity of different vessels to V-PDT was studied using an animal experiment system comprised of structure imaging, function (blood flow perfusion) imaging and singlet oxygen imaging techniques. A clinical monitoring platform was also established comprised of laser Doppler imaging, laser speckle imaging, photoacoustic imaging, optical coherence tomography, and fluorescence detection. During V-PDT, blood vessels structure, blood perfusion, and photosensitizer content can be non-invasively monitored on PWS patients [5].

7 Clinical application

Besides PWS, we also use V-PDT to treat vascular lesions in mucosa, such as radiation proctitis and gastric antral vascular ectasias (GAVE). We found that V-PDT is even easier to get better results in dilated vessels in mucosa than PWS [6], because there is less limit of light penetration in mucosa. Compared with the available endoscopic therapy (Nd:YAG laser photocoagulation therapy, bipolar electrocoagulation, heat probe and argon plasma coagulation), V-PDT has the advantage of high selectivity, structure and function maintaining. Since 2005, we have treated several dozen cases. The preliminary clinical results showed that V-PDT has good hemostatic effect. Its role is moderate and has a good tolerance for patients. With no thermal or mechanical damage, it can be used repeatedly and safely [7].

Acknowledgments: The studies in this article were supported by Nature Science Foundation of China (Grant numbers: '60078021', '60878055', '61036014' and '61108078') and National 863 program (Grant numbers: '2008AA030117' and '2007AA04Z231'). We gratefully acknowledge Prof. Buhong Li (Fujian Normal University), Prof. Ping Xue (Tsinghua University), Prof. Pengcheng Li (Huazhong University of S&T) and Prof. Da Xing (South China Normal University) for their cooperation.

- [1] Gu Y, Li J, Guo Z, Cui X, Liang J. Photodynamic therapy in treatment of port wine stains. Beijing Medical J 1991;13(5):317.
- [2] Gu Y, Li J, Jiang Y, Wang K, Pan Y. A study on the mechanism of photodynamic therapy for port wine stains. Chinese J Laser Med Surg 1992;1(3):141.
- [3] Gu Y, Li J. Clinical application of KTP laser in photodynamic therapy for port wine stains. Chinese J Laser Med Surg 1993;2(3):154-6.
- [4] Gu Y, Huang NY, Liang J, Pan YM, Liu FG. Clinical study of 1949 cases of port wine stains treated with vascular photodynamic therapy (Gu's PDT). Ann Dermatol Venereol 2007;134(3 Pt 1): 241-4.
- [5] Ren J, Li P, Zhao H, Chen D, Zhen J, Wang Y, Wang Y, Gu Y. Assessment of tissue perfusion changes in port wine stains after vascular targeted photodynamic therapy: a short-term follow-up study. Lasers Med Sci 2014;29(2):781-8.
- [6] Li CZ, Cheng LF, Wang ZQ, Gu Y. Photodynamic therapy of esophageal varices: experimental studies in animal veins, and first clinical cases. Endoscopy 2003;35(12):1043-8.
- [7] Qiu H, Mao Y, Gu Y, Wang Y, Zhu J, Zeng J. Vascular targeted photodynamic therapy for bleeding gastrointestinal mucosal vascular lesions: a preliminary study. Photodiagnosis Photodyn Ther 2012;9(2):109-17.

[7.02] Photodynamic therapy by nonlinear upconversion

Jun Song, Xiao Peng, Danying Lin, Wei Yan, Shuai Ye, Junle Qu^{*} and Hanben Niu Key Laboratory of Optoelectronic Devices and Systems of Ministry of Education and Guangdong Province, College of Optoelectronic Engineering, Shenzhen University, Shenzhen 518060, China *Corresponding author: Prof. Junle Qu, jlqu@szu.edu.cn

Abstract: Nonlinear interactions of light in the nearinfrared (NIR) region open a new avenue for transformational advances in photodynamic therapy (PDT) applications. NIR light excitation would provide deep tissue penetration to enable treatment of remote or thick tumors. Visible light emission could match well with the efficient absorption bands of the widely used commercially available photosensitizers, with efficient singlet oxygen generation leading to PDT. Two typical methods for PDT by nonlinear upconversion will be discussed in the paper, i.e. PDT by in situ nonlinear photon conversion, and PDT by upconversion nanoparticles.

Keywords: photodynamic therapy; nonlinear upconversion; near-infrared; upconversion nanoparticles.

1 Introduction

Compared with other treatments, photodynamic therapy (PDT) has specific advantages including high precision, minimal invasiveness, and good reproducibility. The greatest barrier to expanding current PDT methods towards large-scale clinical trials in new areas is the limited penetration depth of the exciting laser. Consequently, many efforts are currently underway to develop new PDT methods that can use near-infrared (NIR) light as the excitation source, to achieve deeper tissue penetration with little or no damage to normal cells or tissues [1]. Development of NIR absorbing photosensitizers is a major area of current PDT research. However, designing and synthesizing an effective photosensitizer with strong absorption in the NIR region is quite challenging [2].

Nonlinear upconversion is a promising alternative approach for NIR-PDT, where NIR excitation contributes to deep tissue penetration, and upconverted emission matches well with the maximal absorption of commercial photosensitizers. Two-photon PDT has already been demonstrated in vivo, and its practicality has already been established [3]. However, because known photosensitizers typically have low two-photon absorption (TPA) cross-sections, modification of their structures to produce stronger TPA or coupling them with other strongly multiphoton absorbing species has been required for multiphoton PDT to be successful. Unfortunately, modification of chemical

structure or combination (conjugation or co-encapsulation) with a TPA unit to enhance the efficiency of nonlinear excitation of the PDT agent can significantly affect the excitation and energy dissipation pathway, with a profound deleterious effect on singlet oxygen generation.

2 Nonlinear optical mechanisms for PDT

Recently, we proposed and demonstrated an entirely different method to activate PDT using the strong one photon absorption of an existing photosensitizer [4]. This approach relies on nonlinear optical effects in the indigenous components of the biological system. As shown in Figure 1, three types of nonlinear effects were utilized in the work: TPA, second-harmonic generation (SHG), and four-wave mixing (FWM). Among them, SHG demonstrated the best efficacy of NIR-PDT. Moreover, SHG is active in collagen which is typically abundant in tumors, while coherent anti-Stokes Raman scattering (CARS), one type of FWM, is more readily generated in lipids, proteins, and nucleic acids. Our experiments indicated that the threshold of nonreversible photonic injury based on the SHG/TPA effect was ~1.5 times lower than that based on the CARS/FWM/TPA effect. Using the same dose of NIR illumination (~4500 J/cm²), we found that CARS/FWM/ TPA excitation just reached the phototoxic threshold, while SHG/TPA excitation had killed or ablated ~70% of pathological cells. If we can combine the proposed nonlinear excitation techniques with the relatively mature TPA-PDT, we will enable a more promising and competitive platform for PDT clinical applications, with high selectivity, large penetration depth, low illumination dose, and enhanced efficacy.

We have obtained preliminary results on CARS imaging of cells during the course of PDT. These results demonstrate the ability to monitor biomolecular organization of irradiated single cells in real time. In conjunction with our earlier results by using two-photon fluorescence lifetime imaging [5] and dynamic fluorescence lifetime imaging based on acousto-optic deflectors [6], these data support the feasibility of establishing qualitative markers of efficient PDT photoactivation (for instance, the change in protein distribution patterns during apoptosis development, or difference in proteins signal ratio before and

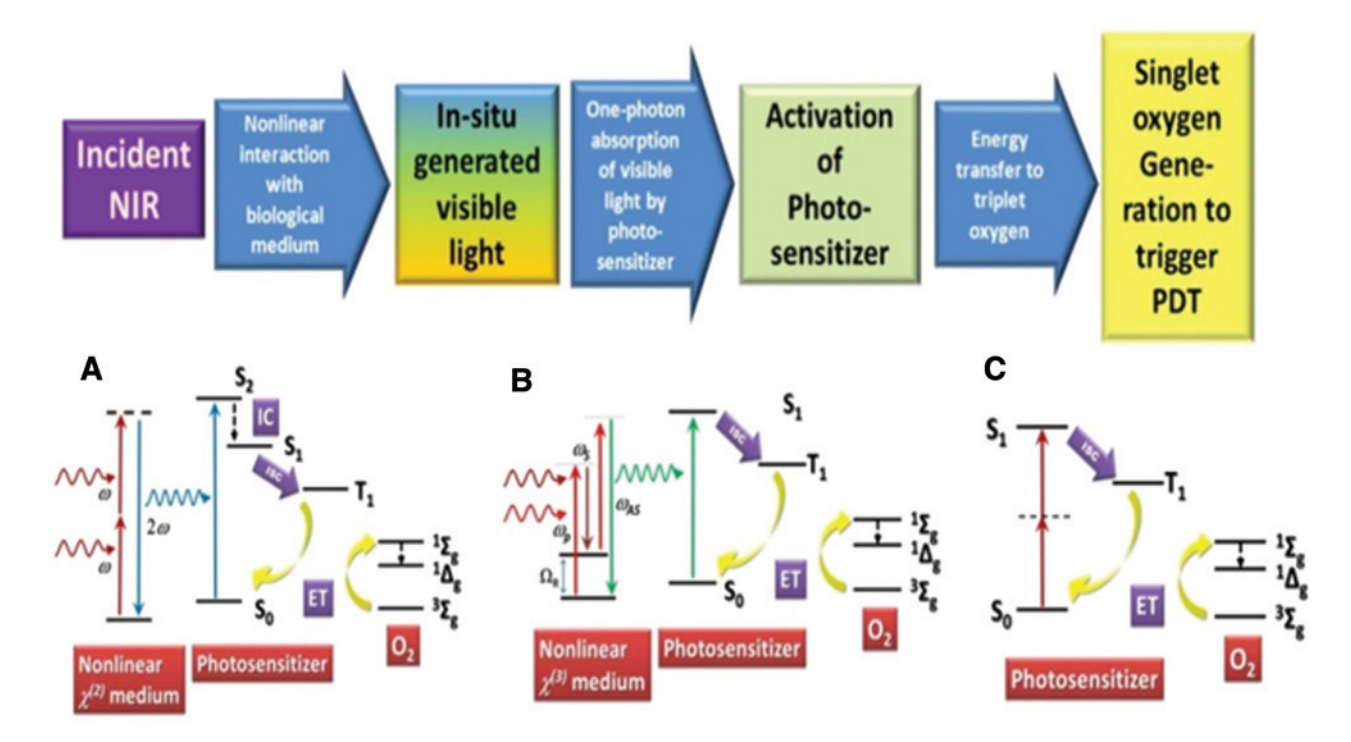


Figure 1: Nonlinear optical mechanisms for photodynamic therapy. Excitation with (A) two-photon absorption, (B) coherent anti-Stokes Raman scattering/four-wave mixing, and (C) second-harmonic generation.

NIR, near-infrared; ISC, intersystem crossing; IC, internal conversion; ET, energy transfer.

after treatment) *in situ*, i.e. using CARS signal simultaneously as an excitation source as well as for monitoring of PDT efficiency.

3 Upconversion nanoparticles

Upconversion nanoparticles (UCNPs) are another technology which has been paid close attention to improve light harvesting for PDT applications in the NIR region. This approach, which employs UCNPs to generate the required visible light for photosensitizer activation in situ, has been actively pursued for NIR-PDT [7]. Figure 2A illustrates our idea to achieve highly effective PDT treatment of deep-seated tumors using mesoporous-silica-coated UCNPs by encapsulating photosensitizers. The nanosystem can efficiently upconvert 800 nm excitation light to red emission light. The local minimal absorption of water is at ~800 nm, which has been considered to be our excitation wavelength to minimize the influence on biological tissues. In addition, the overlap between the spectrum of the upconverted red light and the maximum absorption wavelengths of the photosensitizers enables efficient generation of singlet oxygen within tissues. Coupling with UCNPs in this way can significantly enhance the therapeutic efficacy of PDT. Recently, we have synthesized the core-shell UCNP style with both 800 nm excitation and

red emission [8]. By using NaYF₄:Yb³⁺ @ NaYF₄:Nd³⁺, Ho³⁺ core-shell structure (see Figure 2B), we can obtain a ratio between red and green emission of ~11, whereas the whole emission intensity only decreases ~20%. In our preliminary experiments, ~30% Nd³⁺ doped concentration can contribute to a maximal luminous intensity (see Figure 2C). The present UCNPs are certainly attractive for the treatment of remote or thick tumors for long-time treatments due to low thermal effect at 800 nm excitation.

4 Conclusion

In conclusion, we developed two radically new biophotonic concepts of photoactivation. One utilizes *in situ* generation of light by nonlinear optical interaction of incident NIR laser radiation with components in the natural biological medium. Although the efficacy is limited by low nonlinear coefficients in biomolecules, it is especially suitable for clinical applications because this new approach does not require any chemical modification of the photosensitizer (as is usually the case for two photon excitation). The other makes full use of their ladder-shape energy levels of UCNPs to achieve an efficient upconverting emission, furthermore high curative effect. However, UCNPs' nanotoxicity is an important issue before clinical applications.

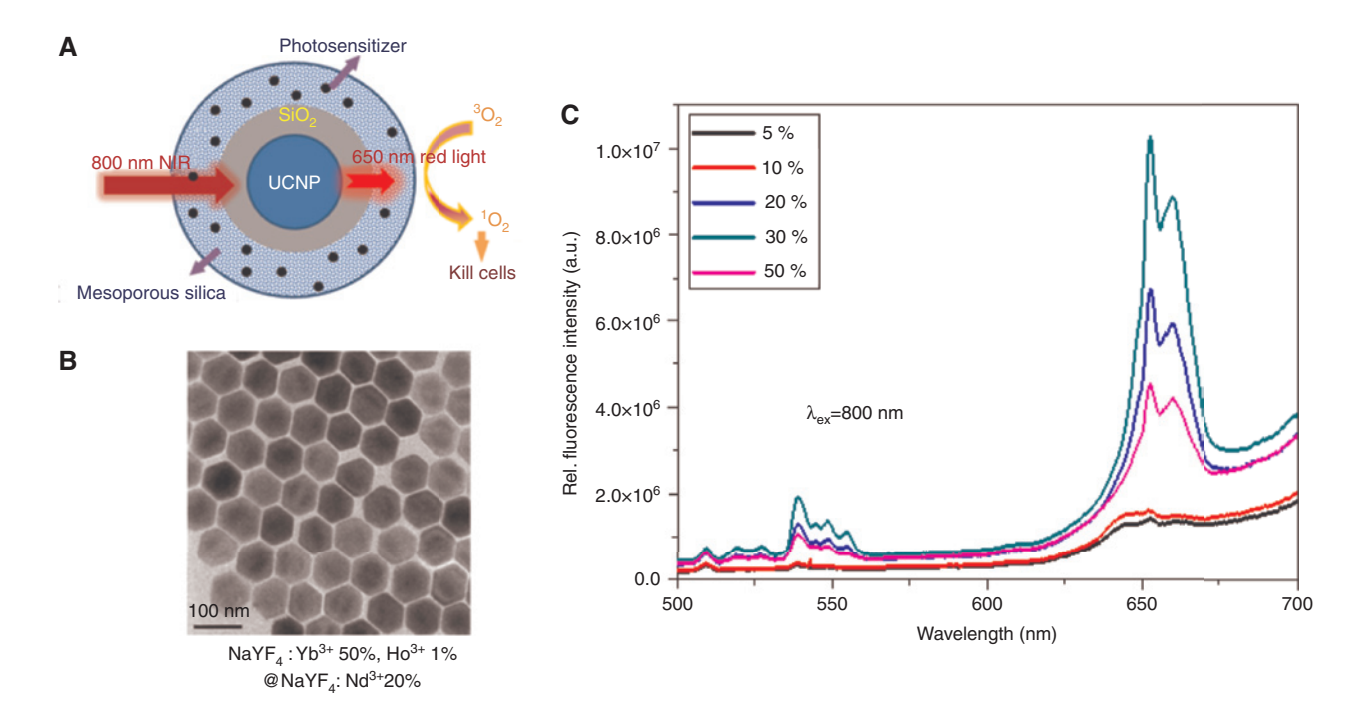


Figure 2: The synthesis of upconversion nanoparticles (UCNPs) for photodynamic therapy (PDT) applications. (A) A schematic of mesoporous SiO_-coated UCNPs co-loaded with photosensitizers for PDT. (B) Transmission electron microscopy (TEM) morphologies of NaYF,: Yb3+50%, Ho3+1% @ NaYF,:Nd3+20%. (C) The photoluminescence spectra of NaYF,:Yb3+, Ho3+ @ NaYF,:Nd3+ with different Nd3+ concentrations.

Acknowledgments: This work has been partially supported by National Natural Science Foundation of China (Grant numbers: '61378091' and '11204226'); National Basic Research Program of China (Grant number: '2015CB352005'); Guangdong Natural Science Foundation (Grant number: '2014A030312008'); Training Plan of Guangdong Province Outstanding Young Teachers (Grant number: 'Yq2013142') and Shenzhen Research Project (Grant numbers: 'ZDSYS20140430164957663' and 'KQCX20140509172719305').

- [1] Prasad PN. Introduction to nanomedicine and nanobioengineering. New York: JohnWiley & Sons; 2012.
- [2] DeRosa MC, Crutchley RJ. Photosensitized singlet oxygen and its applications. Coordin Chem Rev 2002;233-234:351-71.
- [3] Oar MA, Dichtel WR, Serin JM, Frechet JMJ, Rogers JE, Slagle JE, Fleitz PA, Tan LS, Ohulchanskyy TY, Prasad PN. Light-harvesting

- chromophores with metalated porphyrin cores for tuned photosensitization of singlet oxygen via two-photon excited FRET. Chem Mater 2006;18(16):3682-92.
- [4] Kachynski AV, Pliss A, Kuzmin AN, Ohulchanskyy TY, Baev A, Qu J, Prasad PN. Photodynamic therapy by in situ nonlinear photon conversion. Nat Photonics 2014;8(6):455-61.
- [5] Pliss A, Peng X, Liu L, Kuzmin A, Wang Y, Qu J, Li Y, Prasad PN. Single cell assay for molecular diagnostics and medicine: monitoring intracellular concentrations of macromolecules by two-photon fluorescence lifetime imaging. Theranostics 2015;5(9):919-30.
- [6] Yan W, Peng X, Qi J, Gao J, Fan S, Wang Q, Qu J, Niu H. Dynamic fluorescence lifetime imaging based on acousto-optic deflectors. J Biomed Opt 2014;19(11):116004.
- Idris NM, Gnanasammandhan MK, Zhang J, Ho PC, Mahendran R, Zhang Y. In vivo photodynamic therapy using upconversion nanoparticles as remote-controlled nanotransducers. Nat Med 2012;18(10):1580-5.
- [8] Ye S, Chen G, Shao W, Qu J, Prasad PN. Tuning upconversion through a sensitizer/activator-isolated NaYF, core/shell structure. Nanoscale 2015;7(9):3976-84.

[7.03] Photodynamic therapy by a device probe tip

Ashwini A. Ghogare¹, Dorota Bartusik¹, Goutam Ghosh¹, Niluksha Walalawela¹, Inna Abramova¹, Keith A. Cengel², Joann M. Miller², Theresa M. Busch² and Alexander Greer^{1,*}

¹Department of Chemistry and Graduate Center, City University of New York – Brooklyn College, Brooklyn, NY 11210, USA

Abstract: A pointsource photodynamic therapy (PDT) technique has been developed to deliver sensitizer, light and oxygen that are precursors to singlet oxygen (a cytotoxic excited state of O_2) in a highly localized and controllable fashion. The characterization of cell killing radius *in vitro* provides insight into the release kinetics and diffusion of the sensitizer. This opens the door to an instrument that brings all components for PDT to a device tip and may provide long-sought improvements in blood-rich or turbid media and in dosimetry.

Keywords: rectilinear photodynamic therapy; teflon tips; singlet oxygen halo; sensitizer drift.

1 Objective

The discovery of high-precision techniques to eradicate tumors would be of tremendous use for surgeons. Removal of tumors that are directly adjacent to vital tissue is a daunting challenge. Radiation and chemotherapy have been in the limelight for years in non-surgical treatments, but the field needs further advances in high-precision treatment delivery.

2 Method

One solution to this problem is a pointsource photodynamic therapy (PSPDT) device that channels O_2 and red diode laser light through a probe tip to the tumor site (Figure 1) [1]. The probe tip discharges sensitizer molecules that serve as precursors to singlet oxygen ($^{1}O_2$), a key cytotoxic species, placing all components necessary for PDT at the tumor and nowhere else in the body.

3 Results and discussion

Our device has demonstrated photokilling activity and precision in glioma U-87 cells *in vitro* by creating a halo of singlet oxygen (Figure 2) [2]. The photokilling was analyzed by a live/dead assay, with a circle of killing around the probe tip. The probe tip design seemed reasonable. When placed 0.25 mm above U-87 cells spread into a monolayer on a microwell plate, the cell killing radios proceeded from 0.1 to 2.9 mm with increased treatment times.

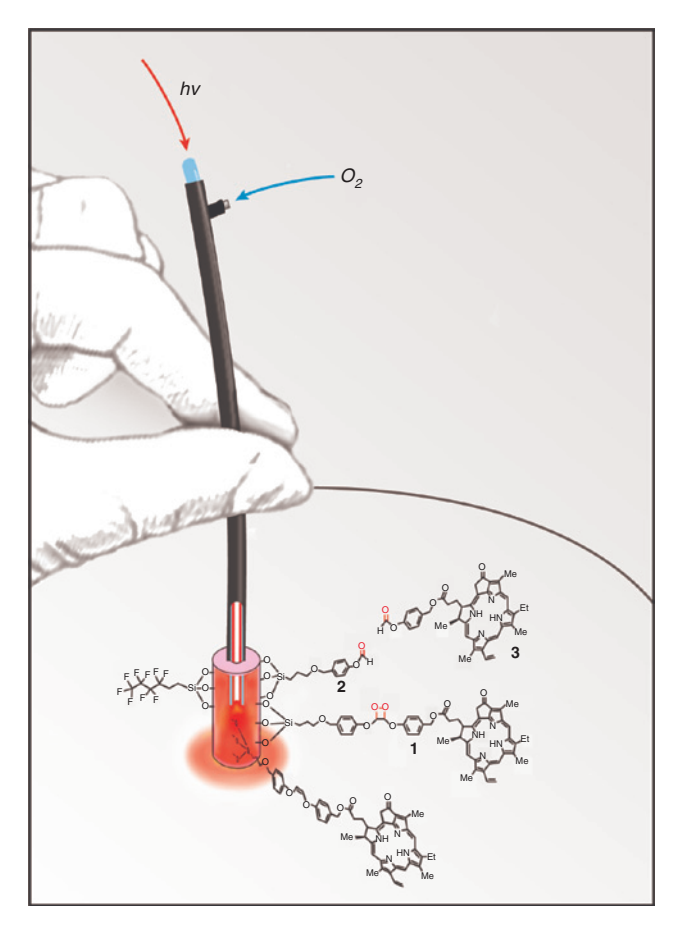


Figure 1: A pointsource device capable of delivering the components necessary for photodynamic therapy in a localized fashion. The device runs on O_2 and diode laser light, fed through the hollow fiber. Sensitizer drug release 3 occurs after scission of dioxetane 1 that arose from a [2+2] addition of singlet oxygen to the ethene bond. Singlet oxygen is produced in the vicinity of the sensitizer which diffuses away from the probe tip.

There is intuition and rationale in the probe tip design. The thinking was that a means for sensitizer release to allow for its excitation while in the tissue was needed due to the short diffusion distance of $^{\rm 1}{\rm O}_2$ delivered extra-cellularly to tissue. Once in use, the device kills cancer cells in regions where the sensitizer diffuses, i.e. beyond the tip's point of application. This combination of sensitizer release and $^{\rm 1}{\rm O}_2$ generation provides a resolution for the $^{\rm 1}{\rm O}_2$ paradox. Nature

²Department of Radiation Oncology, University of Pennsylvania, Philadelphia, PA 19104, USA

^{*}Corresponding author: Prof. Alexander Greer, agreer@brooklyn.cuny.edu

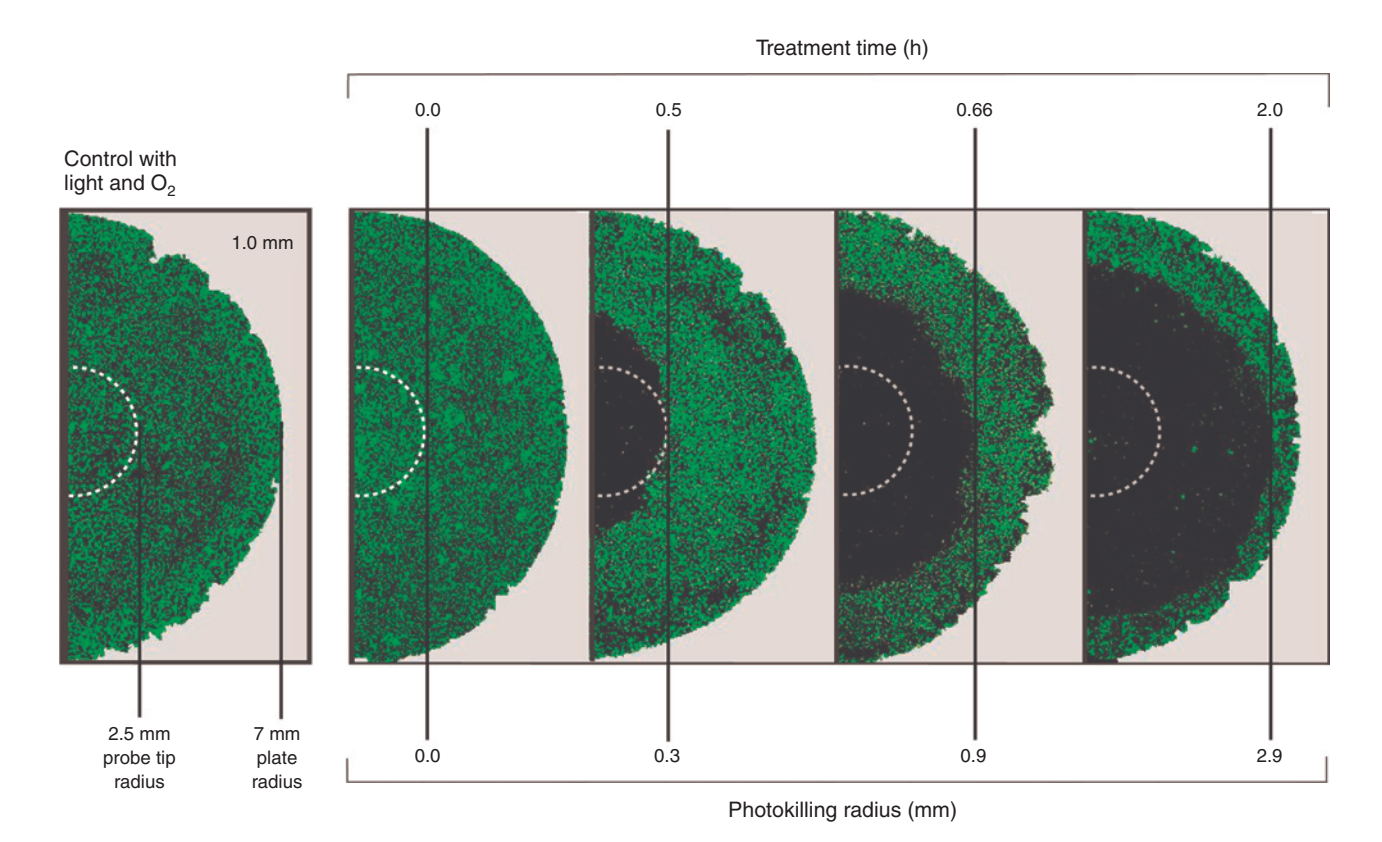


Figure 2: The tip was found to kill U-87 glioma cell monolayers as a function of time. The radius of the probe tip is 2.5 mm (white dashes), where killing extended beyond where the tip actually touched. Viable cells were stained with calcein AM (green), whereas the non-viable cells detached. Magnification 10×.

has provided us laws that govern singlet oxygen's existence, namely its short lifetime and diffusion distance. The released sensitizer effectively lengthens singlet oxygen's diffusion distance in the guise of photocompanion catalysis (synchonizing sensitizer location to ¹O₂ generation). Figure 2 shows there is no requirement for the tip to touch each margin in order to kill cells; notice the killing occurred beyond the dashed white line where the probehead actually touched. Furthermore, these doses do not result in increased heat, and the amount of time required to point the device tip at each cell margin is tunable, as is seen next.

Data from U-87 and OVCAR-5 cells suggested that nonlinear sensitizer release depends on fluorination of the tip [2, 3], which led to curved Eyring plots of $\ln k$ (autocatalytic fitting) vs 1/T. A mechanism was proposed for the sigmoidal photorelease process [4]. In Figure 3 shown in green, with the native silica, there is sensitizer photorelease with non-sigmoidal kinetics. Shown in red, with the fluorinated silica, the rapid photorelease is forestalled until higher concentrations of released sensitizer become available. Shown in blue, immediate acceleration is the result when cleaved sensitizer is added as a dopant at t=0 min. When cleaved sensitizer is spiked into

solution, the induction step is eliminated. That the induction period can be bypassed is quite informative. The steepest sigmoid was seen at 20 °C. As the temperature T increased from 20 to 100 °C, k decreased by 30%. This can be understood in terms of an entropy-controlled reaction with lower product formation at higher temperature from lower reactivity of singlet oxygen with the ethene, and the negative activation energy rises by a tenth of a kJ/mol.

Design and synthesis of sensitizer compounds affect the delivery system characteristics. The extent of sensitizer PEGylation [5], for example, can regulate the time required for the tumor cells to uptake the sensitizer prior to light and O₂ delivery to increase applicability in a clinical setting. Sensitizers bind into membranes at different rates based on PEGylation and other factors. Sensitizer in-diffusion arrival provides the relative position of ¹O₂ that will form. Thus far, we know the phototoxic impact of our device tip can be tuned by sensitizer type and conditioning, such as fluorination.

Probe tip fluorination is found to improve repellent and other properties [6]. In addition to non-fluorinated and fluorinated glass tips, we have also examined polyvinyl alcohol (PVA) and teflon/PVA nanocomposites [7]. Fluorinated media lead to a reduction in the adsorbtive

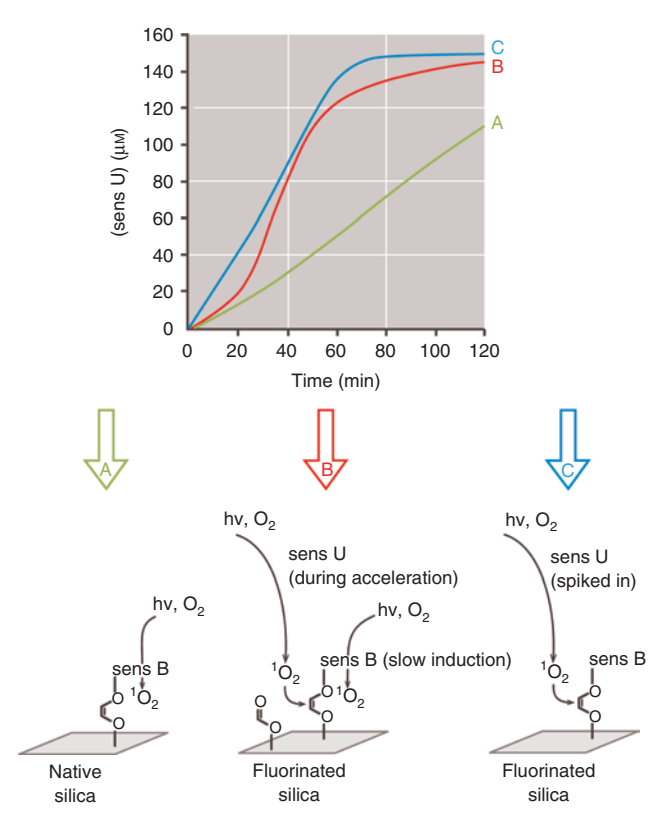


Figure 3: Modes of photorelease of the sensitizer bound (sensB) to the silica surfaces. Silica samples were irradiated with 669 nm light and the turnout of sensitizer unbound (sensU) in n-butanol solution: (A) slow 1st order release from native silica, (B) sigmoidal release for the fluorinated silica sensitizer with a 20-min induction period, followed by an acceleration, and then deceleration and saturation at 50 min signifying that the glass was depleted of sensitizer, and (C) rapid acceleration results with sensitizer spiked in.

affinity of the departing sensitizer with improved release to cellular or liquid surroundings. The advantages of the fluorinated over non-fluorinated surface go beyond the self-cleaning properties, there is a small $\rm O_2$ solubility enhancement caused by the fluorinated surface and also an enhanced percent cleaving efficiency. The fluorinated surfaces also protect $\rm ^1O_2$ from strong surface physical quenching compared to native silica or PVA allowing it to escape beyond the probe tip. The replacement of the O–H groups for the C–H and C–F groups enhanced the $\rm ^1O_2$ lifetime at the tip interface due to less efficient electronic-to-vibronic energy transfer and $\rm ^1O_2$ quenching.

In turning out sensitizer from the tip, control is desired, a reasonable platform for continuous or paced delivery is needed for good dosing. Flooded, acute or abrupt turnout leads to aggregation of the sensitizer and low $^{1}O_{2}$ photoproduction efficiency. Aggregated sensitizers are interlopers in a sense, e.g. they hinder good photophysics by

causing shorter excited-state lifetimes. A counterpart, a probe tip that flows ¹O₂ too rapidly (like throwing fuel on a fire) would also not be the way to go. Thus, our fluorinated probe tips can be suited to pace sensitizer release. Our data show that the fluorinated silica surface becomes privy to autocatalytic-assisted release kinetics, which has significant potential to direct local phototoxicity via singlet oxygen. Autocatalysis (or even oscillating kinetics) provides a mix of good advantages in the operation of the instrument. Control of spatial distance between the sensitizer molecules is also desired so as not to fret when >15 Å distances exist for maximal photocleavage: otherwise, self-quenching by neighboring sensitizer molecules occurs by FRET (pun intended). Optimal sensitizer photorelease has been examined for the probe tip, where crowding of the sensitizer molecules and self-quenching were kept to a minimum [1].

4 Conclusion

We feel the time is ripe for pointsource PDT to be tested in an intraoperative setting in treating residual disease. What needs to be scrutinized is a look beyond pilot feasibility data to a tumor model to see if the technique will be useful *in vivo*. Treatment of head and neck cancers seem promising. With proper controls, future studies can test this device and that if it will work efficiently or better that any currently available treatment. Questions about the device tip's efficacy in assorted geometric shapes or by silicone deposition or three-dimensional printing for rectilinear singlet oxygen delivery also need to be answered [8].

Acknowledgments: AAG, DB, GG, NW, IA and AG acknowledge support from the National Science Foundation (Grant number: 'CHE-1464975') and the NIH (Grant number: 'SC1GM093830'). KAC, JMM and TMB acknowledge support from the NIH (Grant number: 'P01 CA087971'). We also thank Leda Lee for the graphic arts work.

- [1] Zamadar M, Ghosh G, Mahendran A, Minnis M, Kruft BI, Ghogare A, Aebisher D, Greer A. Photosensitizer drug delivery via an optical fiber. J Am Chem Soc 2011;133(20):7882–91.
- [2] Ghogare AA, Rizvi I, Hasan T, Greer A. "Pointsource" delivery of a photosensitizer drug and singlet oxygen: eradication of glioma cells *in vitro*. Photochem Photobiol 2014;90(5):1119–25.
- [3] Bartusik D, Aebisher D, Ghogare A, Ghosh G, Abramova I, Hasan T, Greer A. A fiberoptic (photodynamic therapy type) device with a photosensitizer and singlet oxygen delivery probe tip for ovarian cancer cell killing. Photochem Photobiol 2013;89(4):936–41.
- [4] Bartusik D, Minnis M, Ghosh G, Greer A. Autocatalytic-assisted photorelease of a sensitizer drug bound to a silica support. J Org Chem 2013;78(17):8537–44.

- [5] Kimani S, Ghosh G, Ghogare A, Rudshteyn B, Bartusik D, Hasan T, Greer A. Synthesis and characterization of mono-, di-, and tri-poly(ethylene glycol) chlorin e6 conjugates for the photokilling of human ovarian cancer cells. J Org Chem 2012;77(23):10638-47.
- [6] Bartusik D, Aebisher D, Ghosh G, Minnis M, Greer A. Fluorine end-capped optical fibers for photosensitizer release and singlet oxygen production. J Org Chem 2012;77(10):4557-65.
- [7] Ghosh G, Minnis M, Ghogare AA, Abramova I, Cengel KA, Busch TM, Greer A. Photoactive fluoropolymer surfaces that release sensitizer drug molecules. J Phys Chem B 2015;119(10): 4155-64.
- [8] Aebisher D, Bartusik D, Liu Y, Zhao Y, Barahman M, Xu Q, Lyons AM, Greer A. Superhydrophobic photosensitizers. Mechanistic studies of ¹O₂ generation in the plastron and solid/liquid droplet interface. J Am Chem Soc 2013;135(50):18990-8.

[7.04] Antitumor effect of sinoporphyrin sodium loaded graphene oxide on human liver cancer HepG2 cells

Chao Huang, Chengchao Chu, Jun Zhang, Haiyan Gao and Gang Liu* State Key Laboratory of Molecular Vaccinology and Molecular Diagnostics & Center for Molecular Imaging and Translational Medicine, School of Public Health, Xiamen University, Xiamen 361102, China *Corresponding author: Prof. Gang Liu, gangliu.cmitm@xmu.edu.cn

Abstract: Photofrin-based photosensitizer is the first U.S. Food and Drug Administration (FDA)-approved photosensitizer for clinical application. However, the long-term skin toxicity and low tumor-selectivity limit the clinical application. Various nanocarriers have been developed for the delivery of photosensitizers to improve the poor aqueous solubility and tumor accumulation of photosensitizers. In this study, sinoporphyrin sodium loaded PEGylated graphene oxide (GO-PEG-DVDMS) was prepared to investigate the antitumor effect on human liver cancer cells. HepG2 cells with GO-PEG-DVDMS showed obviously lower cell viability under laser irradiation compared to control experiments without laser irradiation, suggesting the great potential of GO-PEG-DVDMS for liver cancer therapy.

Keywords: graphene oxide; sinoporphyrin sodium; PTT; PDT; liver cancer.

1 Introduction

Phototherapy, represented by photodynamic therapy (PDT) and photothermal therapy (PTT) have aroused wide interest in anticancer therapy due to unique advantages such as remote controllability, improved selectivity, and low systemic toxicity. PDT is an U.S. Food and Drug Administration (FDA)-approved treatment modality, in which a systemically or locally administered photosensitizer is activated locally by irradiating the lesion site with light of a suitable wavelength and power [1]. Furthermore, it has been proved that PDT is an effective treatment method in several cancers. But the long-term skin toxicity and low tumor-selectivity and photobleaching have limited the further clinical application [2, 3].

PTT is a non-invasive therapeutic technique which has unique advantages such as remote controllability,

improved selectivity, and low systemic toxicity. Among various nanomaterials, graphene oxide (GO) has been intensely studied by different groups and functionalized GO, which shows strong near-infrared (NIR) absorbance and high drug-loading capacities, for effective photothermal ablation of tumors as well as cancer combination therapy in animal experiments. More recently, GO has also been widely explored as promising drug delivery systems for improved cancer treatment.

Hepatocellular carcinoma (HCC) is a common disease worldwide. The prognosis of HCC is generally poor. Partial hepatectomy remains the best hope for a cure but is suitable for only 9-27% of patients. The presence of significant background cirrhosis often precludes liver resection in patients with HCC [4]. Herein, we loaded an active compound from Photofrin II, named as sinoporphyrin sodium (DVDMS), onto the PEGylated GO with large specific surface area for the non-invasive therapy of HCC [5]. The new synergistic PTT/PDT platform based on the DVDMSloaded PEGylated GO is an effective approach on cell proliferation inhibition of liver cancer cells.

2 Materials and methods

2.1 Chemicals and reagents

Graphite powder was purchased from Aladdin Reagent Co., Ltd.; mPEG-NH2 (Mw 3500) was purchased from Sigma. Ethylenediamine (EDA), 1-ethyl-3(3-dimethylaminopropyl) carbodiimide (EDC), n-hydroxysuccinimide (NHS) and indocyanine green (ICG) were obtained from J&K Company (Beijing, China), MTT assay kit and 4,6-diamidino-2- phenylindole (DAPI) were purchased form Bioengineering Co., Ltd. (Shanghai, China). Other reagents were purchased from China National Medicine Corporation and used as received. All solutions were freshly prepared using ultrapure water from a Millipore Milli-Q® system.

2.2 Synthesis of GO-PEG-DVDMS

GO nanosheets were prepared from natural graphite by the improved Hummers' method and modified with PEG following established methods [6]. To obtain GO-PEG-DVDMS, DVDMS (4 mg/ml) in phosphate buffered saline (PBS) were slowly added into GO-PEG (1 mg/ml) solution and stirred overnight. Unabsorbed free DVDMS was then removed by filtration through a filter (MW cut off 100 KD) and washed with distilled water for 6–8 times.

2.3 Detection of singlet oxygen

The generation of singlet oxygen was detected following a reported method [7]. Briefly, GO-PEG-DVDMS and ICG at different concentrations were dispersed in PBS solutions containing 32.0 mg/ml 1,3-diphenylisobenzofuran (DBPF) (1.0 ml), and were further irradiated for 5 min (630 nm, 400 mW) for singlet oxygen measurement. The fluorescence intensity at 485 nm was recorded.

2.4 Cell uptake assay

In cellular uptake assay, HepG2 cells were seeded in Lab Tek II 6-well chamber slides with a density of 1×10^4 cells/ml. When cells grew to 60-80% confluency, cells were incubated in the dark with GO-PEG-DVDMS at DVDMS concentration of $4\,\mu$ g/ml for 12 h. Then cells were washed with PBS for three times. After being mounted with a mounting solution containing DAPI for nuclear staining, the cells were observed through an IX81 epifluorescence microscope (Olympus, Japan).

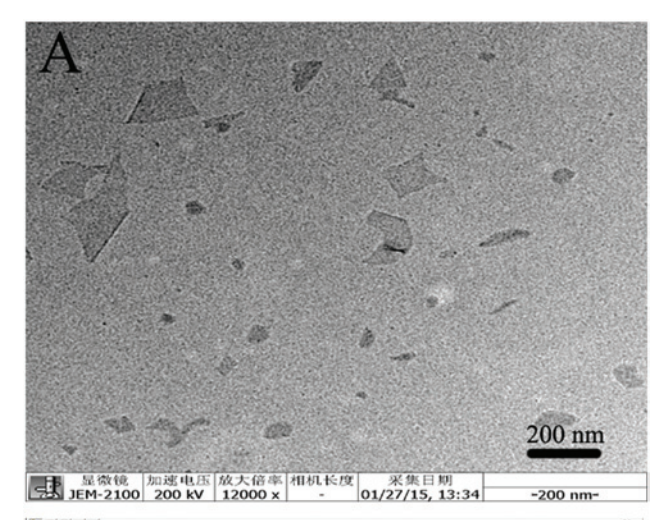
2.5 Cytotoxicity assay and cellular PDT/PTT

HepG2 cells were seeded in 96-well plates at 1×10^4 /well for 24 h and then treated with GO-PEG-DVDMS, free DVDMS, or GO-PEG at a series of concentrations up to 20 μ M. For cytotoxicity study, cells were washed with PBS three times and 20 μ l of MTT solution (5.0 mg/ml) was added to each well. After the 4 h incubation with the MTT, the media were removed and 100 μ l of dimethyl sulfoxide (DMSO) was added.

For PTT and PDT study, the wells were then washed with PBS three times. Then 100 μ l of fresh medium was added into each well, which were immediately irradiated by laser. The plates were kept in the incubator overnight for further cultivation. Cell viability was estimated by the standard MTT assay as described above.

3 Results and discussion

GO nanosheets were prepared from natural graphite by the improved Hummers' method. Amine-terminated PEG was conjugated with GO sheets to improve their aqueous dispersibility, stability, and biocompatibility [6]. DVDMS was



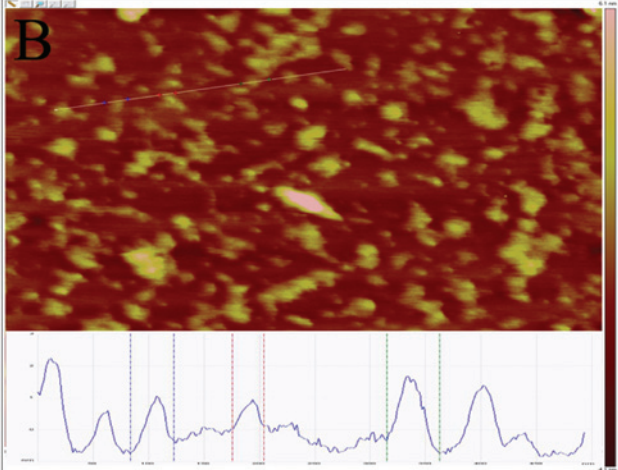


Figure 1: (A) Transmission electron microscopy (TEM) and (B) atom force microscopy (AFM) images of the GO-PEG-DVDMS nanoparticles. Insert: The size graph of GO-PEG-DVDMS nanoparticles from AFM image.

then loaded onto the surface of PEGylated GO nanosheets via π - π stacking [1]. Transmission electron microscopy (TEM) and atom force microscopy (AFM) were used to characterize the prepared GO-PEG-DVDMS nanoparticles (Figure 1A and B). The size of resulting GO-PEG-DVDMS nanoparticles was about 100 nm and the thickness was about 3 nm (Figure 1B).

GO-PEG-DVDMS with different concentrations were tested under 808 nm laser irradiation for 10 min to study the *in-vitro* photothermal property of GO-PEG-DVDMS. As shown in Figure 2A, all the GO-PEG-DVDMS solutions at different concentrations showed obvious temperaturerising phenomenon under the irradiation of 808 nm laser (0.5 W/cm²), demonstrating the potential of GO-PEG-DVDMS in photo-ablating tumor. The generation of singlet oxygen (¹O₂) of GO-PEG-DVDMS and ICG were compared

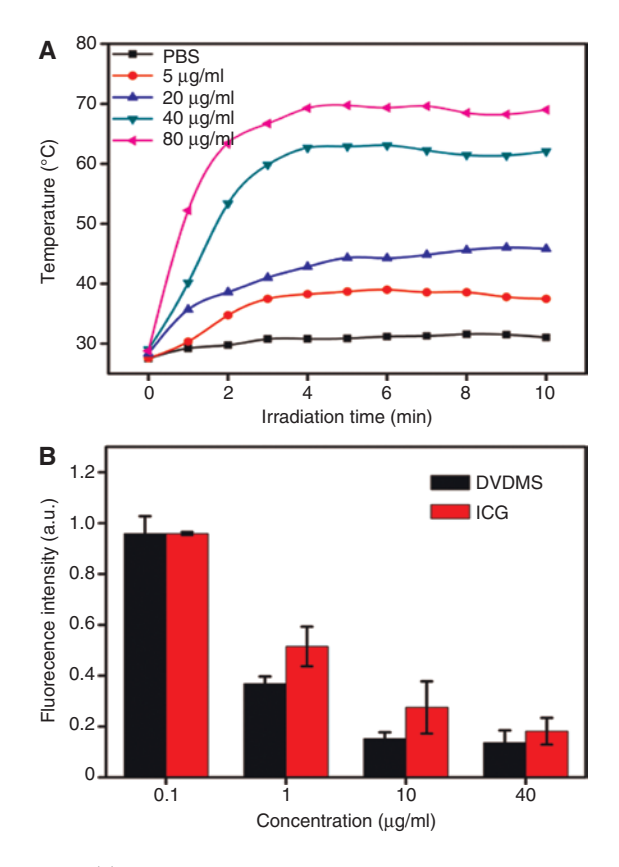


Figure 2: (A) The photothermal heating curves of GO-PEG-DVDMS solutions with different concentrations (under 808-nm laser irradiation at a power density of 0.5 W/cm²). (B) Normalized fluorescence intensity of 1,3-diphenylisobenzofuran (DBPF) after trapping singlet oxygen from DVDMS and ICG at various concentrations under 630 nm, 400 mW, 5 min photoirradiation.

as established methods. As shown in Figure 2B, GO-PEG-DVDMS behaved better than ICG in the generation of ¹O₂.

The GO-PEG nanoparticles partly quenched the fluorescence of loaded DVDMS (Figure 3A). To demonstrate whether GO-PEG-DVDMS can be internalized by cancer cells, we examined the cellular uptake on HepG2 cells. Cells treated with GO-PEG-DVDMS clearly showed red fluorescence in the cytoplasm, demonstrating the excellent cellular uptake of GO-PEG-DVDMS (Figure 3B).

We further evaluated the darkly cytotoxicity and anticancer efficacy of GO-PEG-DVDMS by MTT assay. HepG2 cells were incubated with GO-PEG-DVDMS at equivalent of 4 µg/ml DVDMS (GO-PEG, 2 µg/ml) for 12 h. As shown in Figure 4, HepG2 cells with GO-PEG-DVDMS showed obviously lower cell viability under laser irradiation compared to control experiments without laser irradiation. Without laser irradiation, the cell viabilities of GO-PEG-DVDMS treated group were almost 100%. However, HepG2 cells incubated with GO-PEG-DVDMS exhibited about 40% cell

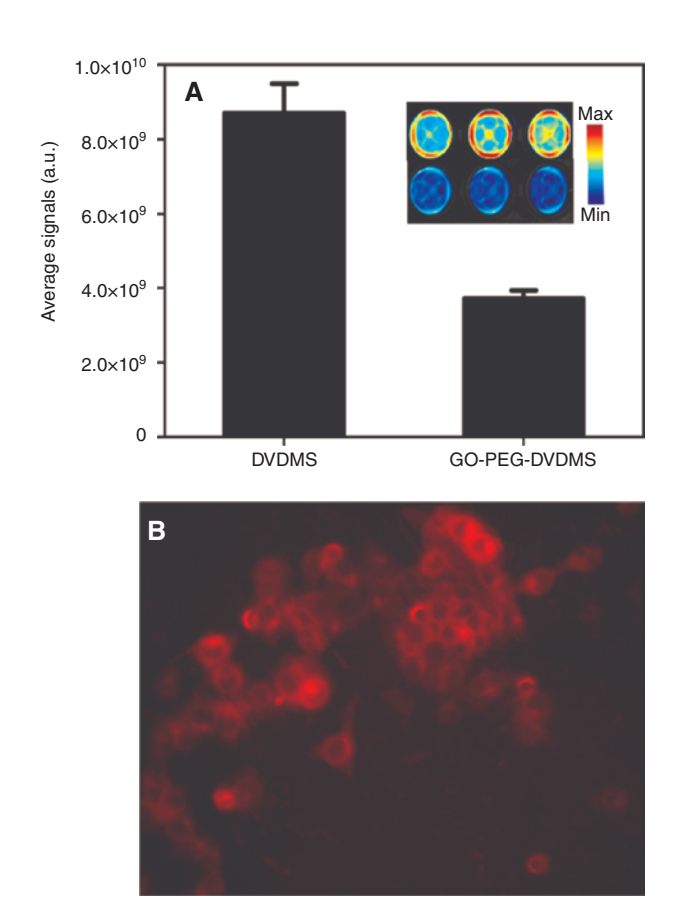


Figure 3: (A) Fluorescence quantity of DVDMS and GO-PEG-DVDMS (Ex: 525 nm, Em: 670 nm). Insert: fluorescence images of DVDMS (top) and GO-PEG-DVDMS (bottom). (B) Fluorecence microscopy image of HepG2 cells incubated with GO-PEG-DVDMS (DVDMS, 10 μg/ml) after 12 h.

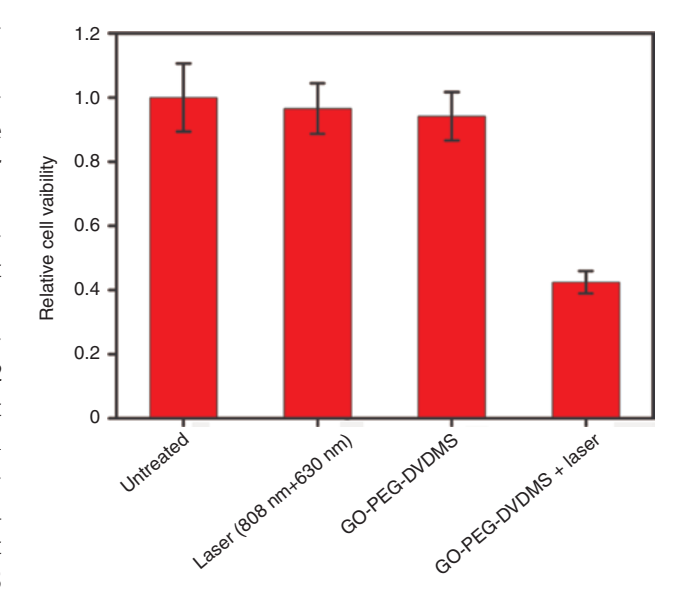


Figure 4: Relative viability of HepG2 cells incubated with GO-PEG-DVDMS after irradiation by 808-nm and 630-nm laser.

viability after NIR laser irradiation (808 nm and 630 nm laser illumination). These results demonstrate that the GO-PEG-DVDMS can act as PTT/PDT reagents for non-invasive therapy of cancer cells in vitro and has great potential for PTT/PDT therapy of liver cancer in vivo.

4 Conclusion

In this work, we successfully loaded the DVDMS onto the surface of the PEGylated GO nanosheets and the obtained GO-PEG-DVDMS was developed as PTT/PDT synergistic therapy platform for liver cancer therapy. With its easy synthetic accessibility and improved fluorescence property, GO-PEG-DVDMS provides a powerful possibility for exploring new material for imaging guided PTT/PDT cancer therapy.

References

[1] Yan X, Niu G, Lin J, Jin AJ, Hu H, Tang Y, Zhang Y, Wu A, Lu J, Zhang S, Huang P, Shen B, Chen X. Enhanced fluorescence

- imaging guided photodynamic therapy of sinoporphyrin sodium loaded graphene oxide. Biomaterials 2015;42: 94-102.
- [2] Chen R, Wang X, Yao X, Zheng X, Wang J, Jiang X. Near-IRtriggered photothermal/photodynamic dual-modality therapy system via chitosan hybrid nanospheres. Biomaterials 2013;34(33):8314-22.
- [3] Huang Z. A review of progress in clinical photodynamic therapy. Technol Cancer Res Treat 2005;4(3):283-93.
- [4] Lau WY, Leung TW, Yu SC, Ho SK. Percutaneous local ablative therapy for hepatocellular carcinoma: a review and look into the future. Ann Surg 2003;237(2):171-9.
- [5] Li C, Zhang K, Wang P, Hu J, Liu Q, Wang X. Sonodynamic antitumor effect of a novel sonosensitizer on S180 solid tumor. Biopharm Drug Dispos 2014;35(1):50-9.
- [6] Yang K, Feng L, Hong H, Cai W, Liu Z. Preparation and functionalization of graphene nanocomposites for biomedical applications. Nat Protoc 2013;8(12):2392-403.
- [7] Guo M, Mao H, Li Y, Zhu A, He H, Yang H, Wang Y, Tian X, Ge C, Peng Q, Wang X, Yang X, Chen X, Liu G, Chen H. Dual imagingguided photothermal/photodynamic therapy using micelles. Biomaterials 2014;35(16):4656-66.

Session 8: Optical techniques in photodynamic therapy applications

[8.01] Photocatalytic inactivation effect of HMME-TiO, nanocomposites on SCC cells under visible light

Yulu He, Cuiping Yao, Jing Wang and Zhenxi Zhang*

Key Laboratory of Biomedical Information Engineering of Ministry of Education, Institute of Biomedical Analytical Technology and Instrumentation, School of Life Science and Technology, Xi'an Jiaotong University, Xi'an, Shaanxi 710049, China *Corresponding author: Prof. Zhenxi Zhang, zxzhang@mail.xjtu.edu.cn

Abstract: In this study haematoporphyrin monomethyl ether (HMME) was conjugated onto the surface of P25 TiO₂ to pursue a higher efficiency of photodynamic therapy (PDT). TEM images confirmed HMME were loaded onto TiO, and a thin layer of HMME was observed on the surface. The interaction between HMME and TiO₂ led to a red shift in absorption spectrum of HMME. FTIR spectra confirmed HMME were loaded TiO, through the interaction between carboxyl groups and TiO₂. Fluorescence microscope images demonstrated HMME-loaded TiO₃ mainly distributed in the cell membrane and cytoplasm of squamous-cell carcinoma (SCC) cells. After treated with HMME-loaded TiO₂ mediated PDT the viability of SCC cells was much lower.

Keywords: photodynamic therapy; HMME-loaded TiO₂; SCC cells.

1 Introduction

As a derivative of porphyrin the second-generation photosensitizer haematoporphyrin monomethyl ether (HMME), which possesses a stable structure, high singlet oxygen yield, stronger photodynamic efficiency, low toxicity and fast clearance, has received considerable attention and been approved for the clinical treatment of port wine stains in China. Due to its low solubility in aqueous solution and deficiency of poor targeting - although the second-generation photosensitizer possesses many advantages - it is still far from an ideal photosensitizer. Many researchers focused on the development of alternative new-generation photosensitizers, but developing an ideal photosensitizer with better selectivity, higher water solubility and low toxicity is still a challenge. The development of nanotechnology, i.e. the application of nanomaterials in the field of biomedical sciences, has become a hot scientific topic.

2 Research approach

TiO, can generate singlet oxygen under light irradiation, which indicates its potential application in photodynamic therapy (PDT). However, the wide band gap (3.0-3.2 eV, only absorbing ultraviolet light of λ <387 nm) of TiO₂ confines its biomedical applications. Researchers have studied the catalytic and photocatalytic applications of porphyrin-sensitized TiO2. However, the photodynamic effect of HMME-sensitized TiO, on squamous-cell carcinoma (SCC) cells has not been involved. In present work HMME-loaded TiO, was prepared through interaction between carboxylic acid anchoring groups in HMME and TiO, nanoparticles. The prepared HMME-loaded TiO, was characterized and its photodynamic effect on SCC cells was investigated under visible light irradiation.

3 Results

TEM images showed that the shape of HMME-loaded TiO₃ nanocomposites was nearly sphere with a size range from 20 to 28 nm. There is a very thin layer on the surface of pure TiO, while the layer becomes much thicker after HMME were loaded.

The interaction between HMME and TiO, led to about 8-nm red shift in absorption spectrum of HMME and the B bands of HMME-loaded TiO₂ are much broader than that of HMME, which is considered due to the adsorption of porphyrin on TiO₂ nanoparticles. Zeta potential of TiO₂ colloid is 27.6 eV, while after HMME was applied to the surface of TiO₃ the Zeta potential becomes -36.8 eV.

FTIR spectra confirmed that HMME was loaded onto TiO, through the interaction between carboxyl groups of HMME and the hydroxyl groups on the surface of TiO₂. Fluorescence microscope results demonstrated that after 6 h incubation HMME-loaded TiO, nanocomposites mainly distributed in the cell membrane and cytoplasm of SCC cells. After treated with HMME-loaded TiO, plus light irradiation (1.8 J/cm², 635 nm), the viability of SCC cells turned to 32.96% which was much lower than that treated with HMME or TiO, plus light irradiation.

The combination of TiO₃ with HMME can effectively enhance the PDT efficiency and promote the potential application of TiO, nanoparticles in biomedical treatment. There are two possible reasons for this: first,

when loaded to the surface of ${\rm TiO_2}$ the aqueous solubility of HMME is improved, which leads to the increase of its accumulation in SCC cells. Second, HMME serve as a sensitizer which extended the absorption of ${\rm TiO_2}$ to the visible light region in turn to generate reactive oxygen species. The coordination of HMME and ${\rm TiO_2}$ results in the improvement of PDT efficiency. Moreover, dark toxicity of HMME-loaded ${\rm TiO_2}$ is no higher than that of HMME [1].

Acknowledgment: This work has been supported by National Nature Science Foundation of China (Grant numbers: '61120106013' and '11274249').

Reference

[1] He Y, Xiong J, Yao C, Wang J, Mei J, Wang M, Wang Z, Song P, Chang Z, Zhang Z. Photocatalytic inactivation effect of HMME-TiO₂ nanocomposites on SCC cells under visible light. Proc SPIE 2015;9449:944910. doi: 10.1117/12.2083110.

[8.02] In vivo tissue optical clearing: A potential technique for PDT

Jiadai He1,2 and Dan Zhu1,*

¹Britton Chance Center for Biomedical Photonics, Wuhan National Laboratory for Optoelectronics, Huazhong University of Science and Technology, Wuhan, China

²Department of Clinical Medicine, School of Medicine, Wuhan University of Science and Technology, Wuhan, China *Corresponding author: Prof. Dan Zhu, dawnzh@mail.hust.edu.cn

Abstract: Advanced optical imaging techniques have provided powerful tools for investigations of photodynamic therapy (PDT), but suffer from the high scattering of tisssue. In this presentation, the principle of tissue optical clearing is introduced. Furthermore, our progress on *in vivo* skin and skull optical clearing methods, and those induced improvement on various optical imaging performance on blood is demonstrated. It indicates that *in vivo* tissue optical clearing will be a potential technique for exploring the mechanisms of PDT, optimizing PDT method, or evaluating the treatment effect of PDT.

Keywords: tissue optical clearing; optical imaging; photodynamic therapy.

1 Introduction

Photodynamic therapy (PDT) consists of a chemical reaction activated by light energy that is used to selectively destroy cells or vascularture. Advanced optical imaging techniques have provided powerful tools for the investigations of PDT, from the basic research to clinical applications. In order to explore the mechanisms of PDT, to optimize the PDT method, or to evaluate the treatment effect of PDT, intravital confocal microscopy, fluorenscence imaging, laser speckle contrast imaging (LSCI), optical coherence tommography etc. were used [1–4]. However, these imaging techniques suffer from the limited penetration depth of light in tissue because of the high scattering, which seriously reduces the imaging depth and contrast. Thus, researchers had to apply dorsal skin fold chambers through surgical procedures to perform *in-vivo* imaging [1–4].

During the past years, researchers have been developing various advanced imaging techniques or contrast agents to resolve this problem. Actually, the tissue optical clearing technique should be an available way to reduce the scattering and make the tissue transparent. It is well known that tissue is packed with various types of substances, such as vessels, cell structures, fibers and interstitial fluid. Each component has different refractive index. The interstitial fluid has lower refractive index, while the fiber's refractive index is much higher. The scattering of tissue is just from the mismatch of refractive indices among various components. If some agents with high refractive index are used to replace the interstitial fluid, the match of refractive indices between the fibers and interstitial fluid will be increased, and then the scattering of tissue will be reduced [5]. Recently, some innovative optical clearing methods were developed, and provided powerful tools for obtaining microstructure of tissue with high resolution by using various microscopies [6]. However, the current *in-vitro* optical clearing methods cannot move to in-vivo animal because the procedure is too time-consuming, especially, the agents used in vitro are serious toxic. In vivo optical clearing methods should be efficient; the process procedure should be enough quick; more imortantly, the optical clearing agents (OCAs) should be safe.

2 Own research

During the past years, we have been focusing on developing *in vivo* optical clearing methods, including skin/skull optical clearing. Based on the mechanisms of tisssue

optical clearing [7–10], in vivo optical clearing agents were screened [11, 12]. Further more, physical and chemical methods were applied to enhance the penetration of OCA into tissue [13-15], and then the efficacy for in-vivo applications were demonstrated [16-21]. In addition, the biocompatibility of tissue optical clearing methods was investigated.

After having topically treated dorsal skin with OCAs, the skin can become transparent within several minutes. And saline treatment can make the skin turn to turbid. The same experiments can be repeated in the following days. So the skin optical clearing method provides a switchable window, which is not only simple and rapid, but also reversible and repeatable [16]. Besides the dorsal skin, the ear skin and footpad skin optical clearing were developed [17]. Considering the complex components and structure of skull, a skull optical clearing method was invented [18]. After treatment of skull optical clearing treatment, the skull could also become transparent within 30 min, and the cortical blood vessels can be visible with naked eye. Based on the in vivo optical clearing window, the various imaging performance were improved notably.

Vascular responses to PDT may influence the availability. After topical application of OCAs, the cutaneous blood vessels can be visible clearly with naked eye, and the image contrast of LSCI for cutaneous blood flow could be increased by 10 times; while it is difficult to detect cutaneous blood flow using LSCI [11, 12, 16, 17, 19]. Through intact skull, the cortical blood vessel is invisible, and LSCI can only extract some information of blood flow of larger vessels, and the contrast is very low. Through the cleared skull, it is easy to get the information even for small vessels, and the resolution is very close to that of removed skull. The image contrast increased by 3 or 4 times for the clear skull and removed skull, respectively [18, 19].

Combination of tissue optical clearing window & LSCI can be used for accessing arteriovenous separation, which is completely impossible for the turbid skin. After skin became transparent, saline injection hardly changes the blood flow and diameter of arteriovenous, while injection of noradrenaline can lead to vasoconstriction, and increase in blood flow immediately. Within 20 min, the changes in arteries recover to the original state. By contrast, the response of veins is slower than that of arteries; it takes longer time to recover for veins. For different veins, there is difference in change values. The cortical response of arteries and veins to noradrenaline was similar to cutaneous response. However, the change of the former is more rapidly and more severious than that of latter [20]. For intact skull, it is impossible for LSCI to access any response to noradrenaline injection.

The *in-vivo* flow cytometry (IVFC) is a promising technique for detecting circulating tumor cells quantitatively in the bloodstream. After ear skin was treated by optical clearing agents, the labeled red blood cells can be detected by the IVFC with higher signal quality and greater detection depth [21]. The results demonstrated that the optical clearing method is very helpful for potential tumor metastasis studies or evaluation of PDT by IVFC in deep tissues.

In addtion, in vivo tissue optical clearing is efficent for enhancing the performance of other imaging techniques, such as, hyperspectral imaging for oxygen saturation, photoacoustic microscopy for vascularture and fluorescence imaging for cells. The oxygen content is a significant parameter of PDT. Hyperspectral imaging (HSI) as an emerging imaging modality can provide oxygen saturation map by analyzing the spectral information in each pixel. Unfortunately, the HSI also faced the same limitation due to high scatter of tissue. After treatment of OCAs for 5 min on skin or 30 min on skull, the skin or skull will became transparent, and the cutaneous or cortical oxygen saturation maps with high resolution and contrast can be also accessed. The photoacoustic imaging (PAM) technique converts diffuse light into clear propagating ultrasound through the photoacoustic effect. It evidently enhance the imaging depth because the ultrasonic scattering is much less than the optical scattering, which would be a promising technique for deeper monitoring of PDT. We used the acoustic-resolution PAM (AR-PAM) and opticalresolution PAM (OR-PAM) to image the cerebral vasularture, respectively. The results showed that the signal intensity for both PAM methods could be increased and more vessels from deeper layers could be obtained. For OR-PAM, the resolution can be enhanced evidently. Moreover, in-vital confocal microscopy can be applied to image labelled tumor cells, which is useful for tumor localization and evaluation of PDT. A footpad optical clearing method was developed. Through the cleared skin, not only stronger fluorescence intensity, but also more cells in deeper tissue could be observed.

3 Conclusion

In summary, in vivo skin/skull optical clearing could enhance performance of various optical imaging techniques, such as the imaging contrast, resolution and sensitivity of LSCI for blood flow and HIS oxygen saturation; the signal intensity and depth or resolution of PAM for blood vessels and fluorescence imaging for cells. For the future, in vivo tissue optical clearing will be applied to the investigation of PDT, including investigating mechanisms of PDT, optimal PDT and evaluating PDT.

Acknowledgments: This study was supported by the National Nature Science Foundation of China (Grant numbers: '81171376' and '91232710'), the Science Fund for Creative Research Group of China (Grant number: '6141064'), and the Director Fund of Wuhan National Laboratory for Optoelectronics.

- [1] van Leeuwen-van Zaane F. de Bruiin HS. van der Ploegvan den Heuvel A, Sterenborg HJ, Robinson DJ. The effect of fluence rate on the acute response of vessel diameter and red blood cell velocity during topical 5-aminolevulinic acid photodynamic therapy. Photodiagnosis Photodyn Ther 2014;11(2):71-81.
- [2] Middelburg TA, de Bruijn HS, Tettero L, van der Ploeg van den Heuvel A, Neumann HA, de Haas ER, Robinson DJ. Topical hexylaminolevulinate and aminolevulinic acid photodynamic therapy: complete arteriole vasoconstriction occurs frequently and depends on protoporphyrin IX concentration in vessel wall. J Photochem Photobiol B 2013;126: 26-32.
- [3] Moy WJ, Patel SJ, Lertsakdadet BS, Arora RP, Nielsen KM, Kelly KM, Choi B. Preclinical in vivo evaluation of NPe6-mediated photodynamic therapy on normal vasculature. Lasers Surg Med 2012;44(2):158-62.
- [4] Khurana M, Moriyama EH, Mariampillai A, Wilson BC. Intravital high-resolution optical imaging of individual vessel response to photodynamic treatment. J Biomed Opt 2008;13(4): 040502
- [5] Zhu D, Luo Q, Tuchin VV. Tissue optical clearing. In: Wang RK, Tuchin VV, editors. Advanced biophontonics – Tissue optical sectioning. Boca Raton, London and New York: CRC Press; 2013, p. 621-72.
- [6] Zhu D, Larin KV, Luo Q, Tuchin VV. Recent progress in tissue optical clearing. Laser Photon Rev 2013;7(5):732-57.
- [7] Wen X, Mao Z, Han Z, Tuchin VV, Zhu D. In vivo skin optical clearing by glycerol solutions: mechanism. J Biophotonics 2010;3(1-2):44-52.
- [8] Wen X, Tuchin VV, Luo Q, Zhu D. Controling the scattering of intralipid by using optical clearing agents. Phys Med Biol 2009;54(22):6917-30.

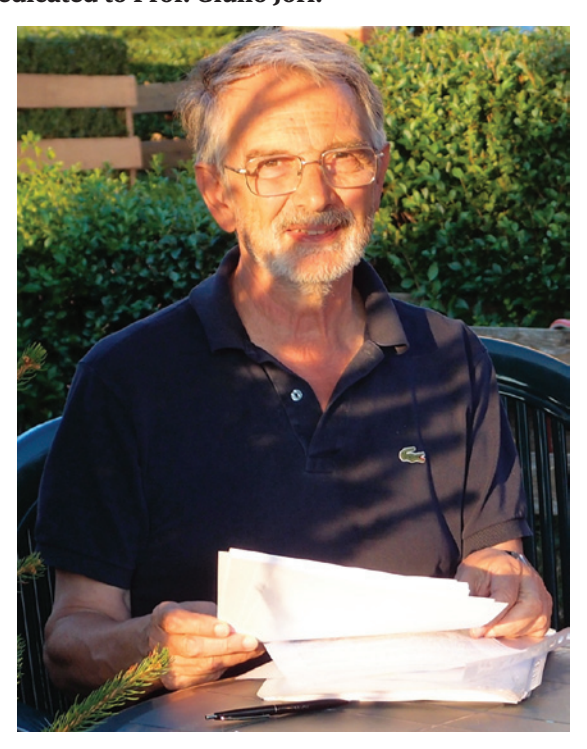
- [9] Mao Z, Zhu D, Hu Y, Wen X, Han Z. Influence of alcohols on the optical clearing effect of skin in vitro. J Biomed Opt 2008;13(2):021104.
- [10] Yu T, Wen X, Tuchin VV, Luo Q, Zhu D. Quantitative analysis of dehydration in porcine skin for assessing mechanism of optical clearing. J Biomed Opt 2011;16(9):095002.
- [11] Wang J, Ma N, Shi R, Zhang Y, Yu T, Zhu D. Sugar-induced skin optical clearing: from molecular dynamics simulation to experimental demonstration. IEEE J Sel Top Quant 2014;20(2):7101007.
- [12] Zhu D, Wang J, Zhi Z, Wen X, Luo Q. Imaging dermal blood flow through the intact rat skin with an optical clearing method. J Biomed Opt 2010;15(2):026008.
- [13] Liu C, Zhi Z, Tuchin VV, Luo Q, Zhu D. Enhancement of skin optical clearing efficacy using photo-irradiation. Lasers Surg Med 2010;42(2):132-40.
- [14] Zhi Z, Han Z, Luo Q, Zhu D. Improve optical clearing of skin in vitro with propylene glycol as a penetration enhancer. J Innov Opt Health Sci 2009;2(3):269-78.
- [15] Liu C, Zhang J, Yue Y, Luo Q, Zhu D. 1064 nm-Nd:YAG lasers with different output modes enhancing transdermal delivery: physical and physiological mechanisms. J Biomed Opt 2013;18(6):61228.
- [16] Wang J, Shi R, Zhu D. Switchable skin window induced by optical clearing method for dermal blood flow imaging. J Biomed Opt 2013;18(6):061209.
- [17] Wang J, Shi R, Zhang Y, Zhu D. Ear skin optical clearing for improving blood flow imaging. Photonics Lasers Med 2013;2(1):37-44.
- [18] Wang J, Zhang Y, Xu T, Luo Q, Zhu D. An innovative transparent cranial window based on skull optical clearing. Laser Phys Lett 2012;9(6):469-73.
- [19] Wang J, Zhang Y, Li P, Luo Q, Zhu D. Review: tissue optical clearing window for blood flow monitoring. IEEE J Sel Top Quant 2014;20(2):6801112.
- [20] Shi R. Chen M. Tuchin VV. Zhu D. Accessing to arteriovenous blood flow dynamics response using combined laser speckle contrast imaging and skin optical clearing. Biomed Opt Express 2015;6(6):1977-89.
- [21] Ding Y, Wang J, Fan Z, Wei D, Shi R, Luo Q, Zhu D, Wei X. Signal and depth enhancement for in vivo flow cytometer measurement of ear skin by optical clearing agents. Biomed Opt Express 2013;4(11):2518-26.

Session 9: Clinical photodynamic therapy

[9.01] Dosimetry aspects for PDT

Ronald Sroka*, Adrian Rühm, Wolfgang Beyer and Herbert Stepp Laser-Forschungslabor, LIFE-Center at Hopsital of University Munich, Feodor-Lynen-Str. 19, 81377 Munich, Germany *Corresponding author: PD Dr. Ronald Sroka, Ronald.sroka@med.lmu.de

Dedicated to Prof. Giulio Jori:



Abstract: This contribution focuses on 5-ALA induced PpIX-mediated photodynamic therapy (PDT) and on dosimetry aspects of light application systems. Terms such as tissue selectivity, transient selectivity and bleaching effects must be recognized to improve the selective tissue reactions. Light dosimetry completely differs when comparing solely surface illumination or irradiation of hollow organs with irregular shape. Backscattering effects must be taken into account. The basic light dosimetric quantities are introduced. Equivalent primary irradiation can lead to a wide range of therapeutic effects when the irradiation geometry of the target tissue may change. When monitoring fluorescence of the photosensitizer the detection of the photobleaching may serve for identification of its consumption. As a necessary task in clinical PDT the documentation of the presence of the photosensitizer fluorescence prior to irradiation is recommended.

Keywords: PDT; light dosimetry; backscattering; fluorescence.

1 Introduction

As the concept of photodynamic therapy (PDT) consists of the interaction of light-excited photosensitizer and oxygen, the research fields expand from photosensitizer (PS) development and light application systems up to the induction of several types of tissue reactions. This summary focuses on 5-ALA induced PpIX-mediated PDT and on dosimetry aspects of light application systems, keeping in mind when changing the photosensitizer other dosimetry factors must be reconsidered to receive clinical responses. PDT is well known as a selective treatment opportunity for tumors. Stressing the term "selectivity" one has to recognize whether there is a selective accumulation of the PS, either in the target tissue on the cellular level or in the tissue supporting vessel structure. Furthermore one has to consider whether the PS showed real selective accumulation or if there is a transient selectivity due to a high contrast between tumor tissue and surrounding normal tissue; in this case the PS-specific drug-light interval should be recognized. Bleaching effects of the PS may also occur while illumination and may improve the selectivity of the tissue reaction due to PDT.

2 Light dosimetry

In case the PS is not that selective or the contrast of PS content within the target compared the surrounding tissue is low the localized and specific light application may support a selective PDT tissue reaction. With regard to light application it should be kept in mind that light dosimetry will be completely different when comparing solely surface illumination or irradiation of hollow organs with irregular shape. In case of hollow organs often isotropic emitters are used and the resulting light distribution is strongly determined by backscattering from the organ wall, thus the hollow organ is working comparable to an integrating sphere.

For clarification, first the basic light dosimetric quantities should be introduced, which are sketched in Figure 1. The power per treated area, measured in mW/cm², multiplied with the treatment duration result in the energy per area, the irradiation. This term is often called power density and energy density. Unfortunately the value of these sizes

500 J/cm²

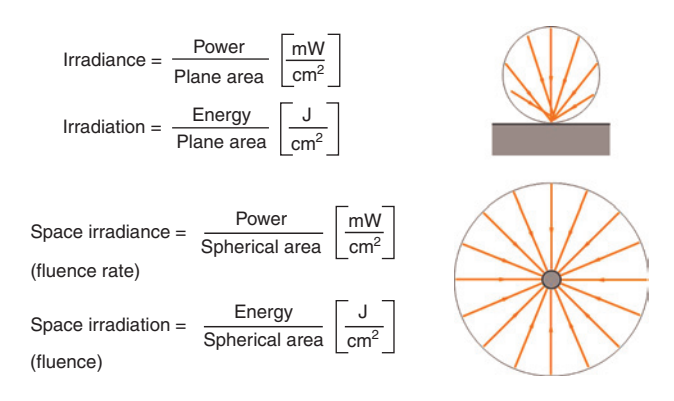


Figure 1: Dosimetric quantities for photodynamic therapy.

Figure 2: Comparison of illuminating a target (from left to right: cell plate, free tissue surface, hollow organ tissue surface) with the same irradiance (e.g. 0.1 W/cm²) for 1000 s resulting in an irradiation of 100 J/cm² (cell plate) but due to internal tissue scattering in different space irradiances (fluences) as indicated.

200 J/cm²

R = 50%

depends on the angle of incidence of the radiation. If this light beam comes from the side a certain amount of the light passes the target area compared to perpendicular irradiation, thus reducing the power or the energy hitting this area.

A living cell on the tissue surface does not care about the direction of the incoming light. The therapeutic effect does not depend on the angle of incidence. Therefore other dosimetric quantities have been defined, for instance the power hitting a small fictive sphere divided by its cross section, the so called space irradiance or fluence rate, and multiplied with the treatment time results in the space irradiation also called fluence. Note that they are measured in the same units like power density and energy density which makes it sometimes difficult to distinguish.

Irradiance and irradiation of the incident light are easy to measure and therefore cited in most papers. But the fluence rate and the fluence are responsible for the therapeutic effect and usually depend on the depth inside tissue. The ratio between these two pairs of sizes depends on the irradiation situation and this makes it necessary to care about. To show the challenge in taking this into account, an example should be discussed which is sketched in Figure 2. A target, tissue or cell, should be irradiated with a light dose of 100 J/cm². In case of an irradiation of a cell culture this number equals to the applied fluence. In case of a tissue a certain part of the light is backscattered and passes the surface again, which can be assumed to be 50%, which is a typical value for most cases. Than a cell on tissue surface obtains an additional light dose. Due to the diffuse angular distribution of the light its contribution to the fluence is higher. A detailed analysis based on the difference between irradiance and

space irradiance leads to an additional factor of 2 for this effects which results instead of 50 J/cm² in additional 100 J/cm² for the total fluence in case of a skin treatment. In case of the integral irradiation of a hollow organ it can be calculated that the fluence is 5 times more than for the cell culture for the same irradiation condition. Thus it can be concluded that the same primary irradiation can lead to a wide range of therapeutic effect. This has to be taken into account if one try to compare light doses for different irradiation situations. One way to overcome this problem of tissue backscattering is to use light application systems consisting of backscattering layers which are in contact to the target tissue surface, because photons escaping the tissue are immediately redirected into the tissue.

3 Conclusion

100 J/cm²

Light dosimetry for PDT is a complex topic and should be reconsidered for each specific application. It should be kept in mind that the same primary irradiation can lead to a wide range of therapeutic effects when the irradiation geometry of the target tissue may change and needs to be taken into account if one try to compare light doses for different irradiation situations. Light may also serve for on-monitoring possibilities, especially when monitoring fluorescence of the PS one can either resume that there is enough PS available for PDT or the irradiation dependent photobleaching may serve for PS consumption. Furthermore, ongoing investigation about monitoring of the transmission or remission of the excitation light show potential for signals which may indicate treatment progress. A very simple but necessary task in clinical PDT should be to clearly identify and document the presence of the PS by its fluorescence.

[9.02] Optimizing light source for photodynamic therapy of port wine stain birthmarks

Yuzhi Wang¹, Kaihua Yuan², Wei Gong³, Jian Zou³ and Zheng Huang^{3,*}

¹Southern Medical University, Guangzhou, China

²Laser Plastic and Aesthetic Center, Guangzhou General Hospital of Guangzhou Military Command, Guangzhou, China ³MOE Key Laboratory of OptoElectronic Science and Technology for Medicine, Fujian Normal University, Fuzhou, China *Corresponding author: Prof. Zheng Huang, zheng_huang@msn.com

Abstract: Port wine stain (PWS) birthmarks are congenital vascular malformations of the skin that affect 0.3% of newborns. The majority of PWS lesions appears on the face and neck area and require medical intervention. Pulsed dye laser (PDL)-mediated photothermolysis is the current standard treatment. Vascular-targeted photodynamic therapy (PDT) might be an alternative for the treatment of PWS. This contribution will provide an overview on our clinical studies on the comparison of PDL and PDT in the treatment of PWS. Current clinical status will be discussed with a focus on developing new light sources for improving the PDT efficacy of large PWS lesion.

Keywords: port wine stain birthmarks; photodynamic therapy; laser; LED.

1 PWS and PDL

Port wine stain (PWS) birthmarks are congenital vascular malformations of the skin that affect 0.3% of newborns. PWS lesions are characterized by ectatic capillaries that are often accompanied with various degrees of hypertrophy of overlying soft tissue. The color of PWS lesions can range from pale pink to red to purple color. PWS lesions can become thick and dark with age. Facial PWS can cause serious emotional and physical impact to patients and their parents. PWS lesions should be treated at younger age to minimize such bad impact.

Pulsed dye laser (PDL)-mediated selective photothermolysis is the current standard treatment for PWS. Good blanching responses might be achieved by the complete photocoagulation of PWS vessels by PDL mediated by yellow light (e.g. 585 nm or 595 nm). But only a small portion of patients can obtain complete blanching of their PWS after PDL treatment. There is a need to develop effective and safe modality for the management of PWS birthmarks.

2 Role of PDT

Vascular acting photodynamic therapy (PDT) is a twostep modality in which a photosensitizer is intravenously administered and activated by the coherent or noncoherent light source of appropriate wavelength(s) at the lesion site while sensitizers are still circulating in blood vessels. Subsequently, light induced oxygen-derived free radicals (e.g. singlet oxygen) can selectively damage the vessel wall and cause vessel closure but sparing surrounding tissue. This modality has been successfully used for treating leaky vessel occurred in the wet form age-related macular degeneration (AMD). Although this modality has been proposed for treating PWS vessels by European and American dermatologists in the later 1980s, it has never got into the clinical use in the Western World, partly because of widely available PDLs and bias on PDT's potentials in PWS treatment.

Anecdotally, vascular acting PDT has been used for the treatment of PWS in China since the early 1990s. So far, several thousands patients have been treated. Similar to PDT of wet form AMD, the selective photodynamic damage to the PWS vessel wall can ultimately close PWS vessels and result in variuos degrees of blanching without the destruction of surrounding skin tissues [1]. The data accumulated from clinical studies in China have demonstrated that PDT is safe and effective in the treatment of childhood and adult PWS [2, 3]. Due to historical reasons, various hepatoporphyrin derivative (HpD)-based sensitizers and laser light sources have been used in China [4]. Currently, the combination of haematoporphyrin monomethyl ether (HMME) and 532 nm laser is undergoing formal clinical trials in China.

3 PDT versus PDL

Fortunately, we have the capacity to do both PDT and PDL treatment in our practice. Our retrospective study of children (PDL=112 and PDT=98) and adults (PDL=163 and PDT=208) suggested that vascular-targeting PDT is as effective as PDL for treating pink PWS and more effective than PDL for purple PWS if not superior [5]. Recently, for the first time, we carried out an inter- and intra-patient side-by-side comparison of the therapeutic responses of PDL and PDT treatment in a small series of patients (n=15). In this prospective study, two adjacent flat areas of PWS lesions were selected from each patient and randomly assigned to either single-session PDL or PDT treatment. PDL treatment was delivered using a 585-nm pulsed laser. PDT was carried out with a combination of HMME and a

low-power copper vapour laser (510.6 nm and 578.2 nm). Clinical outcomes were evaluated colorimetrically and visually during follow-up. This prospective side-by-side comparison demonstrated that PDT is at least as effective as PDL and, in some cases, even superior [6].

Our clinical experience also suggest that PDT might be useful for the management of PDL-resistant PWS lesions. On the other hand, for patients who have large and multiple lesions some residual spots could be present after PDT and in such cases PDL can be used to eliminate those small lesions [7]. Nevertheless, Chinese data support the use of PDT for the management of PWS although the true value of PDT still deserves further investigation.

Vascular-targeted PDT is well tolerated and most cases can be treated on an outpatient basis. Common and rare adverse effects are generally caused by the phototoxicity associated with the mechanisms of action of PDT. In our experience, overtreatment and human error are common risk factors [1, 8]. It should not be overlooked that every safeguard precaution and proper post-PDT treatment care must be routinely and strictly applied by both clinician and patient or parents of pediatric patients in order to prevent and minimize possible adverse effects.

4 Laser versus LED

The light irradiation in vascular-targeted PDT is delivered to PWS lesions while the photosensitizer remains inside the blood vessels, which offers a unique vascular selectivity. However, one major concern or limitation of vasculartargeted PDT is its short drug-to-light interval (DLI), which only offers a very short light treatment window (<1 h) and therefore poses a great technical challenge in light delivery, particularly for patients with large lesions.

Typically, laser light irradiation is carried out at fluence levels of 80–100 mW/cm² immediately after drug injection and the course of light irradiation cannot last longer than 45 min because of (1) the limitation of laser power output, and (2) the concern of drug uptake by the normal skin tissue and possible skin damage. For the typical optic fiber-coupled laser light sources available in our clinic, the maximal diameter of the light spot on the skin surface is set at 7-10 cm and the duration of irradiation is 20-25 min/spot to maintain the fluence levels of 80-100 mW/cm² in order to achieve desired clinical outcomes. The area that can be treated by the laser light source during one single session is therefore highly limited.

Light-emitting diodes (LEDs) have been widely used in topical PDT in the treatment of various skin conditions. In light of rapid recent development in LED technology, it is not unaccepted that to replace the laser with less expensive high power LEDs of suitable wavelength(s) for

fiber-free superficial irradiation of PWS lesions. In terms of providing an even light field for treating large surface in a single session, in addition to adequate power and large emitting surface, the LED panel which consists of carefully designed and arranged arrays of individual LEDs should be able to generate uniform light.

Currently, we are testing several prototypes of LED devices emitting 532 nm light. Preliminary results suggest that the fiber-free LED panel can generate an uniform light field that covers at least twice size of the laser at the same fluence and comparable clinical outcomes to PDL (unpublished data). This demonstrates that with a good assurance of uniform light distribution and adequate power LEDs might offer an ultimate solution for treating larger lesions.

5 Summary

Vascular-targeted PDT combining HpD and laser has been widely used in the treatment of PWS birthmarks in China but not outside China. Chinese data strongly support the use of PDT for the management of PWS but the true value of PDT still deserves further investigation. In the light of recent developments in LED technology, it is not unacceptable to replace the laser with less expensive high power LED to treat large PWS lesions. To test the usefulness of intense pulsed light and PDL as PDT light source is also intriguing.

- [1] Yuan KH, Gao JH, Huang Z. Adverse effects associated with photodynamic therapy (PDT) of port-wine stain (PWS) birthmarks. Photodiagnosis Photodyn Ther 2012;9(4):332-6.
- [2] Zhang B, Zhang TH, Huang Z, Li Q, Yuan KH, Hu ZQ. Comparison of pulsed dye laser (PDL) and photodynamic therapy (PDT) for treatment of facial port-wine stain (PWS) birthmarks in pediatric patients. Photodiagnosis Photodyn Ther 2014;11(4):491-7.
- [3] Huang Z. Photodynamic therapy in China: over 25 years of unique clinical experience Part two - clinical experience. Photodiagnosis Photodyn Ther 2006;3(2):71-84.
- Huang Z. Photodynamic therapy in China: over 25 years of unique clinical experience Part one – history and domestic photosensitizers. Photodiagnosis Photodyn Ther 2006;3(1):3-10.
- Yuan KH, Li Q, Yu WL, Zeng D, Zhang C, Huang Z. Comparison of photodynamic therapy and pulsed dye laser in patients with port wine stain birthmarks: a retrospective analysis. Photodiagnosis Photodyn Ther 2008;5(1):50-7.
- [6] Gao K, Huang Z, Yuan KH, Zhang B, Hu ZQ. Side-by-side comparison of photodynamic therapy and pulsed-dye laser treatment of port-wine stain birthmarks. Br J Dermatol 2013;168(5):1040-6.
- [7] Yuan KH, Li Q, Yu WL, Huang Z. Photodynamic therapy in treatment of port wine stain birthmarks - Recent progress. Photodiagnosis Photodyn Ther 2009;6(3-4):189-94.
- Xiao Q, Li Q, Yuan KH, Cheng B. Photodynamic therapy of portwine stains: long-term efficacy and complication in Chinese patients. J Dermatol 2011;38(12):1146-52.

[9.03] PDT of non-melanoma skin cancer lesions controlled by in vivo OCT imaging

Carsten M. Philipp*

Ev. Elisabeth Klinik Berlin, Abt. Lasermedizin, Lützwostr. 24-26, 10785 Berlin, Germany *Corresponding author: Dr. Carsten M. Philipp, lasermed.elisabeth@pgdiakonie.de

Abstract: Incidence of non-melanoma skin cancer (NMSC) lesions is increasing in Europe, Australia and the United States. Topical photodynamic therapy (PDT) employing protoporphyrin IX is established for thinner lesions as superficial basal cell carcinoma, actinic keratosis and Bowens disease. Larger or ulcerated lesions with a substantial volume may be treated with systemic PDT. Therapeutic decision of the type of PDT and control after treatment is eased by optical coherence tomography.

Keywords: NMSC; BCC; topical PDT; systemic PDT; skin imaging.

1 Introduction

Skin is the largest organ of the human body. Usually it is easy accessible for topical application of drugs, and light dosimetry is easy due to the rather flat appearance in a first approximation. On the other hand a larger number of skin diseases cover a larger area or show multifocal appearance, which favors regional or large field therapies and impedes surgical interventions. As scar formation is another and today highly unwanted result of surgery, the widespread use of photodynamic therapy (PDT) in dermatology is a necessary consequence [1].

Since the introduction of 5-aminolevulinic acid (ALA) as precursor drug topical PDT with protoporphyrin IX (PpIX) has been developed into a reliable and effective tool for the treatment of superficial basal cell carcinoma (BCC) or Bowen's disease (BD) and actinic keratosis. This is even more important as the incidence of those lesions shows a significant increase during the last decade and an even stronger increase has to be expected in the future. The typical fluorescence of PpIX may also be used for fluorescence diagnostic and control of therapy and is another advantage. Overtreatment is unlikely, as PpIX shows a "bleaching" with subsequent decay of reactive oxygen species generation during the light exposure.

2 PDT requirements

Nevertheless, topical PDT is only effective in some tumor types and thickness of the tumors is crucial as penetration of the drug (ALA or its derivatives) and conversion into PpIX is the limiting factor. In larger volumes and other tumor entities systemic PDT with intravenously applied photosensitizers (PS) offer advantages. As photosenzitation of skin in general is one of the typical features that come along with systemic PS, a differentiated light dosimetry becomes much more important. Shielding of non-diseased sites, interval between PS administration and light application, light dose and way of application (surface application or interstitial), single or repeated exposures are examples for the numerous variables in light application that may be applied.

3 OCT imaging

Optical coherence tomography (OCT), established in ophthalmology, may becomes a routine option for imaging of dermal and mucosal structures in dermatology and ENT also. OCT can produce images of the layers of skin and mucosa and their dysplastic changes (leukoplakia, actinic keratosis) as well as dermal and epithelial tumors, such as BCC and BD, and display their vertical and horizontal dimensions proportionally. The imaging depth is slightly variable and depends on the optical density, scattering and absorption parameters of the tissues and may be distorted by hair, hyperkeratosis or else on the surface. However, below 1 mm the imaging quality decreases significantly with currently available systems.

Images obtained by OCT remind of ultrasound images, but with a much higher resolution and from a much smaller volume. The method is "in situ" and "real time", which gives the investigator the chance to depict and delineate suspicious tissues prior to surgery or PDT. It may allow non invasive follow up of treated sites and early detection in case of tumor recurrence also.

While BCC may be displayed in OCT with very high significance and the control of therapy results is eased by OCT, imaging of actinic keratosis and especially its conversion into BD or squamous cell carcinoma (SCC) is less significant and improved techniques with the ability to disclose dysplastic areas from healthy tissues are required. As today we investigate OCT clinically for noninvasive delineation and control of skin lesions prior and after PDT with a high correlation to histological findings [2].

- [1] Philipp CM. PDT in dermatology. In: Abdel-Kader MH, editor. Photodynamic therapy: from theory to application. Berlin and Heidelberg: Springer-Verlag; 2014, p. 131-63.
- [2] Ziolkowska M, Philipp CM, Liebscher J, Berlien H-P. OCT of healthy skin, actinic skin and NMSC lesions. Med Laser Appl 2009;24(4):256-64.

Session 10: Recent advances in clinical photodynamic therapy applications

[10.01] Photodynamic therapy in dermatology

Karin Kunzi-Rapp^{1,2,*}

Institute for Laser Technologies in Medicine and Metrology, Helmholtzstr. 12, 89081 Ulm, Germany

²Department of Dermatology and Allergology, University of Ulm, Albert-Einstein-Allee 23, 89081 Ulm, Germany

*Corresponding author: Dr. Karin Kunzi-Rapp, karin.rapp@ilm.uni-ulm.de

Abstract: Photodynamic therapy (PDT) is a modern therapy modality in dermatology. PDT has been established in the treatment of non-melanoma skin cancers as actinic keratoses, Bowen disease and superficial basal cell carcinoma. The advantages are the excellent cosmetic results, especially in the treatment of extensive field cancerization, the good controllability by the physician and the good efficacy in the immunosuppressed patients. The associated pain and the low tissue penetration are the most frequent limiting factors of PDT. The talk reviews the recent developments in dermatological PDT. Key oncological and non-oncological indications are presented as well.

Keywords: PDT; 5-ALA; daylight-PDT; intensified PDT; pain.

1 Introduction

In Egypt, China and India skin lesions were treated by cumarin containing plant extracts and sun light more than 1000 years B.C. The concept of topical photodynamic therapy (PDT) was resumed at the beginning of the 20th century and increasingly used since 1990. Today PDT is a modern therapy modality mainly employed to treat patients with superficial non-melanoma skin cancer and dysplasia. It allows treatment of large areas with high response rate and excellent cosmetic outcome. In Europe the prodrugs 5-aminolevulinic acid (5-ALA) and ALA-methylester are approved for topical application. Systemical applications in dermatology with 5-ALA (oral application), indocyan green, methylen blue or verteporphin are still experimental. Because of higher optical penetration depth in the red spectrum and a small peak in the absorption spectrum of protoporphyrin IX (PpIX), irradiation is performed by lasers or light emitting diode (LED) light sources emitting wavelength of 635 nm or by broad spectrum lamps (550-700 nm). For conventional PDT incubation time of the sensitizer averages 3-4 h.

2 Medical indications

2.1 Oncological indications

The main oncological indications in dermatology are actinic keratosis (AK), especially field cancerization, initial squamous cell carcinoma (SCC), Bowen's disease and superficial basal cell carcinoma (BCC). PDT is unsuitable for tumors >2 mm in histological thickness and for morpheic or pigmented BCC, likely due the limited availability of photosensitizer and light in deep or pigmented lesions.

Besides conventional PDT, individualized therapy options are created as simplified PDT with daylight irradiation and intensified PDT. Indications for simplified PDT are grade I or II AKs, field cancerosis and older patients. The idea of daylight irradiation is continuous photoactivation with blue and red light at Pp IX low levels. Side effects like edema and crusting occur, but the treatment with daylight results in a significant decrease in pain score compared with conventional PDT. Intensified PDT is indicated for the treatment of thicker lesions as initial BCC or initial SCC. Chemical or physical pretreatments like topical retinoids or ablative fractional laser treatments before topical sensitizer incubation achieve deeper penetration of sensitizer and light. Temperature elevation during sensitizer incubation (heat pad 38–40°C for 1 h), iontopheresis or iron-chelating substances which interact with heme biosynthetic pathway results in higher concentration of PpIX. But intensified therapy leads to intensified reactions and higher risks of side effects.

Immunosupressed organ transplant recipients have a significantly increased risk of skin cancer due to the long-term immunosuppressive therapy especially for SCC. Most of these carcinomas develop from precancerous AKs. Periodical preventive PDT treatments are recommended in chronically sun-damaged skin with areas with fieldcancerization to prevent SCC.

2.2 Non-oncological indications

Besides precancerous lesions and non-melanoma skin cancers, PDT is also used in non-oncological indications. With modification of the therapy protocols immunmodulatory mechanisms of PDT become active. Especially inflammatory skin diseases such as acne, viral warts, morphea and even cutaneous leishmaniasis profits from this mechanism. Even in skin rejuvenation the beneficial combination of ALA and intense pulsed light is reported.

Topical PDT is effective, safe and allows treatment of large areas. However, the main drawback of PDT is the pain during irradiation. Besides premedication with oral analgesic drugs, local or regional anaesthesia (intra cutaneous, sub cutaneous or nerve blockade, no effect of topical anesthetics!), various strategies for controlling pain during PDT have been studied. Most utilized is cooling by pre-cooled air stream and/or water spray. Furthermore pausing irradiation, pulsed-dye laser (PDL, 595 nm)-mediated PDT, low dose irradiation or daylight irradiation and even pre-irradiation with small doses of blue light before irradiation with red are reported to be helpful.

3 Conclusion

In conclusion, topical PDT is a safe and effective method of treatment for initial non-melanoma skin cancer. It is commonly used for the therapy of AK especially for large areas of photodamaged skin. Cosmetic results are excellent in comparison to curettage, cryosurgery or excisional surgery. The individualized therapy shows a good controllability by the physician. Periodical preventive PDT treatments demonstrate good efficacy in immunosupressed organ transplant recipients.

[10.02] Recent progress of ALA-PDT in China

Xiuli Wang*

Shanghai Skin Diseases Hospital, Baode Rd 1278, Shanghai 200443, China *Corresponding author: Prof. Dr. Xiuli Wang, xlwang2001@aliyun.com

Abstract: Our research group started to utilize 5-aminolevulinic acid (ALA)-mediated photodynamic therapy (ALA-PDT) as a possible treatment of skin cancers in 1995. Nowadays, ALA-PDT has become one of the most popular modalities in dermatology and venereology in China. In particular, the pioneering work done by our group in ALA-PDT of urethral condylomata acminata helped Shanghai Fudan Zhangjiang Bio-Pharmaceutical Co., Ltd. to obtain the regulatory approval from the China Food and Drug Administration (CFDA) for ALA to be used in the topical PDT of Condyloma acuminatum in 2007. Since then, ALA and dermatological PDT have been rapidly developed in China. To date, ALA-PDT has been carried out routinely in over 600 clinics across China. Approved and off-label indications include condylomata acminata, acne, flat warts, photoaging, actinic kerotosis, folliculitis, extramammary Paget's disease, lichen sclerosus, and superficial skin cancers. Meanwhile, numerous research teams have been actively engaged in basic researches of ALA-PDT. This presentation will provide an overview on clinical and basic researches carried out by our group and other groups in China.

Keywords: ALA-PDT; Condyloma acuminatum; acne; skin cancer.

1 Backgound

Our research group started to utilize 5-aminolevulinic acid (ALA) photodynamic therapy (PDT) as a possible treatment of skin cancers in 1995. Nowadays, ALA-PDT has become one of the most popular modalities in dermatology and venereology in China. In particular, the pioneering work done by our group in ALA-PDT of urethral Condyloma acminatum helped Shanghai Fudan-Zhangjiang Bio-Pharmaceutical Co., Ltd. to obtain the regulatory approval from the China Food and Drug Administration (CFDA) for ALA to be used in the topical PDT of condylomata acuminata in 2007. Compared with conventional therapies, topical ALA-PDT is a simple, effective, safe and well-tolerated treatment for urethral condylomata acuminata that is associated with a low recurrence rate. The mechanism might be the triggering of both apoptosis and necrosis by ALA-PDT in human papillomavirus-infected keratinocytes. Since then, ALA and dermatological PDT have been rapidly developed in China. To date, ALA-PDT has been carried out routinely in over 600 clinics across China. Approved and off-label indications include condylomata acuminata, acne, flat warts, photoaging, actinic kerotosis, folliculitis, extramammary Paget's disease, lichen sclerosus, and superficial skin cancers. Meanwhile, numerous research teams have been actively engaged in basic and clinical researches of ALA-PDT.

2 Medical indications

2.1 Condyloma acuminatum

The indication of ALA-PDT in China is Condyloma acuminatum. In 2004, our group firstly reported that topical ALA-PDT was used to treat urethral condylomata acuminata with a low recurrence rate. Compared with conventional treatment, such as repeated local drug application and laser ablation, ALA-PDT is a simple, effective, safe and well-tolerated treatment for urethral condylomata acuminata. Meanwhile, we detected protoporphyrin IX (PpIX) pharmacokinetics after topical application of ALA in urethral condylomata acuminata. The results suggest

that the topical application of 5–10% ALA solution for 3-5 h is the optimal condition for the PDT of urethral condylomata acuminata. The selective damage of the condylomata acuminata lesions in the epidermis without damaging the dermis ensures a better control of recurrence and side effects such as ulceration or scarring. In 2007, Prof. H. Gu and Prof. K. Chen investigated the efficacy and safety of topical application of ALA-PDT for condylomata acuminata in China [1]. They found that topical application of ALA-PDT is a simpler, more effective and safer therapy with a lower recurrence for treatment of condylomata acuminata compared with conventional CO₃ laser therapy. This work proved the efficacy of ALA-PDT for condylomata acuminata via a randomized clinical trial. In 2008, our group [2] found ALA-assisted photodynamic diagnosis could be employed for the detection of the lesion, subclinical lesion of genital warts, even latent human papillomavirus (HPV) infection. It explained why ALA-PDT could reduce the recurrence rate of condylomata acuminata. In further clinical studies we found ALA-PDT combined with imiguimod had a good effect on the treatment of genital Bowenoid papulosis with low recurrence and less side effect [3]. There are also a few studies showing ALA-PDT is effective for flat warts, common warts and plantar wart [4].

2.2 Acne

Acne is an off-label indication of ALA-PDT in China, In 2010, our group found ALA-PDT was a simple, safe and effective therapeutic option for the treatment of severe acne [5]. In total, 22% of patients showed excellent improvement after one-course ALA-PDT, another 34% showed excellent improvement after two-course ALA-PDT, and the rest (44%) required three-course treatment to further reduce the number and size of residual lesions. Adverse effects were minimal. The symptoms and signs in recurrent cases (14%) were much milder and responded well to conventional topical medication. After that, dermatologist in China began to treat severe acne with ALA-PDT widely. In 2013, a self-controlled multicenter clinical trial carried out in 15 centers throughout China was reported [6]. In total, 397 acne patients of grade II-IV in 15 centers received ALA-PDT treatment. The results showed that a low-dose topical ALA-PDT regimen using 5% ALA, 1 h incubation and a red light source of 3 treatment sessions was suggested as optimal scheme for the treatment of different severity of acne vulgaris in Chinese patients. Superior efficacy was found in severe cystic acne of grade IV with mild side effects. In addition, ALA-PDT could not only clear the acne but also have cosmetic results. Our studies showed

that after ALA-PDT the appearance of photoaging lesions improved, the stratum corneum hydration increased and the transepidermal water loss decreased.

2.3 Skin cancers

Actinic keratosis and basal cell carcinoma are the indications of ALA-PDT in USA or Europe. But our group started to use ALA-PDT to treat skin cancers in China as early as in 1995. In recent 20 years, we have made progress in ALA-PDT for skin cancer. So far, we have treated 100 cases of skin cancer and pre-cancer using topical ALA-PDT. They included squamous cell carcinoma, basal cell carcinoma, Bowen's disease, mammary and extramammary Paget disease, actinic keratosis and erythroplasia of Queyrat. Especially, we used PDT-combined surgery group to treat extramammary Paget's disease and found multiple ALA-PDT could be applied to reduce the severity of extramammary Paget's disease lesions and improve the success of surgery [7]. Our study shows that ALA-PDT treated tumor cells can stimulate the maturations of dendritic cells (DCs), including morphology maturation, phenotypic maturation, and functional maturation [8]. Most interestingly, PDT-induced apoptotic tumor cells are more capable of potentiating maturation of DCs than PDT-treated or freeze/thaw-treated necrotic tumor cells. ALA-PDT-DC vaccine based on apoptotic tumor cells can activate the adaptive immune system more effectively, providing protection against skin squamous cell carcinoma in mice, far stronger than that of freeze-thaw DC vaccine. Our results indicated that immunogenic apoptotic cells induced by ALA-PDT can enhance DC vaccine for squamous cell carcinoma.

3 Conclusion

In conclusion, this presentation will provide an overview on clinical and basic researches carried out by our group and other groups in China.

- [1] Chen K, Chang BZ, Ju M, Zhang XH, Gu H. Comparative study of photodynamic therapy vs CO₂ laser vaporization in treatment of condylomata acuminata: A randomized clinical trial. Br J Dermatol 2007;156(3):516–20.
- [2] Wang HW, Wang XL, Zhang LL, Guo MX, Huang Z. Aminolevulinic acid (ALA)-assisted photodynamic diagnosis of subclinical and latent HPV infection of external genital region. Photodiagnosis Photodyn Ther 2008;5(4):251–5.
- [3] Wang XL, Wang HW, Guo MX, Huang Z. Combination of immunotherapy and photodynamic therapy in the treatment of Bowenoid papulosis. Photodiagnosis Photodyn Ther 2007;4(2):88-93.

- [4] Li Q, Jiao B, Zhou F, Tan Q, Ma Y, Luo L, Zhai J, Luan Q, Li C, Wang G, Gao T. Comparative study of photodynamic therapy with 5%, 10% and 20% aminolevulinic acid in the treatment of generalized recalcitrant facial verruca plana: a randomized clinical trial. J Eur Acad Dermatol Venereol 2014;28(12):1821-6.
- [5] Wang XL, Wang HW, Zhang LL, Guo MX, Huang Z. Topical ALA PDT for the treatment of severe acne vulgaris. Photodiagnosis Photodyn Ther 2010;7(1):33-8.
- [6] Ma L, Xiang LH, Yu B, Yin R, Chen L, Wu Y, Tan ZJ, Liu YB, Tian HQ, Li HZ, Lin T, Wang XL, Li YH, Wang WZ, Yang HL, Lai W. Low-dose topical 5-aminolevulinic acid photodynamic therapy in the
- treatment of different severity of acne vulgaris. Photodiagnosis Photodyn Ther 2013;10(4):583-90.
- [7] Wang HW, Lv T, Zhang LL, Lai YX, Tang L, Tang YC, Huang Z, Wang XL. A prospective pilot study to evaluate combined topical photodynamic therapy and surgery for extramammary Paget's disease. Lasers Surg Med 2013;45(5):296-301.
- [8] Ji J, Fan Z, Zhou F, Wang X, Shi L, Zhang H, Wang P, Yang D, Zhang L, Chen WR, Wang X. Improvement of DC vaccine with ALA-PDT induced immunogenic apoptotic cells for skin squamous cell carcinoma. Oncotarget 2015;6(19):17135-46.

[10.03] Photodynamic therapy in dermatology: Actual indications and new alternative therapies

Georg Däschlein^{1,*}, Matthias Napp², Andreas Söhnel³, Sebastian von Podewils¹, Stine Lutze¹, Andreas Arnold¹ and Michael Jünger¹

¹Department of Dermatology of the Ernst Moritz Arndt University, Sauerbruchstrasse, 17475 Greifswald, Germany

- ²Department of Surgery of the Ernst Moritz Arndt University, Sauerbruchstrasse, 17475 Greifswald, Germany
- ³Department of Dental Medicine of the Ernst Moritz Arndt University, Sauerbruchstrasse, 17475 Greifswald, Germany
- *Corresponding author: PD Dr med. Georg Däschlein, Georg.daeschlein@uni-greifswald.de

Abstract: Photodynamic therapy (PDT) is known for over 100 years in medicine and has shown considerable power in the antimicrobial treatment of various infectious diseases involving bacteria, viruses, parasites, and fungi. In the era of worldwide emerging multi-resistance, novel treatment options are strongly warranted and PDT may be a suitable alternative to antibiotics against multidrug-resistant pathogens. We were able to show excellent PDT (with toluidine blue as sensitizer) in vitro results against clinically highly relevant species like Methicillin-resistant Staphylococcus aureus (MRSA) and multidrug-resistant Proteus mirabilis and Klebsiella pneumonia (extended beta-lactamase buildner, ESBL) not being inferior in comparison to another novel treatment, cold atmospheric plasma (CAP).

Keywords: photodynamic therapy; infectious disease; bacteria; wIRA; toluidine blue; cold atmospheric plasma.

1 Materials and methods

1.1 Experiments

We conducted an in vitro trial to test the antimicrobial power of a photodynamic therapy (PDT) with toluidin blue (TBO) as photosensitizer in comparison with 2 sources of cold atmospheric plasma (CAP).

As multidrug-resistant (MDR) pathogens we tested Proteus mirabilis (PME894.2) and Klebsiella pneumonia (KPNESBL) both extended beta-lactamase buildner (ESBL) and hospital (h) as well as community (c) associated Methicillin-resistant Staphylococcus aureus (MRSA) collected from wounds of dermatologic patients in our clinic. As not multiresistant strains we investigated

clinical strains of Staphylococcus epidermidis (Ederm and ATCC12228), Micrococcus luteus (EMLderm), Klebsiella pneumonia (non ESBL E688.1), Candida albicans (CA54/05 and ATCC10231), Enterococcus faecalis (EFderm and ATCC1657), Methicillin susceptible S. aureus (MSSA ATCC 1924; American Type Culture Collection Manassas, VA, USA), Streptococcus pyogenes (ATCC19615), Pseudomonas aeruginosa (ATCC 15442), M. luteus (ATCC1030) and Escherichia coli (ATCC11229).

All strains were grown overnight on Columbia agar and grown colonies thereafter diluted in sterile saline to obtain concentrations between 10E8 and 10E9 colony forming units (CFU) per milliliter. After dilution, TBO (Sigma Aldrich, Germany) was added to a final concentration of 0.02 mg/ml to the suspension. 400 µl of the suspension of each isolate were irradiated in 6-well plates (Sarstedt, Nümbrecht, Germany) by water-filtered infrared-A (wIRA) using the Hydrosun-radiator system emitter (Hydrosun-System; Hydrosin-750 Strahler, Hydrosun Medizintechnik GmbH, Müllheim, Germany) at a distance of 25 cm to the wIRA bulb over 20 min; the applied energy in the form of wIRA is between 200 and 225 mW/cm² (75% wIRA, 25% visible light). During treatment the plates were cooled by ice blocks manually added into a water bath surrounding the plates. The reduction factor (RF) was calculated for each isolate by the difference between the decadic logarithm of CFU of the control assay (nonirradiated suspensions) and those grown after irradiation after visual enumeration of the grown CFU on Columbia agar overnight at 36°C aerobically (200 µl of the respective suspension were plated onto the agar).

In a second trial, the same suspensions as described above for PDT treatment were used for investigating the susceptibility against CAP. For this purpose the wells were irradiated over 3 min with either a dielectric barrier discharge plasma (DBD) (Tefra®; Tefra, Berlin Germany) or an atmospheric pressure plasma jet (APPJ). Both plasma sources were manually positioned in order to allow constant contact of the discharge plume with the fluid surface (keeping the tip in continuous meandric movements). RF was calculated in the same way.

1.2 Plasma sources

The APPJ device used was a kINPen 09® (Neoplas Tools Greifswald e.V., Greifswald, Germany) jet plasma generator. The argon flow through the capillary as the feed gas is adjusted to 6 l/min) and the radio frequency voltage of 1–5 kV, 1.5 MHz is coupled to the central electrode. The temperature at the tip of the beam did not exceed 37°C. For detailed characterization of the APPJ, the reader is referred to Weltmann et al. [1]. The Tefra® plasma works via a pencil-shaped evacuated gas electrode with a tip of around 1.5 cm².

2 Results

The *in vitro* PDT treatment over 20 min was followed by a significant reduction of the bacterial growth in all cases showing some interspecies differences ranking between 3.4 (*S. epidermidis*, Ederm) and 8.4 found treating *E. faecalis* (EFderm) (Figure 1). The MDR species MRSA (both *h*MRSA and *c*MRSA) and *P. mirabilis* (PME894.2) and *K. pneumoniae* (KPNESBL) did not show lower RF compared with the non-MDRspecies. The typical skin habitat species *S. epidermidis* (ATCC 12228 and the clinical strain Ederm) and *M. luteus* (ATCC 1030) with RF of 3.7, 3.4 and

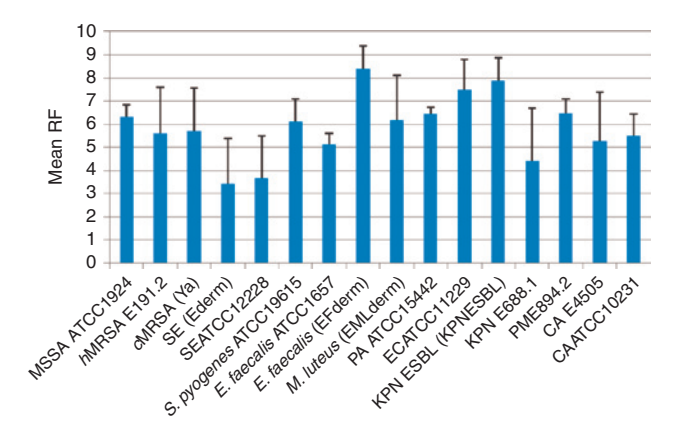


Figure 1: Mean reduction factors (RF) obtained after 20 min *in vitro* irradiation with wIRA-PDT with toluidine blue as photosensitizer against normo- and multi-resistant bacteria.

6.2 respectively were not more susceptible or resistant to PDT compared with the typical wound pathogens MRSA (hMRSA RF 5.6, cMRSA 5.7), E. coli (RF 7.5), K. pneumoniae (non ESBL, RF 4.4), P. aeruginosa (RF 6.4), and S. pyogenes (RF 6.1). After 3 min of CAP treatment of the suspensions no growth was recorded 48 h after incubation of enumerating plates in any case of a treated suspension indicating a RF of ≥ 8 for every tested species and each of the used plasma sources (data not shown) indicating a much stronger effect against most species by CAP.

3 Discussion

Our data demonstrate a powerful TBO-PDT efficacy against the most important multiresistant skin and wound pathogens in vitro. These results together with the good tolerability of TBO (concentrations <1%) support a potential use of this treatment in the clinic against skin and wound pathogens including MDR strains like MRSA, vancomycin-resistant enterococci (VRE) and multidrug-resistant gramnegative rods (MRGN). Antimicrobial PDT has been referenced since decades focusing nearly any kind of bacterial, fungal, parasitic or viral infection [2–8] but the global spread of multi-resp. extreme resistant pathogens opens new horizons in the anti-infective philosophy because now potent alternatives to antibiotic drugs are urgently warranted. Recently Tseng et al. [9] faced this challenge comparing TBO-PDT susceptibility of cMRSA and hMRSA in vitro and found a significant inhibition of both pathogens with cMRSA being less susceptible to the treatment than hMRSA. They hypothesized the background of this effect in different sequencing types and staphylococcal cassette chromosome mec (SCCmec) types. The authors also found a distinct damaging of genetic structures thus allowing finally putting the pathogens in check by down modulating their virulence factors even when the killing effects are less pronounced. This is of crucial importance because it implicates the opportunity to benefit from the surviving pathogens which one times defused now are valuable candidates to colonize the susceptible tissue thus protecting it against recontamination with new pathogens, a phenomenon which turns non-desired effects (weak killing power) into a positive one. Finally antimicrobial PDT can cause classical photodamage of cells propagating direct lethal effects disrupting plasma membranes as well as chromosomal and plasmid DNA [10] and also indirect cell death provoked by DNA misreplication and fragmentation via deoxyguanosin derivates [11], additionally it was shown to cause chromosomal DNA fragmentation and plasmid DNA degradation in MRSA [9]. Other studies support the virulence modulating effect of PDT in E.coli and P. aeruginosa [12, 13]. Additionally it could

be shown that sublethal TBO concentrations are able to inhibit the activities of virulence proteins of MRSA like bacterial protease, lipase, hemolysin, and enterotoxin type B [9]. The suitability of TBO-PDT against MRSA was further described by Wainwright et al. [14] and in the light of these results clinical trials to evaluate the clinical suitability of PDT in infection prevention of these pathogens now seem reasonable.

Since especially chronic recalcitrant wounds (lower leg ulcer wounds in most cases) are not typical indications for PDT treatment, these wounds (often harbouring MDR pathogens) should yet be focused at first for clinical PDT treatment. We recommend such an in vivo trial as supportive treatment in parallel to conventional methods.

In comparison with CAP showing RF≥8 after 3 min treatment the PDT which took 20 min of irradiation was less effective. To further investigate whether less exposure time is required for bacterial killing we treated MSSA and MRSA over 0.5, 1, 2, 3, 4 and 5 min and found the first significant RF increase starting after 3 min of irradiation (data not shown). However we cannot recommend less exposure time using wIRA-PDT because 20 min was the most often referenced treatment time found to support wound healing. Second, we do not recommend stronger RF than those found with PDT because the obtained RF easily fulfil the RF recommendations for skin disinfection.

In contrast to CAP wIRA therapy mainly relies on thermic energy released into tissue thus promoting healing and only indirectly reinforcing antimicrobial treatment via i.e. restoring phagocytic activity by neutrophils and providing oxygen supply [15]. This healing promoting property by wIRA is widely referenced and meanwhile this therapy constitutes an effective healing supporting therapy in patients with acute and chronic wounds [16] with recommended treatment time of 20 min for one treatment session. However, in combination with TBO-PDT we cannot exclude pain during (and after) PDT provoked by the effect of TBO in wounded tissue what has to be investigated in clinical trials before implementing a combined treatment study.

In opposite to PDT the antimicrobial CAP treatment is based upon a bundle of biophysical effects with membrane oxidation by reactive oxidative species like hydroxyl radicals and peroxides being of particular importance [1, 17], however, the antimicrobial scenario of CAP used vet is not fully understood [18]. Like wIRA, CAP has shown important wound healing effects which in sum besides antimicrobial activity support cell differentiation and repair [17]. Up to now CAP in contrast to wIRA is not part of established wound therapy because double-blinded randomized controlled multi-centered studies are lacking.

CAP was shown to exhibit broad and potent antimicrobial efficacy against all clinically relevant skin and wound pathogens, including multiresistant species like MRSA, VRE and MRGN in vitro [19-22]. This potency was clinically evaluated in clinical trials demonstrating potent reduction of the colonization flora of chronic wounds [23, 24]. Other applications are chronic wounds in cardiac surgery showing good results in the treatment of infected transdermal driveline catheter wounds [25]. An important step in chronic wound therapy regarding both treatment tools will be the involvement of large biofilms. Albeit PDT with TBO [26] and CAP were shown to have potent antibiofilm activity in vitro [27, 28], in case of larger biofilm involvement in wounds we recommend a prior surgical debridement in order to improve access of reactive species to living tissue or to use a special CAP system which in contrast to wIRA and conventional CAP is able to debride in parallel to its antimicrobial activity, however this is requiring local anaesthesia in most cases. This kind of plasma, i.e. the KLS Argon beam® (KLS Martin, Tuttlingen, Germany) treatment is more versatile compared with nondebriding systems and was recently referenced as suited treatment in the therapy of chronic ulcer wounds in dermatology by our group [29].

Finally, the antimicrobial reduction of bacterial bioburden is a cornerstone in the treatment of acute infected wounds and is an important step in the treatment of recalcitrant wounds when bacterial burden is involved in healing deterioration. Accordingly, PDT using TBO like CAP treatment are promising candidates in the treatment and prevention of MDR pathogens and may serve as alternative to antimicrobial chemotherapy and conventional surface disinfection in hospital hygiene. Up to now albeit some referenced and also significant differences in susceptibility in some species like hMRSA and cMRSA the principle susceptibility of all up to now worldwide distributed notorious resistant pathogens against CAP and also PDT seems given and in sum, the obtained RF of both treatments are high enough to suppose good clinical effectiveness, since colonizations like infections are not known to significantly exceed these bacterial concentrations.

4 Conclusion

In conclusion, TBO-PDT as a new treatment tool and alternative to less effective antimicrobial drugs seems suited to defeat colonization with MDR bacteria like MRSA, ESBL and MRGN. This therapy could establish a new era in hospital infection prevention breaking the fatal circle of drug overuse and selection of resistant clones leading to the now predominating excessive global multidrug-resistance problem with the reality of complete lack of therapeutic options for many patients. However, evidence must be driven from clinical trials in order to prove reliable and also well-tolerated treatment. This is of crucial importance since i.e. sanitization of heavily colonized patients warrants whole-body treatment which has not been successfully demonstrated up to now. For this purpose it has to be demonstrated that TBO is well tolerated after application also to the around 2 m² of body surface in the adult patient. Another goal will be the topical wound treatment where TBO meets wounded tissue not covered by protecting epidermis and as mentioned above it has to be investigated whether the TBO-PDT is tolerated or whether pain relief is mandatory.

Nevertheless in the light of dramatic lack of new drug development as alternative we recommend TBO-PDT as potential option in infection therapy as well as infection prevention.

- [1] Weltmann KD, Kindel E, Brandenburg R, Meyer C, Bussiahn R, Wilke C, von Woedtke T. Atmospheric pressure plasma jet for medical therapy: plasma parameters and risk estimation. Contrib Plasma Phys 2009;49(9):631–40.
- [2] Malik Z, Ladan H, Nitzan Y. Photodynamic inactivation of Gramnegative bacteria: Problems and possible solutions. J Photochem Photobiol B 1992;14(3):262-6.
- [3] Hamblin MR, Hasan T. Photodynamic therapy: a new antimicrobial approach to infectious disease? Photochem Photobiol Sci 2004;3(5):436–50.
- [4] Mohr H, Lambrecht B, Selz A. Photodynamic virus inactivation of blood components. Immunol Invest 1995;24(1-2):73-85.
- [5] Ferro S, Coppellotti O, Roncucci G, Ben Amor T, Jori G. Photosensitized inactivation of *Acanthamoeba palestinensis* in the cystic stage. J Appl Microbiol 2006;101(1):206–12.
- [6] Wiegell SR, Kongshoj B, Wulf HC. Mycobacterium marinum infection cured by photodynamic therapy. Arch Dermatol 2006;142(9):1241–2.
- [7] Calzavara-Pinton PG, Venturini M, Capezzera R, Sala R, Zane C. Photodynamic therapy of interdigital mycoses of the feet with topical application of 5-aminolevulinic acid. Photodermatol Photoimmunol Photomed 2004;20(3):144–7.
- [8] Maisch T. A new strategy to destroy antibiotic resistant microorganisms: antimicrobial photodynamic treatment. Mini Rev Med Chem 2009;9(8):974–83.
- [9] Tseng SP, Hung WC, Chen HJ, Lin YT, Jiang HS, Chiu HC, Hsueh PR, Teng LJ, Tsai JC. Effects of toluidine blue O (TBO)photodynamic inactivation on community-associated methicillin-resistant *Staphylococcus aureus* isolates. J Microbiol Immunol Infect 2015. doi: 10.1016/j.jmii.2014.12.007.
- [10] Bertoloni G, Lauro FM, Cortella G, Merchat M. Photosensitizing activity of hematoporphyrin on *Staphylococcus aureus* cells. Biochim Biophys Acta 2000;1475(2):169–74.
- [11] Sayed Z, Harris F, Phoenix DA. A study on the bacterial phototoxicity of phenothiazinium based photosensitisers. FEMS Immunol Med Microbiol 2005;43(3):367–72.

- [12] Tseng SP, Teng LJ, Chen CT, Lo TH, Hung WC, Chen HJ, Hsueh PR, Tsai JC. Toluidine blue O photodynamic inactivation on multidrug-resistant *Pseudomonas aeruginosa*. Lasers Surg Med 2009;41(5):391–7.
- [13] Kömerik N, Wilson M, Poole S. The effect of photodynamic action on two virulence factors of gram-negative bacteria. Photochem Photobiol 2000;72(5):676–80.
- [14] Wainwright M, Phoenix DA, Laycock SL, Wareing DR, Wright PA. Photobactericidal activity of phenothiazinium dyes against methicillin-resistant strains of *Staphylococcus aureus*. FEMS Microbiol Lett 1998:160(2):177–81.
- [15] Schumann H, Calow T, Weckesser S, Müller ML, Hoffmann G. Water-filtered infrared A for the treatment of chronic venous stasis ulcers of the lower legs at home: a randomized controlled blinded study. Br J Dermatol 2011;165(3):541–51.
- [16] Künzli BM, Liebl F, Nuhn P, Schuster T, Friess H, Hartel M. Impact of preoperative local water-filtered infrared A irradiation on postoperative wound healing: a randomized patient-and observer-blinded controlled clinical trial. Ann Surg 2013;258(6):887–94.
- [17] Kong MG, Kroesen G, Morfill G, Nosenko T, Shimizu T, van Dijk J, Zimmermann JL. Plasma medicine: an introductory review. New J Phys 2009;11:115012.
- [18] Moisan M, Barbeau J, Moreau S, Pelletier J, Tabrizian M, Yahia LH. Low-temperature sterilization using gas plasmas: a review of the experiments and an analysis of the inactivation mechanisms. Int J Pharm 2001;226(1–2):1–21.
- [19] Daeschlein G, Napp M, von Podewils S, Scholz S, Arnold A, Emmert S, Haase H, Napp J, Spitzmueller R, Gümbel D, Jünger M. Antimicrobial efficacy of a historical high-frequency plasma apparatus in comparison with 2 modern, cold atmospheric pressure plasma devices. Surg Innov 2015;22(4):394– 400.
- [20] Daeschlein G, von Woedtke T, Kindel E, Brandenburg R, Weltmann KD, Jünger M. Antibacterial activity of an atmospheric pressure plasma jet against relevant wound pathogens in vitro on a simulated wound environment. Plasma Process Polym 2010;7(3-4):224-30.
- [21] Daeschlein G, Scholz S, Arnold A, von Podewils S, Haase H, Emmert S, von Woedtke T, Weltmann KD, Jünger M. *In vitro* susceptibility of important skin and wound pathogens against low temperature atmospheric pressure plasma jet (APPJ) and dielectric barrier discharge plasma (DBD). Plasma Process Polym 2012;9(4):380–9.
- [22] Daeschlein G, Napp M, von Podewils S, Lutze S, Emmert S, Lange A, Klare I, Haase H, Gümbel D, von Woedtke T, Jünger M. *In vitro* susceptibility of multidrug resistant skin and wound pathogens against low temperature atmospheric pressure plasma jet (APPJ) and dielectric barrier discharge plasma (DBD). Plasma Process Polym 2014;11(2):175–83.
- [23] Isbary G, Morfill G, Schmidt HU, Georgi M, Ramrath K, Heinlin J, Karrer S, Landthaler M, Shimizu T, Steffes B, Bunk W, Monetti R, Zimmermann JL, Pompl R, Stolz W. A first prospective randomized controlled trial to decrease bacterial load using cold atmospheric argon plasma on chronic wounds in patients. Br J Dermatol 2010;163(1):78–82.
- [24] Brehmer F, Haenssle HA, Daeschlein G, Ahmed R, Pfeiffer S, Görlitz A, Simon D, Schön MP, Wandke D, Emmert S. Alleviation of chronic venous leg ulcers with a hand-held dielectric barrier discharge plasma generator (PlasmaDerm® VU-2010): results of a monocentric, two-armed, open, prospective, randomized

- and controlled trial (NCT01415622). J Eur Acad Dermatol Venereol 2015;29(1):148-55.
- [25] Hilker et al. Personal communication. 2015.
- [26] Daeschlein et al. Unpublished data. 2014.
- [27] Kamgang JO, Briandet R, Herry JM, Brisset JL, Naïtali M. Destruction of planktonic, adherent and biofilm cells of Staphylococcus epidermidis using a gliding discharge in humid air. J Appl Microbiol 2007;103(3):621-8.
- [28] Joaquin JC, Kwan C, Abramzon N, Vandervoort K, Brelles-Mariño G. Is gas-discharge plasma a new solution to the old problem of biofilm inactivation? Microbiology 2009;155(Pt 3):724-32.
- [29] Daeschlein G, Napp M, Lutze S, Arnold A, von Podewils S, Guembel D, Jünger M. Skin and wound decontamination of multidrug-resistant bacteria by cold atmospheric plasma coagulation. J Dtsch Dermatol Ges 2015;13(2):143-50.

Author Index

[1.01] – [10.03] represent the short report numbers

Abramova, I. [7.03]	He, H. [5.01]	Maisch, T. [4.01]	Wan, Z. [1.02]
Arnold, A. [10.03]	He, J. [8.02]	Mao, H. [1.02]	Wang, H. [5.04]
	He, Y. [8.01]	Miller, JM. [7.03]	Wang, J. [8.01]
Bao, W. [6.02]	Helmreich, M. [2.01]		Wang, P. [3.01]
Bartusik, D. [7.03]	Hoelzel, H. [2.01]	Napp, M. [10.03]	Wang, X. [10.02]
Berlien, H-P. [6.01]	Hopf, A. [2.01]	Ng, DKP.[5.01]	Wang, XS. [4.02], [4.06]
Beyer, W. [9.01]	Huang, C. [7.04]	Ni, Y. [6.02]	Wang, Yi. [1.07], [4.06],
Biedermann, M. [2.01]	Huang, J. [3.04]	Nie, G. [5.04]	[7.01]
Busch, TM. [7.03]	Huang, MD. [2.02]	Niu, H. [7.02]	Wang, Yu. [9.02]
	Huang, N. [7.01]	Nuñez, SC. [4.03]	Wang, YC. [4.06]
Cengel, KA. [7.03]	Huang, Z. [9.02]		Wei, J. [5.04]
Chen, D. [1.07]	Hui, Z. [5.03]	Peng, X. [7.02]	Wei, Y. [2.03]
Chen, H. [1.02]		Pfitzner, M. [1.04]	Wen, T. [5.03], [5.04]
Chen, Z. [2.02]	Ji, T. [5.04]	Philipp, CM [6.01], [9.03]	Wenqi, L. [5.03]
Chen, ZY. [6.02]	Jiang, X-J. [5.01]	Pohl, J. [4.05]	Wilson, BC. [1.05]
Chu, C. [7.04]	Jünger, M. [10.03]	Preuß, A. [1.01], [4.04]	Wu, X. [5.03], [5.04]
Cui, D. [5.02]	Jux, N. [2.01]		Wu,S. [4.06]
Cui, S. [3.02]	,,,,,,,,,,,,,,,,,,,,,,,,,,,,,,,,,,,,,,,	Qiu, H. [7.01]	
	V- MD [2 0/] [5 0/]	Qu, J. [7.02]	Yan, W. [7.02]
Däschlein, G. [10.03]	Ke, MR. [3.04], [5.01]	24,7.[7.02]	Yang, J. [4.06]
Ding, Z. [6.02]	Köhl, M. [1.06]	Röder, B. [1.01], [1.03], [1.04],	Yao, C. [8.01]
z3, z. [etez]	Kunzi-Rapp, K. [10.01]	[4.04], [4.05]	Ye, S. [7.02]
Eder, K. [2.01]		Rühm, A. [9.01]	Yin, D. [3.02]
Fang, W. [2.03]	Lan, W. [3.04]	Kuiiii, A. [9.01]	Yuan, K. [9.02]
Tang, W. [2.09]	Lau, JTF. [5.01]	C-bl-th IC [4 04] [4 02]	
C II [7.07]	Li, B. [1.05], [1.07]	Schlothauer, JC. [1.01], [1.03],	Zeng, J. [7.01]
Gao, H. [7.04]	Li, K. [4.02]	[1.04]	Zhang, J. [7.04]
Gao, W. [3.02]	Li, P. [6.02]	Shangguan, Z. [6.02]	Zhang, JY. [7.01]
Ge, J. [3.01]	Li, R. [2.02]	Shen, Y. [6.02]	Zhang, Z. [8.01]
Ghogare, AA. [7.03]	Li, YL. [1.02]	Shi, J. [5.04]	Zhao, D. [3.04]
Ghosh, G. [7.03]	Li, YY. [5.04]	Shi, X. [5.04]	Zhao, J. [3.03]
Gong, W. [9.02]	Lin, D. [7.02]	Söhnel, A. [10.03]	Zhao, R. [5.04]
Greer, A. [7.03] Gu, Y. [1.05], [1.07], [4.06],	Lin, L. [1.05]	Song, J. [7.02]	Zhao, Y. [5.04]
	Liu, G. [7.04]	Sroka, R. [9.01]	Zheng, B. [3.04]
[7.01] Gu, YQ. [3.02]	Liu, L. [2.03]	Stepp, H. [9.01]	Zheng, K. [2.02]
Guo, M. [1.02]	Liu, X. [5.04]	van Dadawila S. [40,02]	Zhou, A. [2.03]
Guo, IVI. [1.02]	Lo, P-C. [5.01]	von Podewils, S. [10.03]	Zhou, Q. [4.02]
H. H. H. C. M. C. T. C. C.	Luo, Y. [4.06]		Zhu, D. [8.02]
Hackbarth, S. [1.01], [1.03]	Lutze, S. [10.03]	Walalawela, N. [7.03]	Zou, J. [9.02]

Subject Index

[1.01] – [10.03] represent the short report numbers

5-ALA [10.01] Acne [10.02] Active targeting [2.01] ALA-PDT [10.02] Amino-terminal fragment of urokinase

[2.02]

Antibiotic resistance [4.01] Anticancer [3.04] Antifungus [3.04]

Backscattering [9.01] Bacteria [4.04], [10.03]

BCC [9.03]

Biofilm(s) [4.03], [4.04], [4.05], [4.06]

Bodipy [3.03]

Carbon dots [3.01] Ce6 [5.02] Chitosan [3.02]

Cold atmospheric plasma [10.03] Condyloma acuminatum [10.02]

Davlight-PDT [10.01] Decolonization [4.01] Dental infections [4.03] Diffusion [1.01]

Enhanced permeation and retention effect (EPR) [2.01]

Enzyme activity [1.06]

Fluorescence [9.01] Fluorescent imaging [5.02]

Folate [3.02] FRET [3.03]

Gold nanoclusters [5.02] Gold nanoprisms [5.02] Gold nanorod(s) [5.02], [5.04] Graphene oxide [7.04] Green algae [4.05]

HMME-loaded TiO, [8.01] Human serum albumin [2.02]

Imaging [1.04], [1.05] In vivo singlet oxygen detection [1.04] Inactivation of bacteria [4.02] Infectious disease [10.03] Infrared spectroscopy [1.03], [1.06] Intensified PDT [10.01] Intracellular delivery [1.02]

Intraepithelial neoplasms [6.01]

Kinetics [1.01] Laser [9.02]

Laser irradiation protocol [6.01]

LED [9.02] Light dose [1.01] Light dosimetry [9.01] Liver cancer [7.04]

Local field enhancement [5.04]

Luminescence [1.07] Lysosomal disruption [1.02]

Mechanism [7.01]

Methicillin-resistant Staphylococcus aureus

(MRSA) [4.06] Micelles [1.02]

Microbial resistance [4.03]

Mold fungi [4.04] MRSA [4.01]

Near-infrared [7.02] NMSC [9.03]

Noble metal nanostructures [5.03] Nonlinear upconversion [7.02]

Optical coherence tomography [6.02]

Optical diagnostic [6.01] Optical imaging [8.02] Oral disease [4.03]

Pain [10.01]

Passive targeting [2.01] Photobleaching [7.01] Photocatalysts [5.03] Photochemistry [3.03] Photodynamic antimicrobial chemotherapy (PACT) [4.01]

Photodynamic inactivation (PDI) [4.04],

[4.05], [4.06] Photodynamic therapy (PDT) [1.07], [2.01], [2.03], [3.01], [3.02], [3.04], [4.02],

[4.03], [5.01], [5.02], [5.04], [6.01], [6.02], [7.02], [7.04], [8.01], [8.02], [9.01], [9.02],

[10.01], [10.03] Photoinactivation [4.03] Photomultiplier [1.03] Photon counting [1.03]

Photosensitizer(s) [3.04], [5.01], [5.03], [5.04] Photothermal therapy (PTT) [5.04], [7.04]

Phototrophic microorganisms [4.05] Phthalocyanine(s) [3.04], [5.01] Phthalocyanine zinc [2.02]

Plasmon [5.03]

Port wine stain birthmarks [9.02]

Port wine stains (PWS) [7.01] Pseudomonas aeruginosa [4.06] Pulse repetition rate [1.07] Pulsed laser [1.07]

Quenching [1.06]

Rectilinear photodynamic therapy [7.03]

SCC cells [8.02] Sensitizer drift [7.03]

Single photon avalanche diode [1.03] Singlet oxygen [1.02], [1.06], [1.07], [2.03], [3.02], [4.01], [4.04], [4.05], [5.01]

Singlet oxygen halo [7.03]

Singlet oxygen luminescence [1.01], [1.04], [1.05]

Singlet oxygen quantum yields [3.01]

Sinoporphyrin sodium [7.04] Skin cancer [10.02] Skin imaging [9.03] Spatially resolved [1.05] Subcellular localization [1.01] Superconducting nanowire [1.03]

Systemic PDT [9.03]

Teflon tips [7.03]

Therapeutic outcome [6.02]

Time-resolved luminescence spectroscopy

[1.04]

Time-resolved [1.05] Tissue optical clearing [8.02] Toluidine blue [10.03] Topical PDT [9.03]

Transition metal complex [3.03]

Triarylmethane [4.02] Triplet state [3.03] Tumor [2.03] Tumor targeting [2.02]

Upconversion nanoparticles [3.02], [7.02] Upconversion nanoprobe [2.03]

Urokinase receptor [2.02]

Vascular lesions in mucosa [7.01] Vascular-targeted photodynamic therapy (V-PDT) [7.01]

Vasculature imaging [6.02]

Vesicles [1.02]

Water [1.06] wIRA [10.03]